NATURAL RADIOACTIVITY IN SOILS OF THE WALVIS BAY – HENTIES BAY COASTAL AREA, NAMIBIA.

A THESIS SUBMITTED IN PARTIAL FULFILMENT

OF THE REQUIREMENTS FOR THE DEGREE OF

MASTER OF SCIENCE

OF

THE UNIVERSITY OF NAMIBIA

BY

SIMON ANDREW SHIMBOYO

JANUARY 2013

Supervisor: Professor James Akindele Oyedele (University of Namibia)

ABSTRACT

Naturally occurring radionuclides such as ^{238}U, ^{232}Th and ^{40}K are present in the soil where they disintegrate spontaneously releasing ionizing radiation which could pose health hazards to the inhabitants of a given location especially when the concentrations of the radionuclides are high. In Namibia, the Walvis Bay – Henties Bay coastal area is known to have many mineral resources including uranium and therefore the concentrations of the radionuclides in the soils and the associated radioactivity may be high in some towns in the area. It is therefore important to study the concentrations of radionuclides and the radioactivity in the soils of the major towns in the area. In this study, the concentrations of the radionuclides ^{238}U, ^{232}Th and ^{40}K and their progeny, and their contribution to natural radioactivity in the soils of six major towns in the Walvis Bay – Henties Bay coastal area have been determined. These towns are Usakos, Arandis, Swakopmund, Walvis Bay, Wlotzkasbaken and Henties Bay.

A total of 305 soil samples were collected across the six towns and dried under laboratory temperature for 72 hours. These samples were pulverised and passed through a 2 mm mesh screen and sealed in 500 ml polythene bottles. The specific activities of the radionuclides ^{238}U, ^{232}Th and ^{40}K in the samples were subsequently analysed using a well-shielded high-purity germanium (HPGe) detector. The average concentration for ^{238}U varies from a minimum of 14.5 ± 2.5 Bq kg^{-1} in Walvis Bay to a maximum of 104.1 ± 28.1 Bq kg^{-1} in Wlotzkasbaken, with a mean of 52.6 ± 24.5 Bq kg^{-1} for the six towns. Also, the average concentration for ^{232}Th varies from a minimum of 18.0 ± 3.0 Bq kg^{-1} in Walvis Bay to a maximum of 334.4 ± 86.9 Bq kg^{-1} in Arandis, with a mean of 104.3 ± 85.9 Bq kg^{-1} while the average concentration for ^{40}K varies from a minimum of 363.3 ± 41.3 Bq kg^{-1} in Walvis Bay to a maximum of 1336.5 ± 142.0 Bq kg^{-1} in Usakos, with a mean of 778.7 ± 204.6 Bq kg^{-1} for the six towns. These values were used to calculate the mean absorbed dose rate and the annual effective dose. The average annual effective dose varies from a minimum of 0.04 ± 0.01 mSv in Walvis Bay to a maximum of 0.35 ± 0.07 mSv in Arandis**,** with a mean of 0.15 ± 0.08 mSv for the six towns. These values

are lower than the maximum permissible limit of 1.0 mSv recommended by the International Commission on Radiological Protection (ICRP) for the public so that the towns do not have high natural radioactivity.

DEDICATION

This thesis is dedicated to my late mother, **Elizabeth "Ella" Christiaans** and to my wife and son, Rosalina Esperanca Shimboyo and Andrew Lorenzo Domingo's Shimboyo.

ACKNOWLEDGEMENTS

Firstly, I would like to thank our heavenly Father for all his blessings and the gifts HE provides. To my wife, thank you for your patience and understanding when I had to travel and work late nights. My mentor, colleague and friend, Professor James Akindele Oyedele THANK YOU for all you have done and continue doing for this person from the dusty streets of Katutura. I would also like to express my heartfelt thanks to everyone that was instrumental in the production of this Thesis, my colleagues in the Department of Physics and Faculty of Science at the University of Namibia, Windhoek.

The author would also like to thank the following institutions for their contributions;

University of Namibia

International Atomic Energy Agency

Ministry of Health and Social Services: National Radiation Protection Authority

Municipality of Usakos

Municipality of Arandis

Municipality of Swakopmund

Municipality of Walvis Bay

Municipality of Henties Bay

Erongo Regional Council

Dr. Christopher Strobl, Herr Michael Thomas, Frau Angela Poppitz-Spuhler, Frau Carola Cronfeld, Herr Hartmut to name a few at the Federal office for Radiation Protection, Oberschleissheim, Germany.

DECLARATION

I, Simon Andrew Shimboyo, hereby declare that this study is a true reflection of my own research, and that this work, or part thereof has not been submitted for a degree in any other institution of higher education.

…….. Date:…….

Simon Andrew Shimboyo

ACRONYMS

UNAM	University of Namibia
IAEA	International Atomic Energy Agency
ICRP	International Commission on Radiological Protection
UNSCEAR	United Nation Scientific Committee on Effects of Atomic Radiation
ICRU	International Commission on Radiation Units and Measurements
SANUMARC	Sam Nujoma Marine & Coastal Resources Research Centre
NRPA	National Radiation Protection Authority (Namibia)
NORM	Naturally Occurring Radioactive Materials

LIST OF TABLES

LIST OF FIGURES

LIST OF APPENDICES

Table of Contents

CHAPTER 1

1. INTRODUCTION

1.1 Radioactivity

Henri Becquerel, a French scientist in 1896 accidentally discovered that uranium salt crystals emit an invisible radiation that could pass through a black, lightproof paper shielding a photographic plate and darken or "expose" the film (Patel, S.B., 1988 and Giancoli, C.G., 1998). This phenomenon was further investigated in 1897 by the husband and wife team of Pierre and Marie Curie who, after studies on pitchblende - the ore from which uranium is extracted - found that it emits "Becquerel rays" with a much stronger intensity than its uranium content would. They later discovered two new elements, radium and polonium, and they gave the name 'radioactive' to these substances that emitted the so called "Becquerel rays". This phenomenon soon became known as radioactivity. In the years that followed, Ernest Rutherford found that a beam from a radium sample splits into three when passed through a strong magnetic or electric field. He established that there existed three distinct types of radiation, which he named "alpha (α)"-, "beta (β)"-, and "gamma (γ)"- rays (Tykva R. & Sabol J., 1995). Radioactivity occurs when certain nuclides undergo spontaneous disintegration and energy (in the form of radiation) is liberated in the process. New nuclides are formed in the process and radiations such as gamma rays, alpha particles and beta particles are emitted.

Nuclides undergoing spontaneous disintegration are said to be unstable or radioactive (Hodgson, P.E., Gadioli, E. & Gadioli Erba, E., 1997). Such nuclides are uranium, thorium, polonium and radium. These nuclides can be radioactive for several years. For example, a uranium sample will be radioactive for more than a billion years. The different radiations emitted have different properties and are usually referred to as ionizing radiation (Burcham, W.E. & Jobes, M., 1995; and Knoll, G.F., 2000). Gamma rays are photons or quantum of light having very high energy. Their energies range from a few keV to several MeV. A gamma ray (γ ray) carries no charge and there is no change in a nuclide when it emits γ ray. In beta decay, an electron (in β^- decay) or a positron (in β^+ decay) is emitted so that a new or different nuclide is formed after the decay. When a nucleus emits alpha particle (α particle) it loses two protons and two neutrons so that the new nucleus is different from the original nucleus (Heyde K., 1999; and Patel, 1988). The detection of radioactivity is based on the properties of these radiations and the intensities of the radiations indicate the concentration of the radioactive element.

1.2 Natural background radiation

Natural background radiation is the amount of radiation that a member of the general population receives from exposure to natural sources, such as terrestrial radiation from naturally occurring radionuclides in the soil, rocks, vegetation, air and cosmic radiation originating from outer space. Also naturally occurring radionuclides exist in small traces in the human body taken up through the diet (Annex A, United Nation Scientific Committee on Effects of Atomic Radiation (UNSCEAR), 1993).

The most commonly encountered naturally occurring primordial radionuclides are ^{238}U, ^{232}Th, their decay products and the long-lived nuclide ^{40}K. Most elements are stable, however those that are naturally unstable parent nuclides have long half-lives and their decay products are also present in nature. Half –life is the time it takes for a radioactive nuclide to lose 50% of its activity by decay. Each radionuclide has a unique half-life (Tykva & Sabol, 1995). The half-lives of some radionuclides are long while those of others are short as shown in Table 1.1. Figure 1.1 (a) shows the decay scheme for the naturally occurring radionuclide ^{40}K.

Table 1.1: The half-lives of some radionuclides

Radionuclide	Half-life ($T_{1/2}$)
Polonium-216	0.15 *s*
Radon-220	55.6 *s*
Proactinium-234m	1.2 *min*
Sodium-22	2.602 *years*
Cobalt-60	5.271 *years*
Caesium-137	30.0 *years*
Potassium-40	1.28×10^9 *years*
Uranium-238	4.47×10^9 *years*
Thorium-232	1.41×10^{10} *years*

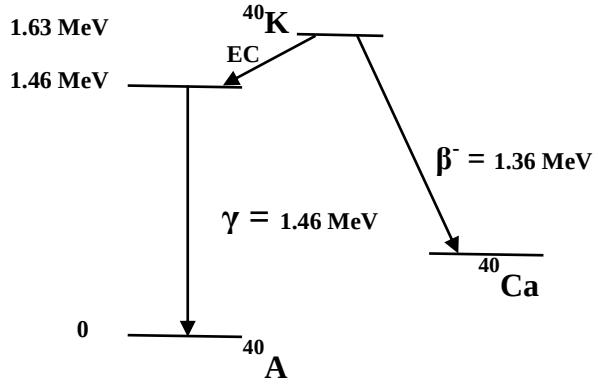

Figure 1.1 (a): The decay scheme of ^{40}K.

From the half-lives of some radionuclides presented (in Table 1.1) above, only nuclides with half-lives comparable with the age of the earth exist in terrestrial materials (UNSCEAR, 1993). The principal primordial radioactive elements are ^{238}U ($T_{1/2}$ = 4.47 x 10^9 years), ^{232}Th ($T_{1/2}$ = 1.41 x 10^{10} years) and ^{40}K ($T_{1/2}$ = 1.28 x 10^9 years) which are present in soil and rocks that have condensed with the earth 4500 million years ago. In nature, there exist three natural radioactive decay chains, namely the Uranium series, Thorium series and Actinium series. The parent radionuclide of the Uranium series is the radionuclide ^{238}U while that of the Thorium series is ^{232}Th and ^{235}U is the parent radionuclide of the Actinium series. Half-lives of these parent radionuclides (^{238}U and ^{232}Th) need to be much longer than that of any other radionuclides in the series. This sufficiently long period must have elapsed to allow for ingrowth of the decay products. The activity of the parent radionuclide undergoes no appreciable changes during many half-lives of its decay products (Argonne National Laboratory EVS, 2005).

To reach a lighter stable nucleus these nuclei and they daughters decay either by alpha (α), beta (β) or gamma (γ) emission (Firestone R.B., Chu S.Y.F., Baglin C.M. and Zipkin J., 1996). It should be mentioned that there are unstable nuclides or radioisotopes that are produced in the laboratory or that are man-made: such radioisotopes are ^{137}Cs, ^{22}Na and ^{60}Co (Giancoli, 1998; and Hodgson et al., 1997). The radioactivity of naturally occurring unstable isotopes are called “natural radioactivity” while those of the man-made unstable isotopes are called “artificial radioactivity”. There are unstable isotopes or radioactive

elements in the soil, rocks, water and air around us (Burcham & Jobes, 1995; and Knoll, 2000).

Background radiation can vary with location and altitude, because of the different concentrations of naturally occurring radioisotopes in the soils, water and from cosmic radiation at these locations. About 70% of natural background radiation comes from the earth crust including rocks and soils (UNSCEAR, 1993). The other contributions are from photons originating from the core of the sun and other extra-terrestrial bodies in the outer universe, also contributions could be from man-made activities like nuclear weapons testing and accidents at nuclear power plants.

The exposure of human beings to ionizing radiation from natural sources is a continuing feature of life on earth. However, some people live in areas with low or normal background radiation (mean effective dose less than 1.0 mSv y^{-1}) while others live in areas regarded as high background radiation areas (Ramli, A. T., Wahab, A., Hussein, H. A. and Wood, A.K., 2005 and Oyedele, J.A., 2005). It is not desirable for human beings to live in high background radiation area (mean effective dose greater than 1.0 mSv y^{-1}) because ionizing radiations are hazardous or can cause biological damage.

1.3 Biological effects of radiation

The 1945 atomic bombing in the Japanese cities of Hiroshima and Nagasaki and the Chernobyl nuclear plant disaster in the Ukraine in 1986 have shown that the biological

effects of radiation could be very severe. Many people died due to the release of ionizing radiation from these events. In the bombings of the Japanese cities the immediate effects of the blast killed approximately 70,000 people in Hiroshima and many people continued to die in the years that followed from burns Figure 1.1(a) and radiation related diseases, such as leukaemia, cataracts, acute radiation syndrome and solid cancers. Also, in Nagasaki estimates for immediate deaths ranged from 40,000 to 75,000 and most people did not die directly from the actual explosion, but from the radiation released or burns as shown in Figure 1.1(b) (UNSCEAR, 2008).

At Chernobyl, the resulting radioactive release was equivalent to ten Hiroshima's and many people died and are still dying from the radiation released (UNSCEAR, Scientific Annex D, 2008). In general, the biological effects of ionizing radiation depend on the type and dose of the radiation (Ghiassi-nejad, M., Mortazavi, S. M. J., Cameron, J. R., Niroomand-rad, A. & Karam, P. A., 2002; and Knoll, 2000). The occurrence of biological effects from exposure to ionizing radiation is complicated with a lot of factors involved namely, the type of radiation, magnitude of dose received, the rate at which the dose is received, part of the body exposed, age of the person and biological differences.

(a)

(b)

Figure 1.1(b): Victims with serve burns after the explosion of atomic bombs in (a) Hiroshima and (b) Nagasaki in 1945 (http://www.hiroshima-remembered.com/photos/effects/image7.html)

The biological effects from ionizing radiation are broadly divided into two categories: stochastic and deterministic. In the former, the effects are usually associated with exposures to low levels of radiation exposure over a long period of time and occur in a statistical manner. The probability of their occurrence increases with radiation dose as shown in Figure 1.2 (a). Hence the name “stochastic” which means pertaining to chance. The induction of cancer and genetic defects are two of the most familiar consequences attributed to stochastic effects. There is also no threshold level of radiation exposure below which we can say with absolute certainty that no cancer or genetic defect will occur and the probability of a cancer or genetic defect occurring doubles when the radiation dose doubles.

Deterministic effects are associated with much higher levels of radiation exposure received over a short period of time. There is a causal relationship between the dose and the effect. This means that the effects manifest early (and/or late) in the exposed individual as a result of high radiation doses received over a short time. Severity increases with the magnitude of the radiation dose as could be expected, and there is a threshold below which no effect is observed as shown in Figure 1.2 (b). The biological effects of radiation could be quantitatively described in terms of the dose-response relationship, that is, the incidence or severity of a given effect expressed as a function of the dose (Turner, J.E., 2004).

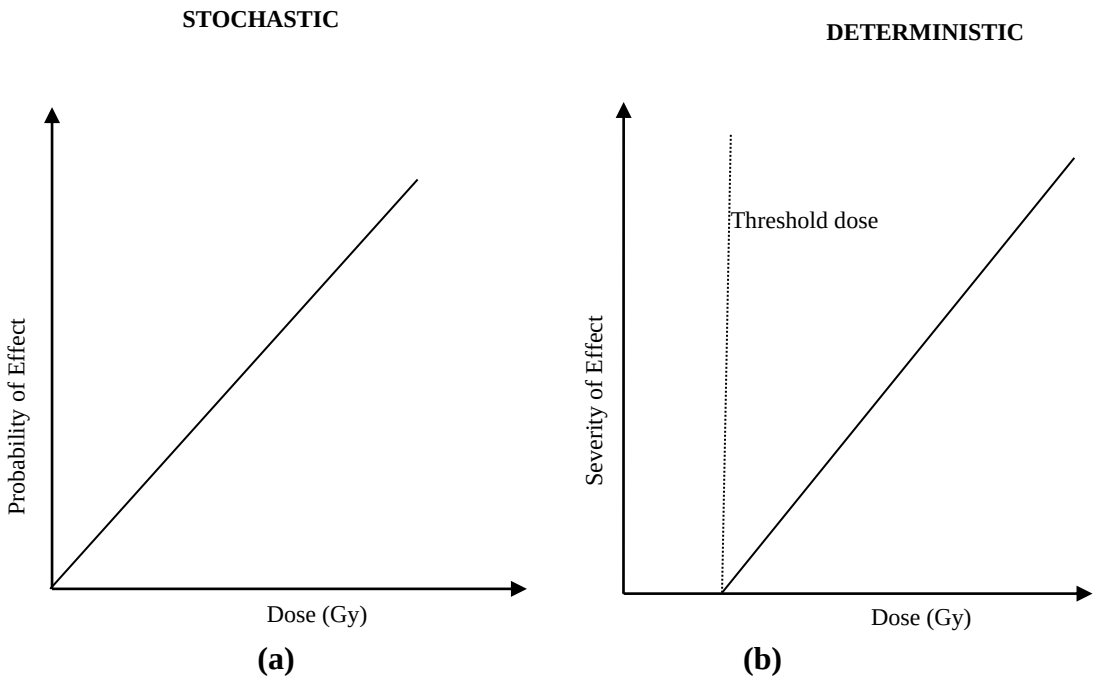

Figure 1.2: Differences between (a) stochastic and (b) deterministic effects of radiation. In (a), the probability of occurrence of a stochastic effect (e.g. cancer) increases with dose and there is no threshold dose. In (b), the severity of a deterministic effect (e.g. burns) increases with dose but there is a threshold dose.

There exists no evidence that directly demonstrates genetic damage to children of people exposed to radiation, although the potential effects of radiation based on animal studies was prominent in the 1950s and earlier. In the National Council on Radiation Protection and Measurement (NCRP) Report No. 116 the genetic risks were found to be smaller and cancer risks larger at that time. The United Nations Scientific Committee on the Effects of Atomic Radiation in its 2000 report states that, "No radiation-induced genetic (hereditary) diseases have so far been demonstrated in human populations exposed to ionizing radiation. However, ionizing radiation is a universal mutagen and experimental studies in plants and animals have clearly demonstrated that radiation can induce genetic effects; consequently, humans are unlikely to be an exception in this regard." (UNSCEAR, 2000)

The size of the radiation dose is expressed by specifying the amount of energy deposited by the incident radiation. The basic measure of radiation dose is called absorbed dose and this is equal to the amount of energy deposited in the body divided by the mass of the body volume irradiated. The unit of absorbed dose that is received by an organ or tissue is the Gray (Gy) and 1Gy = 1J/kg. One joule of energy is quite a small amount, but one gray is a considerable dose and this fact brings about the questioning aspect of radiation that even high radiation doses cannot be felt by the senses of humans when they are being irradiated. In the International Commission on Radiological Protection (ICRP) Publication 60, the ICRP introduced a new quantity named the *equivalent dose* ($H_{T,R}$) that is obtained from the absorbed dose ($D_{T,R}$) averaged over a tissue or organ T due to a radiation R, multiplied by a radiation weighting factor w_R that accounts for the different

biological effects of various radiation. The following equation shows how the quantities are related:

$$H_{T,R} = w_R \cdot D_{T,R} \tag{1.1}$$

Table 1.2 shows the values of the weighting factor w_R for different radiation. The unit for equivalent dose is sieverts (Sv) while the absorbed dose is expressed in grays. When there are different types of radiation and the total equivalent dose (H_T) is given by a sum over all radiation types:

$$H_T = \sum_R H_{T,R} = \sum_R w_R \cdot D_{T,R} \tag{1.2}$$

The effective dose is related to the absorbed dose, but it takes into account the different abilities of the different types of radiation to induce cellular damage, plus the sensitivities of the different types of tissues in the body.

A set of tissue weighting factors w_T are introduced to allow for the calculation of what is known as the *effective dose* (E):

$$E = \sum_T w_T \cdot H_T \tag{1.3}$$

Table 1.3 shows the values of the weighting factor w_T for different tissues. The effective dose, E, is an estimate of the overall effect of a given exposure to radiation. It should also

be emphasized that this estimation is intended only as guidance in approximating the potential effects of ionizing radiation (Knoll, 2000).

Table 1.2: Table of Radiation Weighting Factors for different types of radiation and their energy range (Knoll, 2000).

Radiation	**Energy Range**	**Radiation Weighting Factor, w_R**
X- and γ- rays	All energies	1
Electrons (e^-), positrons (p^+) and muons (μ^-)	All energies	1
Neutrons	< 10 keV	5
	10 keV to 100 keV	10
	> 100 keV to 2 MeV	20
	> 2 MeV to 20 MeV	10
	> 20 MeV	5
Protons, (other than recoil protons)	> 2 MeV	5
α particles, fission fragments, heavy nuclei		20

Table 1.3: Table of Tissue Weighting Factors for different types of tissues (UNSCEAR, 2000).

Tissue	**Tissue Weighting Factor, W_T**
Gonads	0.20
Red bone marrow	0.12
Colon	0.12
Lung	0.12
Stomach	0.12
Bladder	0.05
Breast	0.05
Liver	0.05
Esophagus	0.05
Thyroid	0.01
Bone surfaces	0.01
Remainder	0.05

1.4 Henties Bay – Walvis Bay Area

This project will be carried out in the Walvis Bay – Henties Bay coastal area which is located in the south – western part of the Republic of Namibia as shown in Figure 1.4. The coastal area is in the Erongo region (Figure 1.3) which is well known for its deep water harbour, tourism, uranium mines among other activities. This region is named after the Erongo Mountain, a well-known landmark in this area and in Namibia.

The Erongo region has it's shoreline with the Atlantic Ocean in the west and borders with the following regions in the north Kunene, the east Otjozondjupa , the south east Khomas and in the south Hardap region as shown in Figure 1.3. There are a number of important and historic towns in the region. These are Usakos, Arandis, Henties Bay, Swakopmund, Walvis Bay and Wlotzkasbaken as shown in Figure 1.4. All these towns are of interest in this project and more detailed information about the towns are provided below.

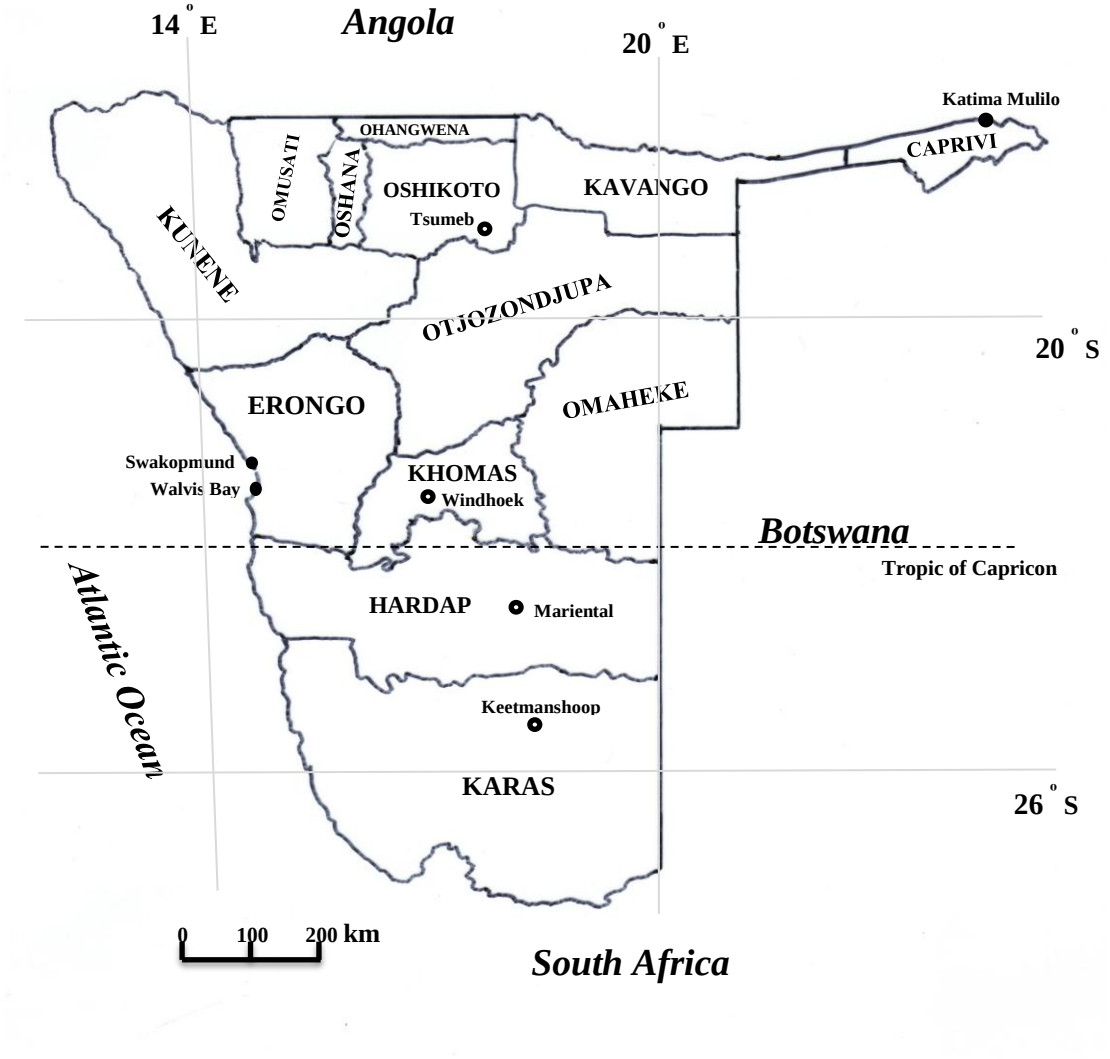

Figure 1.3: Map of Namibia showing its regions and some administrative towns including Walvis Bay.

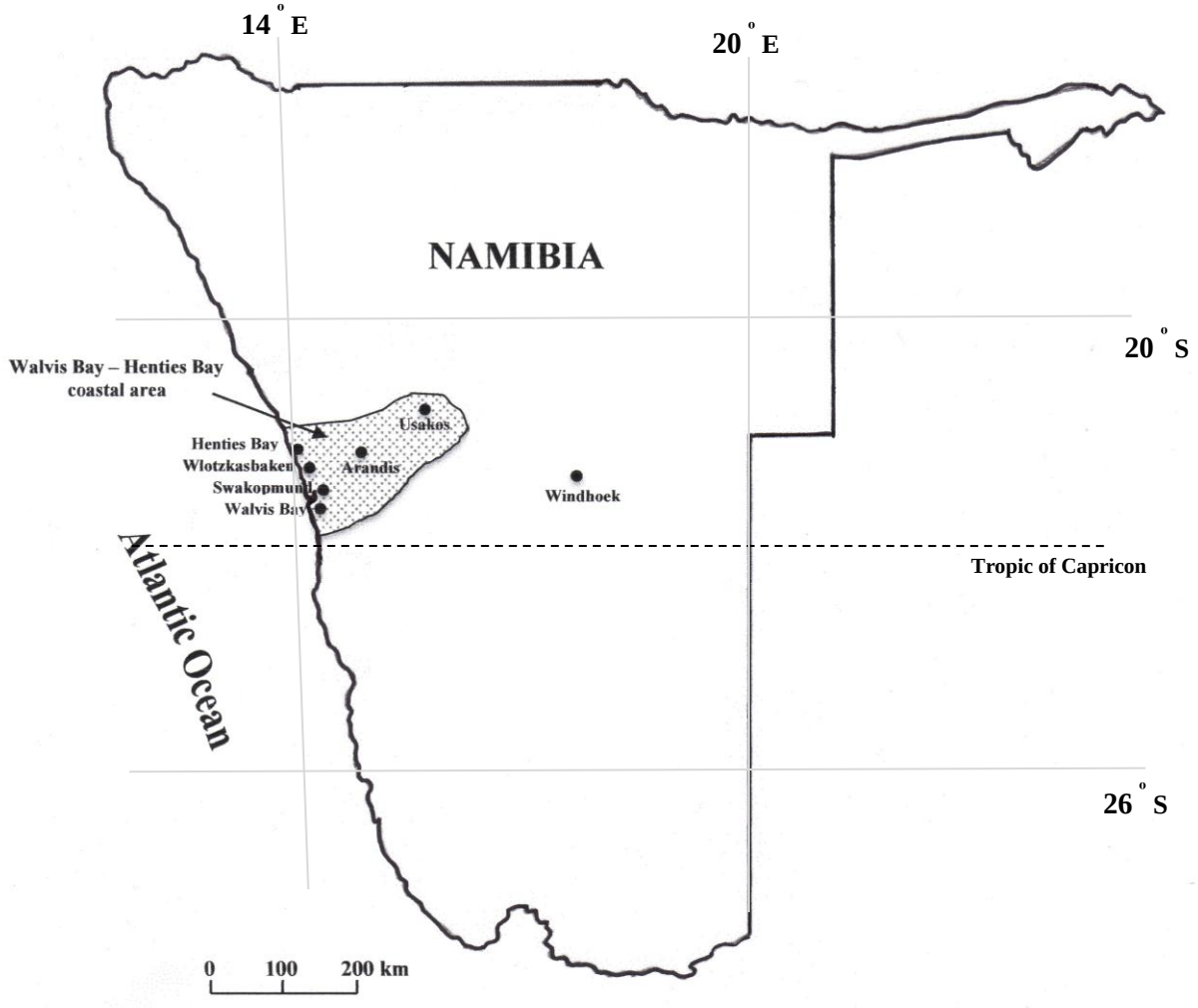

Figure 1.4: Map of Namibia showing the Walvis Bay –Henties Bay coastal area and the towns of interest in this study.

Usakos is a town located on the banks of the river Khan 140 kilometres north-east of Swakopmund. Its geographical coordinates are latitude 22° 0′ 0′′ South, and longitude 15° 36′ 0′′ East. The town's name derived from the Damara language means "grab the heel". The town has about 3,000 inhabitants and covers an area of 58 km^2. Founded in 1900 the town was a watering station for locomotives when railway construction workers from the Otavi Minen- und Eisenbahgesellschaft (Otavi Mining and Railway Company, OMEG) arrived there on their way from Swakopmund to Tsumeb. The town, much like many towns in the region, has rich German colonial architecture that can still be seen in the town. It is a tourism hub and many travellers both nationally and internationally pass the town on route to the coastal towns (Henckert, W., 2009).

The town of Arandis is at latitude 22° 25′00′′ S and longitude 14° 58′ 00′′ E. It is about 65 km north-east of Swakopmund and located about 14 km from the Rossing Uranium Mine, which has one of the largest open pit uranium mines in the world. The mine currently produces about 7.7% of the world's uranium. Arandis was first established in 1976 and it was developed by Rössing Uranium Limited to provide accommodation for its workers and their families. Rössing Uranium Limited managed Arandis from 1976 until 1992 when it was subsequently given to the Namibian Government as an Independence gift. In 1995 Arandis was proclaimed a fully-fledged town and it has approximately 7 000 residents. (Arandis Town Council, n.d)

Swakopmund is at latitude 22° 41′00′′ S and longitude 14° 32′ 00′′ E. The name of the town Swakopmund is German for "Mouth of the Swakop" as the town is situated at the

mouth of the Swakop River. It is a city on the coast of western Namibia, 280 km west of Windhoek, Namibia's capital. Founded 1892, Swakopmund is the capital of the Erongo region administrative district. The town has about 42 000 inhabitants and owns 193 km^2 of land. It is one of the most popular holiday and tourist destination. Many conferences and workshops by Government Ministries and institutions both locally and internationally take place in Swakopmund every year. Many people who work at Rössing Uranium Mine and Langer Heinrich Uranium Mine in the area live in Swakopmund (Namibia Travel Adviser, 1998).

The town of Walvis Bay is located at latitude 22° 57′ 22′′ S and longitude 14° 30′ 29′′ E. it is situated just north of the Tropic of Capricorn in the Kuiseb River delta and lies at the end of the TransNamib Railway to Windhoek. Its name in Afrikaans is “Walvisbaai”, while in German it is “Walfischbucht” or “Walfischbai”, all meaning "Whale Bay", which is the name of the bay on which it lies. The town has about 85 000 inhabitants and retains a total of 1 124 km^2 of land. It is one of the most common holiday and tourist destinations both locally and internationally. The Bay has long been a sanctuary for sea vessels because of its natural deep water harbour, protected by the Pelican Point sand spit. This natural harbour is the only one of its size along the country's coastline.

The Walvis Bay Export Processing Zone Management Company is an important aspect of the local economy as it is an entry and exit point for most import and exports from Namibia and other Southern African land locked countries in the Southern African Development Community (SADC) (Municipality of Walvis Bay, 2011).

The town of Henties Bay is located at latitude 22° 07′ 06′′ S and longitude 14° 16′ 57′′ E. It is located 70 km north of Swakopmund and is an important holiday town. Also, the seal colony of Cape Cross is situated 70 km to the north of the town. The name of the town in English is literally “Henty's Bay”, in Afrikaans, “Hentiesbaai” and in German, “Hentiesbucht”. It is a coastal town in the Erongo Region, of Namibia and it has about 3,300 inhabitants and owns 121 km^2 of land. It is also known for its excellent fishing opportunities. In fact, Henties Bay is one of the foremost angling destinations for many anglers flocking to the coast throughout the year. The town is nestled in between the Atlantic Ocean and the Namib Desert (Henties Bay Tourism Association, n.d). Henties Bay is home to the University of Namibia’s Dr. Sam Nujoma Marine & Coastal Resources Research Centre (SANUMARC). Many Scientists, both local and international, visit and work at the Centre.

Wlotzkasbaken is a settlement located at latitude 22° 25′ 00′′ S and longitude 14° 27′ 00′′ E. It is located 31 km north of Swakopmund on the road to Henties Bay. It is named after Mr. Paul Wlotzka for whom it was a halfway house on his regular trips by horse cart from Swakopmund to Henties Bay as well as the only remaining trigonometrical beacon of a survey of the Skeleton Coast during the 1930’s. Paul Wlotzka was also the first one to build a temporary shelter there it still mirrors these unique temporary houses each with its own water tank. Wlotzkasbaken has gained popularity as a fishing spot since 1936. Soon more temporary houses were set up.

The South West Africa (SWA) Administration in 1955 surveyed 24 erven, which were leased on a long term basis. In the years that followed the increasing development at the settlement forced the Peri-Urban Board to control Wlotzkasbaken. Hence, an advisory committee consisting of residents was formed to discuss matters pertaining to Wlotzkasbaken. After independence, under the Local Authorities Act, Act No. 23 of 1992, Wlotzkasbaken was a village. However, by Government Notice 22 of 1993 it became a settlement area in terms of the Act and was then, in terms of the provisions of the Act, under the jurisdiction of the Erongo Regional Council (Goosen L., 2009).

1.5 Local geology of study area

The onshore coastal geology of the Erongo region consists of old crystalline rocks that form the basement to the Permo-Triassic Karoo Sequence and young deposits of the Namib Dessert. The crystalline basement in the Erongo region is presented by rocks of the Abbabis Complex and the Nosib and Swakop Groups of the Damara Sequence that comprises mostly a thick pile of metasedimentary rocks as shown in Figure 1.5. Based on stratigraphy, structure and metamorphic grade, the Damara Orogen is subdivided into zones, that comprise of the Central Zone, the Northern Zone and the Southern Kaoko Zone.

The Nosib Group is predominantly siliciclastic and is subdivided into the lower Etusis and upper Khan Formation, which generally have an interfingering relationship. The Etusis Formation consists predominantly of pinkish to buff-coloured, medium- to coarse grained meta-arkoses and micaceous to feldspathic quartzites and paragneisses.

Conglomerate, mica schist, calc-silicate bearing quartzite and marble occur locally the Khan Formation is predominantly made up of massive to bedded, greyish-green calc-silicate rocks. Layers of meta-conglomerate also occur locally. A unit of interbedded amphibolite and biotite schist is present near the Rössing Dome (Schreiber, U.M., 1996).

The Swakop Group is subdivided into the Rössing, Chuos, Arandis, Karibib and Kuiseb Formations. A bluish-grey dolomitic marble, minor quartzite, metaconglomerates, schist, gneiss and calc-silicate rocks are evident in the Rössing Formation. Bulk of the Chuos Formation consists of dark-grey to greenish-grey diamictites. Subordinate interbedded quartzite and marble occur within pebble-bearing schists. The Arandis Formation contains schists, calc-silicate rocks and marbles. A marble-dominated Karibib Formation is widely distributed and underlies large parts of the flat, poorly exposed coastal region. Also, the study area is home to many uranium mines such as Rössing Uranium, Langer Heinrich Uranium, Reptile Uranium Mine, Tjrekkope, Uramin Inc. and Valencia Uranium Project (Coastal Zone Management Project (CZM), 1999).

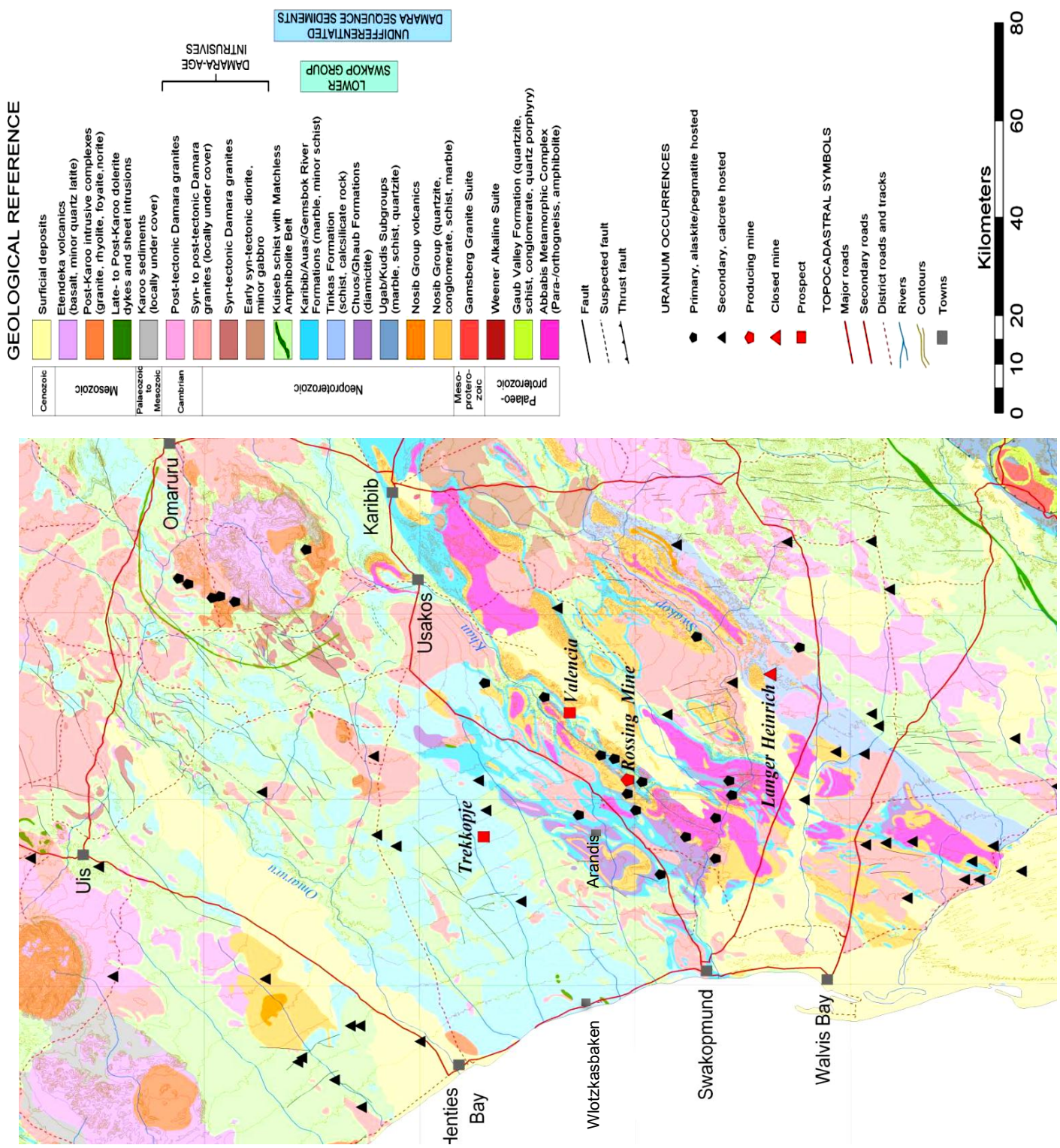

Figure 1.5: Map of the Central Damara Uranium Province showing the towns of interest and the location of some uranium mines. Adapted from (Schreiber U. , n.d).

1.6 Statement of the Problem

Namibia is a country having many mineral resources including uranium which is one of the naturally occurring radioisotopes or radionuclides. Uranium in particular is concentrated on the south-western coast or the Walvis Bay – Henties Bay coastal area of the country (Figure 1.4), and one of the world's largest open-pit uranium mines is in the area. Therefore, there may be significant low-level radiation arising from the naturally occurring radionuclides that are present in the soils of the areas. Such low-level radiation will result in a continuous exposure of the inhabitants of the area to low-level radiation. Some environmental groups have already raised awareness on the possible effect of higher levels of radiation due to uranium mining in the south-western coast. In contrast, mining companies have said that there are no significant negative environmental impacts associated with the mining activity (Rossing website: www.rossing-com.info and www.softchem.co.za/pdfs/Lhuim.).

Low-level radiation exposures have been measured in some regions of some countries such as Brazil and India and found to be surprisingly very significant (Brazilian Academy of Sciences, 1975). Efforts are being made to monitor this low-level radiation exposure in many countries. It is therefore desirable to know the distributions of radionuclides in the soils of Namibia especially in areas such as the south-western coast or the Walvis Bay – Henties Bay coastal region where uranium is found and to also know the low-level radiation due to the radionuclides. In fact, such determination or study is in tune with the efforts of the Government of Namibia to monitor different

hazardous radiations in the Country. This project aims to study the distribution of radionuclides and associated hazardous radiation in different towns in the Erongo region. It may be useful to mention that on February 18, 2009, the Government of Namibia, through the Ministry of Health and Social Services, inaugurated the Atomic Energy Board of Namibia which was established in fulfilment of Section 3(1) of the Atomic Energy and Radiation Protection Act, 2005 (Act No 5 of 2005). The key mandate of the board is to advise Government and relevant persons or entities on all matters relating to radiation sources and nuclear energy (Atomic Energy Board of Namibia, Annual Report 2009-2010, 2011). Section 33(1) of the Act No. 5 of 2005 establishes an independent National Radiation Protection Authority (NRPA). One of the functions of the Authority is to advise the Board on the extent of radiation exposure in Namibia and the exposure includes those of radiation workers, the public and the environment. The extent of radiation exposure to the public in Namibia is not well documented and there is therefore a need to determine the radioactivity levels in the environment as planned in this project. This research project is therefore very important and relevant to Namibia.

1.7 Objectives of the research project

The objectives of this research project is to:

1. Determine the concentrations and distributions of the naturally occurring radionuclides namely ^{238}U, ^{232}Th and ^{40}K in soil samples collected across different towns in the Walvis Bay – Henties Bay coastal area of Namibia.
2. Calculate the mean absorbed dose rate for each town in the area from the measured radionuclide concentrations.
3. Estimate the mean annual effective dose for each town in the coastal area and thereby obtain information on the degree of continuous exposure of people to ionizing radiation in each town.
4. Determine which town is having a normal background radiation and which town is having a high background radiation.

CHAPTER 2

2. LITERATURE REVIEW

2.1 Interaction of radiation with matter

Ionizing radiation interacts with matter in various ways. Most commonly known types of ionizing radiation are alpha rays, beta rays, gamma rays, X rays and neutron rays. In the case of alpha or beta particle, the interaction has a direct ionization effect. This is due to the fact that the particles are charged. However, in the case of gamma ray which is not charged, there are three processes by which the ionization (removal of an electron from an atom by a photon) can take place. These processes are Photoelectric absorption, Compton scattering and Pair production. The different radiations (alpha, beta and gamma) and their interactions with matter are discussed in the following sub-sections.

2.1.1 Alpha Radiation

The alpha (α) particle is basically a helium ($^4_2$He) nucleus that has two protons and two neutrons. It is the largest type of radiation and its interaction with matter is very strong because of its electrical charge of 2 units. As a result of the strong interaction, alpha particle has a short range and it can be stopped easily by a thin sheet of paper or the surface layer of the skin. Major energy loss mechanism for alpha particles is electronic excitation and ionization. Alpha particles basically do not pose any major radiological concern externally. However when it is ingested, it may cause harmful biological effects as it interacts strongly with the surrounding internal tissue. Almost all naturally occurring alpha emitters are heavy elements with atomic number $Z \geq 83$ (Turner J.E.,

p.61, 2007). An example of alpha decay is the decay of $^{226}_{88}$Ra with the emission of $^{4}_{2}$He (or alpha particle) as shown below.

$$^{226}_{88}\text{Ra} \rightarrow {}^{222}_{86}\text{Rn} + {}^{4}_{2}\text{He} \quad (2.1)$$

2.1.2 Beta Radiation

A nucleus that decays spontaneously by emitting an electron or a positron is said to undergo beta decay. There are three different types of beta decay: beta-minus (β^-), beta-plus (β^+) and electron capture. Beta (β) particles are charged particles that have a relatively light mass, like an electron (e^-) or a positron (e^+). Their interaction with matter is characterized as average and they have a longer range than alpha particles and can be stopped by a layer of clothing or by a few millimetres of aluminium. A beta-minus particle (β^-) is an electron. It comprises the transformation of a neutron into a proton ($^{1}_{1}\text{p} = {}^{1}_{1}\text{H}$), an electron and a third particle called an antineutrino (as shown in equation 2.2.1). It is the most common source of fast electrons in radiation measurements. In beta-plus (β^+) a proton decays with the emission a positron, the electrons antiparticle is emitted together with a neutrino. The basic process is shown in equation 2.2.2. The third type of beta decay is electron capture. There are a few nuclides for which β^+ emission is not energetically possible, but in which an orbital electron (usually in the K shell) can combine with a proton to form a neutron and a neutrino (equation 2.2.3). The neutron remains in the nucleus and the neutrino is emitted (Young, H.D and Freedman, R.A., 2006).

$$^{1}_{0}\text{n} \rightarrow {}^{1}_{1}p + \beta^- + \bar{\nu} \quad (2.2.1)$$

$$^{1}_{1}\text{p} \rightarrow {}^{1}_{0}n + \beta^+ + \nu \quad (2.2.2)$$

$$^{1}_{1}p + \beta^- \rightarrow \text{n} + \nu \quad (2.2.3)$$

where ${}_{0}^{1}n$ is a neutron, ${}_{1}^{1}p$ is a proton, ν is a neutrino and $\bar{\nu}$ is an antineutrino. The extremely small interaction probability with matter that neutrinos and antineutrinos have makes them undetectable for all practical purposes, thus only the fast electrons or the beta particle itself is the only significant ionizing radiation produced by beta decay. Each specific beta decay transition is characterized by a fixed decay energy that varies from decay to decay and can range from zero to the "beta endpoint energy", which is numerically equal to the Q-value. The difference in excitation energies will reflect in the beta spectrum if the transition involves an excited state of either the parent or the daughter nuclei. Figure 2.1 gives a representative beta energy spectrum that displays the resulting beta particle energy distribution.

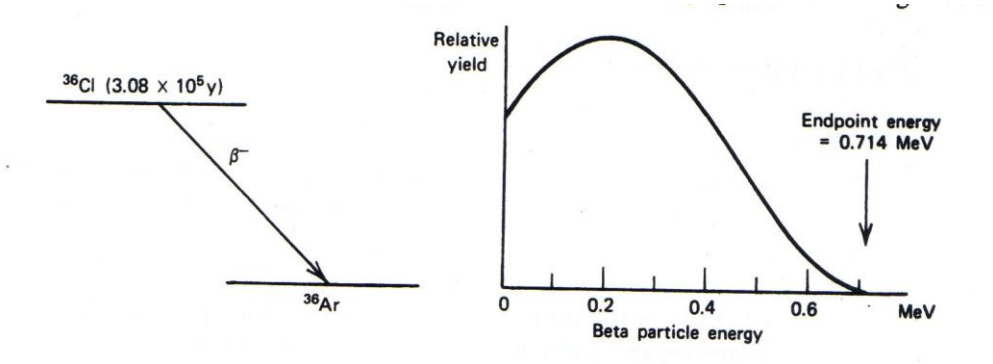

Figure 2.1: The decay scheme of ^{36}Cl and the resulting beta particle energy distribution (Knoll, 2000).

Table 2.1: Some "Pure" electron sources (Knoll, 2000).

Nuclide	Half-Life	Endpoint Energy (MeV)
^{3}H	12.26 y	0.0186
^{14}C	5730 y	0.156
^{32}P	14.28 d	1.710
^{33}P	24.4 d	0.248
^{35}S	87.9 d	0.167
^{36}Cl	3.08×10^5 y	0.714
^{45}Ca	165 d	0.252
^{63}Ni	92 y	0.067
^{90}Sr/^{90}Y	27.7 y / 64 h	0.546/2.27
^{99}Tc	2.12×10^5 y	0.292
^{147}Pm	2.62 y	0.224
^{204}Tl	3.81 y	0.766

Table data from Lederer and Shirley (Knoll, 2000)

2.1.3 Gamma Radiation

Gamma rays are produced as a result of energy state transformations of the atomic nucleus. They are electromagnetic radiations with very short wavelengths and thus have very high penetrative power. Gamma rays are part of the electromagnetic spectrum and comprise the part of the spectrum with energy, E > 40 keV, whereas electromagnetic radiation with E < 40 keV are denoted as X-rays. They travel at the speed of light c, have a discrete energy, E, wavelength, λ and frequency, f. The energy E, is related to the frequency and wavelength according to the expression,

$$E = hf = \frac{hc}{\lambda} \tag{2.3}$$

where, h is the Planck's constant (h = 6.6261 × 10^{-34} J·s) and c is the speed of light.

The interaction of gamma rays with matter is through three principal processes, namely Photoelectric absorption, Compton scattering and Pair production. These processes are described further in the following sub-sections.

2.1.4 Photoelectric absorption

An incident photon cannot be totally absorbed by a free electron, from considerations of the conservation of momentum. If the electron is initially bound to the atom total absorption can take place and by the recoil of the atom momentum is conserved. The most tightly bound electrons have the most likely probability of absorbing an incident photon (Krane, 1988 and Damon, 2005). The entire atom is involved in the process of

the interaction with the incident photon. It may therefore be perceived as the interaction of the primary photon with the electron cloud of the atom as illustrated in Figure 2.2.

The emitted electron or photoelectron will have a kinetic energy which is equal to the difference in the energy of the photon and the binding energy of the electron (which is energy binding the electron to the atom). That is,

$$K.E = h\nu - B.E \tag{2.4}$$

where K.E is the kinetic energy of the emitted electron, hν is the energy of the photon and B.E is binding energy of the ejected electron. The ejected electron is usually from the K- or L- shell of the atom.

The photoelectric process is the predominant mode of interaction for gamma-rays of relatively low energies and is enhanced for materials of high atomic number, Z. There is no single analytic expression that is valid for the probability, σ, of photoelectric absorption per atom over all ranges of hν and Z, but a first order approximation is

$$\sigma \propto \frac{Z^n}{h\nu^{3.5}} \tag{2.5}$$

where the exponent *n* varies between 4 and 5 over the energy region of interest. The use of materials with high atomic numbers Z (such as lead) as gamma-ray shielding and in detectors is due to this severe dependence of the photoelectric absorption probability on the atomic number of the absorber material (Damon, 2005 and Knoll, 2000).

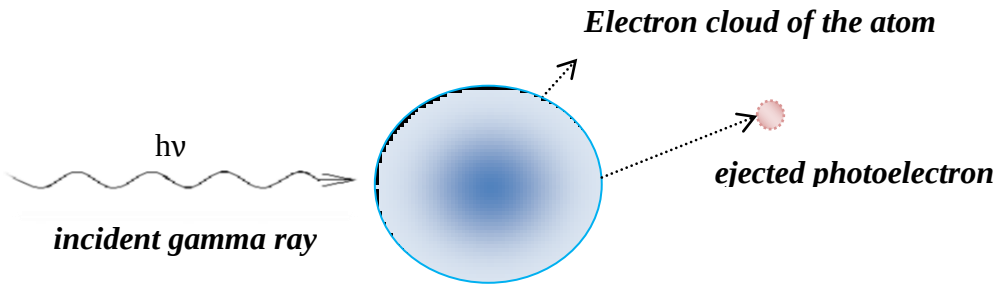

Figure 2.2: Illustration of an atom ejecting a photoelectron.

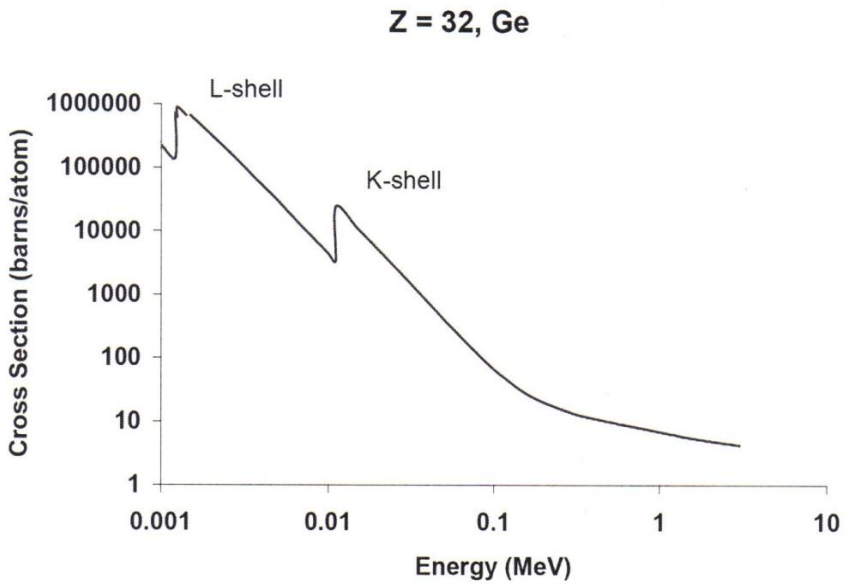

Figure 2.3: The Photoelectric absorption cross-section for germanium (Ge) (Damon, 2005).

The photoelectric absorption cross-section for a common gamma-ray detector material, germanium (Ge), is shown in Figure 2.3. In the low-energy region, discontinuities in the curve or "absorption edges" appear at gamma-ray energies that correspond to the binding energies of electrons in the various shells of the absorber atom. The edge lying highest in energy therefore corresponds to the binding energy of the K-shell electron. For gamma-ray energies slightly above the edge, the photon energy is just sufficient to undergo a photoelectric interaction in which a K-electron is ejected from the atom. For gamma-ray energies slightly below the edge, this process is no longer energetically possible and therefore the interaction probability drops sharply. Similar absorption edges occur at lower energies for the L, M, N electron shells of the atom (Knoll, 2000).

Photoelectric absorption is therefore an ideal process if one is interested in measuring the energy of the original gamma-ray. The total electron kinetic energy equals the incident gamma-ray energy and will always be the same if monoenergetic gamma-ray are involved. Under this conditions, the differential distribution of electron kinetic energy for a series of photoelectric absorption events would be a simple delta function (i.e a function that has an even distribution about a fixed reference point) as shown in Figure 2.4. The single peak appears at a total electron energy corresponding to the energy of the incident gamma-rays (Knoll, 2000).

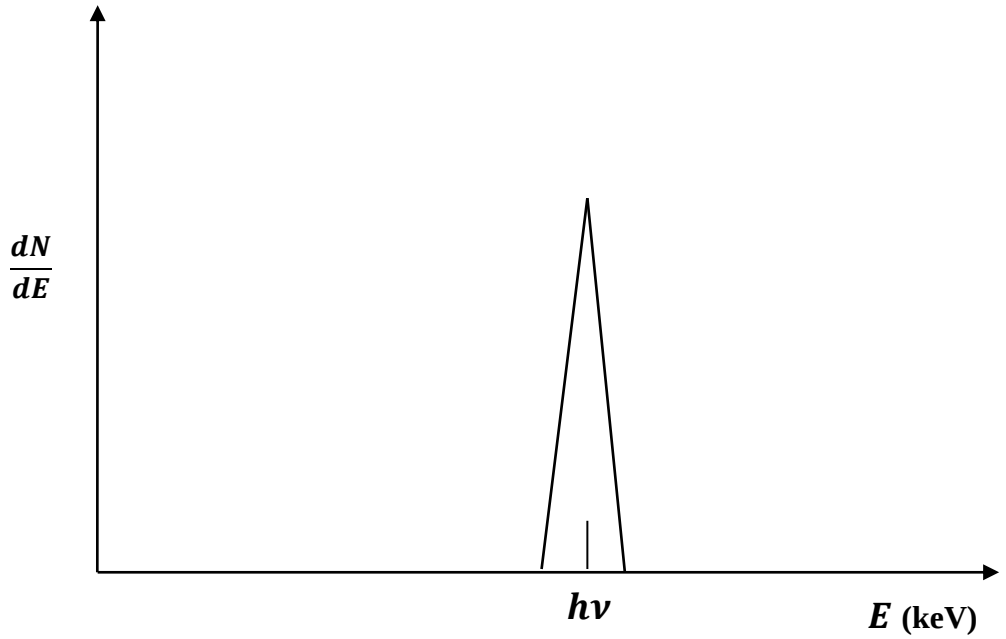

Figure 2.4: Photoelectric absorption energy peak corresponding to the energy of the incident gamma-ray (Knoll, 2000).

2.1.5 Compton scattering

In Compton scattering, the photon interacts with an atomic electron in such a way that it (the photon) is not completely absorbed but scattered into a different direction so that it has a reduced energy. That is, the photon transfers a portion of its energy to the electron (Patel, 1991 and Knoll, 2000). As shown in Figure 2.5, if the photon is scattered through an angle θ, then the energy of the scattered photon, $h\nu'$, is related to its initial or incident energy hν by the expression

$$h\nu' = \frac{h\nu}{\left(1+\frac{h\nu}{m_0 c^2}(1-\cos\theta)\right)} \tag{2.6}$$

where $m_o c^2$ is the rest-mass energy of the electron or 0.511 MeV. For small scattering angle θ, very little energy is transferred. Some of the original energy is always retained by the incident photon, even in the extreme case of $\theta = \pi$. Two extreme cases can be identified:

1. A grazing angle scattering, or one in which $\theta \cong 0$. In this case, equation (2.6) predicts that $h\nu' \cong h\nu$. The recoil Compton electron has very little energy and the scattered gamma-ray has nearly the same energy as the incident gamma-ray.
2. An head-on collision in which $\theta = \pi$. The incident gamma-ray, in this extreme, is backscattered toward its original direction, whereas the electron recoils along the direction of incidence. This extreme presents the maximum energy that can be transferred to an electron in a single Compton interaction.

The probability of Compton scattering per atom of the absorber depends on the number of electrons available as scattering targets and therefore increases linearly with the atomic number, Z. The dependence on gamma-ray energy generally falls off gradually with increasing energy.

The angular distribution of scattered gamma-rays is predicted by the Klein-Nishinda formula for the differential scattering cross-section $\frac{d\sigma}{d\Omega}$:

$$\frac{d\sigma}{d\Omega} = Zr_0^2 \left(\frac{1}{1+\alpha(1-\cos\theta)}\right)^2 \left(\frac{1+cos^2\theta}{2}\right) \cdot \left(1 + \frac{\alpha^2(1-\cos\theta)^2}{(1+cos^2\theta)[1+\alpha(1-\cos\theta)]}\right) \quad (2.7)$$

where $\alpha \equiv \frac{h\nu}{m_o c^2}$ and $r_0 = \frac{e^2}{4\pi\,\varepsilon_0 mc^2}$ is the classical radius of the electron . This distribution shows a strong tendency for forward scattering at high gamma-ray energies (Knoll, 2000).

2.1.6 Pair Production

When the energy of the photon is very large or larger than 1.02 MeV, its absorption can result in the creation of a positron and an electron (Burcham & Jobes, 1995 and Hodgson et al., 1997). The total energy of the positron-electron pair is equal to that of the photon. It should be mentioned that a positron is a positively charged electron. The probability of this process occurring remains zero until the gamma-ray energies equals or exceeds twice the rest mass energy of an electron, $h\nu \geq 2m_0c^2$. The gamma-ray in this process is replaced by an electron-positron pair. The excess energy that remains after pair production takes place goes into kinetic energy shared by the positron E_{e^+} and electron E_{e^-}. This gives the energy balance;

$$h\nu = E_{e^+} + E_{e^-} + 2m_0c^2, \tag{2.5}$$

where E_{e^+} and E_{e^-} are the kinetic energies of the positron and electron respectively (Krane, 1988). Because the positron will subsequently annihilate after slowing down in the absorbing medium, two annihilation photons of energy 511 keV each are normally produced as secondary products of the interaction as shown in Figure (2.6).

The crystal can either absorb the photons or they can escape from the medium. The so-called "*escape peaks*" that can be observed in the gamma-ray spectrum is evidence of this.

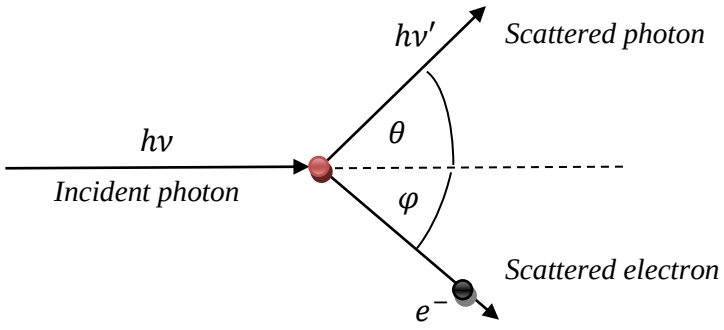

Figure 2.5: Compton scattering process

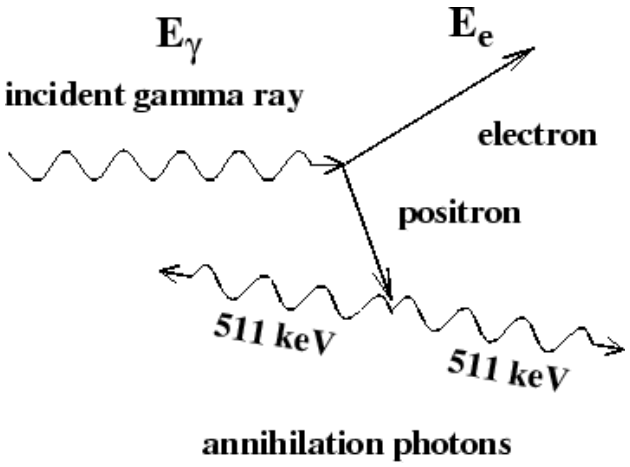

Figure 2.6: Pair production and annihilation processes (Damon, 2005).

If one of the 511 keV photons escapes the detector crystal, then a "*single escape peak*" could be observed at $(h\nu - m_0c^2)$ and if both photons escape then a "*double escape peak*" is observed at $(h\nu - 2m_0c^2)$ (Damon, 2005). The electrons or charged particles produced in the above processes can further produce ionization. Furthermore, the electrons produced can be easily detected and this is the basis for many radiation detectors.

The probability that a photon will interact with matter, expressed by the cross-section δ (m^2), depends on the photon energy, E, and the composition of the matter. Gamma rays of natural terrestrial origin (with E up to 2615 keV) and for matter comprising of rock, water and air, Compton scattering is the dominant interaction process. The γ ray photons typically lose energy through successive Compton scattering events until eventually the resulting low-energy photons are absorbed through the photoelectric effect, as shown in Figure 2.7. The intensity of γ rays interacting with matter decreases with the distance of the source from the detector (IAEA, TECDOC-1363, 2003).

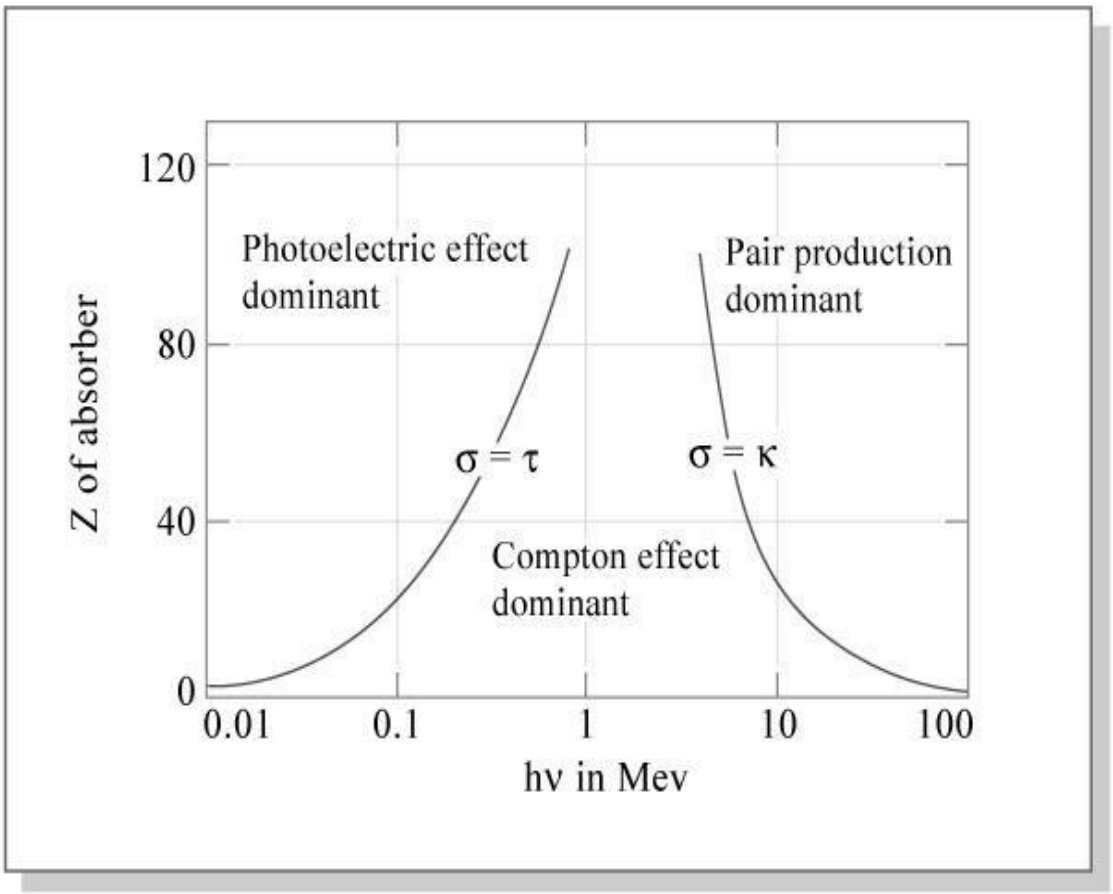

Figure 2.7: Interaction processes of gamma rays with matter.

2.2 Radiation detection and measurement

The basic principles of operation of most detectors are used for nuclear radiation detection and measurement and they follow the same characteristics. Basically, radiation enters the detector and interacts with the atoms of the detector material losing part or all of its energy, whereby it releases a large number of fairly low-energy electrons from their atomic orbits. These electrons are then collected and moulded into a voltage or current pulse for analysis by the electronic components of the detector.

The type of radiation and information about it depends on the type of material used for the radiation detector. To measure the energy of the radiation, a detector should carefully chosen such that the output pulse amplitude is proportional to the energy of the radiation. Here, a material in which the number of electrons released is large should be chosen, so that if statistical fluctuations are experienced or a few electrons are not counted, it does not substantially affect its ability to determine the energy (Krane, 1988). In this study, the approach to be taken is to detect gamma rays being emitted by the naturally occurring radionuclides (^{238}U, ^{232}Th and ^{40}K) in the soil, classify them according to their energies and then calculating the activities of the radionuclides in Becquerel.

As could be expected, there are different types of detectors for detecting ionizing radiations (Knoll, 2000). Some of these detectors will be discussed in the following sub-sections.

2.2.1 Earlier detectors: Cloud Chambers and Bubble chambers

The Cloud Chamber , also commonly known as the Wilson chamber (named after C.R.T Wilson a Scottish physicist who invented it in 1911) was one of the earlier detectors of ionizing radiation. The ions produced as an ionising particle passes through clean air that is saturated with water or alcohol vapour, acts as centres of condensation upon which tiny drops of water or alcohol are formed. These drops formed all along the particle's path so a visible track appears in the air. The tracks formed by α-rays are thick and straight; those formed by β-rays are thin and curved. γ-rays eject electrons from air molecules which in turn produce a tangle of β-ray tracks (figure 2.8 (a)). (Pfeffer, J.I., & Nir, S., 2000)

The Bubble Chamber, developed in 1952 by Donald A Glaser, operates almost similar to the cloud chamber. The detector is made from a vessel that is filled with a transparent fluid, typically liquid hydrogen, is under a pressure and a temperature (superheated) for which it is on the liquid gas boundary. An ionizing particle passing through the superheated liquid generates ions which initiates a string of bubbles along its path. These tiny bubbles appear as a visible track in the liquid, which can then be photographed and analysed (Pfeffer & Nir, 2000). An image from 1960 (Figure 2.8 (b)) is of real particle tracks formed in CERN's first liquid hydrogen bubble chamber. Negatively charged pions with an energy of 16 GeV enter from the left. One of them interacts with a proton

in the liquid hydrogen and creates sprays of new particles, including a neutral particle (a lambda) that decays to produce the "V" of two charged particle tracks at the centre. Lower-energy charged particles produced in the interactions spiral in the magnetic field of the chamber (The European Organization for Nuclear Research (CERN), 1970).

(a)

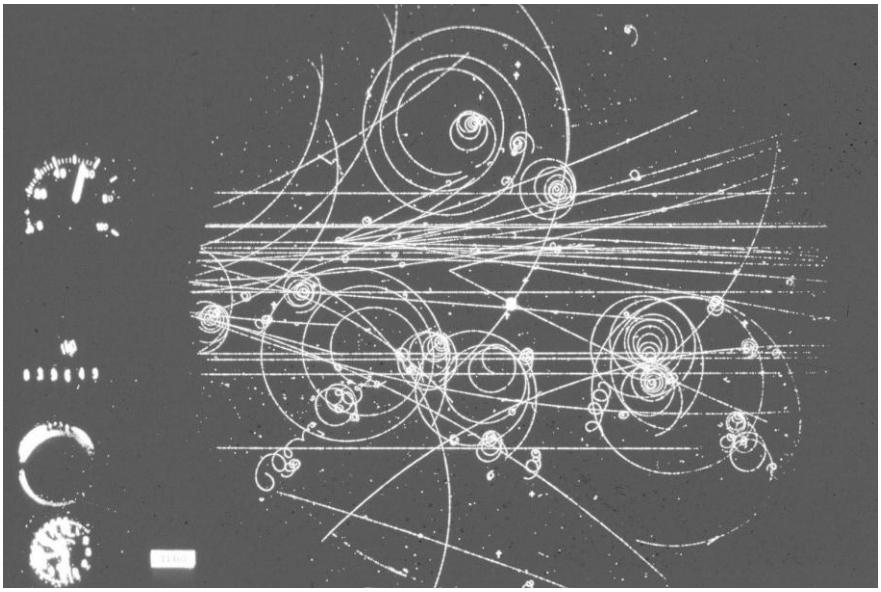

(b)

Figure 2.8: (a) The α, β and γ particle tracks in a cloud chamber (Coffey, J., 2010) and (b) Pion decay tracks in a bubble chamber photographed at CERN in 1960 (CERN,1970).

2.2.2 Geiger Muller counters

A Geiger-Muller counter (GM counter) consists of a gas-filled tube equipped with a metal cylinder (the cathode) and a thin conductive wire (the anode) mounted along the tube axis. Normally argon, with an admixture of halogen vapour, is used as gas filling. GM counters are 2 to 30 cm long and 1 to 4 cm in diameter, and they operate with applied voltage of several hundred volts. GM counters make use of the progressive growth of ionization in a strong electric field between the anode and the cathode. An incident photon interacts with the cathode and releases an electron that may be directed into the GM tube. The growth of ionization between the anode and the cathode amplifies the signal and generates an electric current between the electrodes. This results in a voltage pulse at the anode output of the GM counter. The multiplication coefficient of the gas ionizing chain reaction is of the order of 10^6, and the output pulse is not proportional to the absorbed gamma ray energy. The detection efficiency of GM counters is very low (less than 2%) and the dead time is of the order 10^{-4} s (IAEA, TECDOC-1363, pg.12, 2003).

2.2.3 Scintillation counters

When radiation enters and loses energy in a luminescent material (called a scintillator or phosphor), it causes electronic transitions to excited states in the material. These excited states decay by emitting photons (light) which can be observed and which provide quantitative information on the radiation. Usually, the photon or light emitted is fed into a photomultiplier tube. Here, a photosensitive cathode converts a fraction of the photons into photoelectrons, which are then accelerated through an electric field toward another

electrode, called a dynode. On striking the dynode, each electron ejects a number of secondary electrons, giving rise to electron multiplication. These secondary electrons are similarly accelerated through a number of additional dynode stages (e.g. 10), achieving electron multiplication in the range $10^7 – 10^{10}$. An electrical signal is finally produced which is proportional to the light output which in turn is proportional to the energy loss that produced the scintillation.

A good scintillator should efficiently convert the energy deposited by a charged particle or photon into detectable light. The alkali halides such as sodium iodide are good scintillators. Scintillator detectors usually have poor energy resolutions.

2.2.4 Semi- conductor detectors

The usefulness of semiconductors for radiation measurements stems from the special properties created at a junction where n and p type semiconductors are brought into good thermodynamic contact usually called an n-p junction. In semiconductor diode detectors, electron-hole pairs are created within the depleted region of the semiconductor material when an ionizing radiation is incident on or passes through them. These electron-hole pairs are swept out of the region by an electric field and their motions constitute a basic electrical signal which provides information on the incident radiation. The high-purity germanium detector (HPGe) is a good example of a semiconductor detector.

2.2.5 HPGe detectors

Germanium detectors are semiconductor diodes having a p-i-n structure in which the instrinsic region is sensitive to ionizing radiation, particularly X-rays and gamma-rays. Under reverse bias, an electric field extends across the intrinsic or depleted region. When photons interact with the material within the depleted volume of a detector, charge carriers (hole and electrons) are produced and are swept by the electric field to the P and N electrodes. This charge, which is in proportion to the energy deposited in the detector by the incoming photon, is converted into a voltage pulse by an integral charge sensitive preamplifier.

Because germanium has relatively low band gap, these detectors must be cooled in order to reduce the thermal generation of charge carriers (thus reverse leakage current) to an acceptable level. Otherwise, leakage current induced noise destroys the energy resolution of the detector. Liquid nitrogen, which has a temperature of -196.15 $^{\circ}$C, is the common cooling medium for such detectors. The detector is mounted in a vacuum chamber which is attached to or inserted into a LN_2 dewar. The sensitive detector surfaces are thus protected from moisture and condensable contaminants.The energy resolution of these detectors is very high, but because of their small volume, their sensitivity is low and it may take several minutes to record a spectrum. Arrangement of p-type and n-type semiconductor detectors is shown in Figures 2.9 (a) and (b).

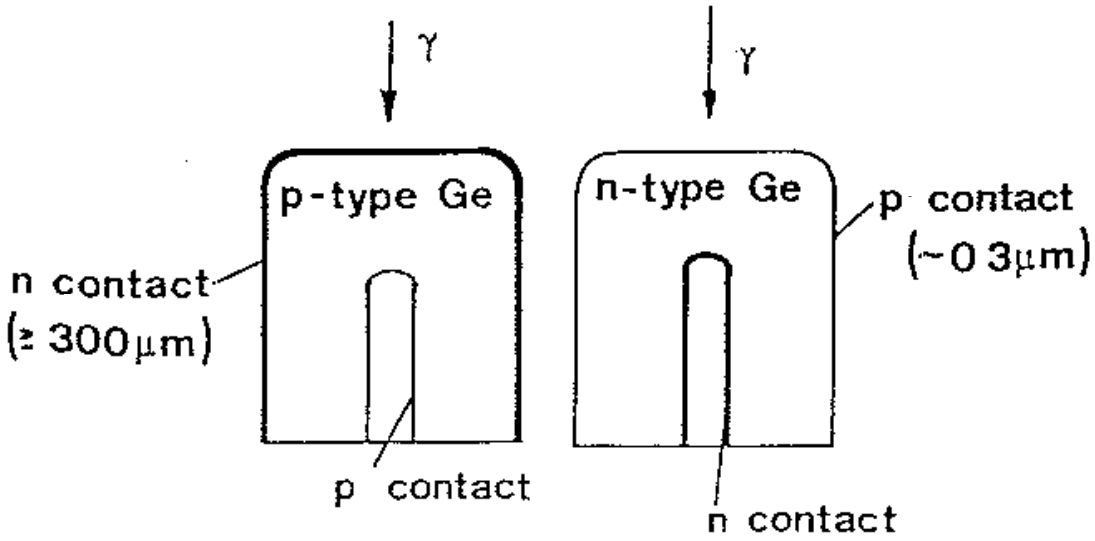

(a)

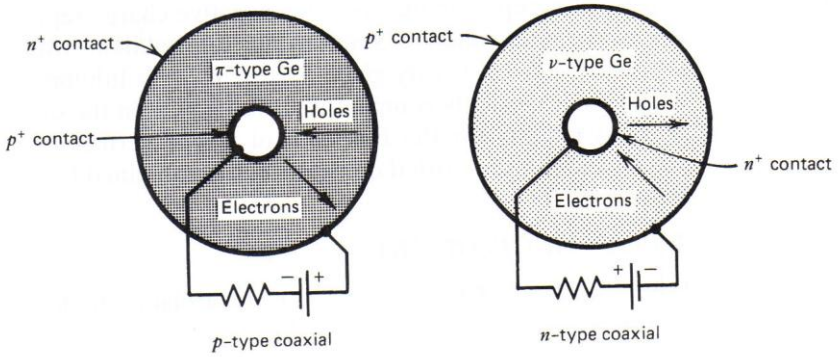

(b)

Figure 2.9: (a) Configuration of closed end coaxial n-type and p-type semiconductor detectors (ICRU Report 53, 1994, p.5) and (b) Cross sections perpendicular to the cylindrical axis of the high-purity germanium p or n type crystal and corresponding electrode configuration for each type. (Knoll, 2000, p.409).

CHAPTER 3

3. REVIEW OF STUDIES ON NATURAL RADIOACTIVITY

3.1 Measurements of concentrations

Radionuclides such as ^{238}U, ^{232}Th and ^{40}K are present in various degrees in soils. The radionuclides emit radiations and contribute significantly to natural background radiation as discussed in Section 1.2. Since it is not desirable for human beings to live in high background radiation areas (mean annual effective dose equivalent greater than 1 mSv) as discussed in Section 1.2, there have been many studies to determine the concentrations of primordial radionuclides in soils and the levels of the associated radiation in different parts of the world.

The distribution of natural radionuclides in the soils of Kaiga in the south west coast of India was studied by a group of scientists and the results published in 2001 (Karunakara, N., Somashekarappa, H. M., Avadhani, D. N., Mahesh, H. M., Narayana, Y. and Siddappa, K., 2001). Gamma-ray spectroscopy was employed in the study and an HPGe detector was used to detect the gamma rays. The activity of ^{226}Ra was found to have a mean value of 31.3 Bq kg^{-1} while that of ^{232}Th was 27.5 Bq kg^{-1} and that of ^{40}K was 159.9 Bq kg^{-1}. These concentrations should not cause any health problem. It was also reported that the contributions of ^{238}U, ^{232}Th and ^{40}K to the total gamma absorbed dose rate were 39.9%, 40.7 % and 16.0% respectively.

A similar study of the activity concentrations of naturally occurring radionuclides in soils was carried out in the Punjab province of Pakistan, a neighbour of India (Tahir, S. N. A., Jamil, K., Zaidi, J. H., Arif, M., Ahmed, N. and Ahmad, S. A., 2005). A p-type coaxial HPGe-based gamma ray spectrometer was used in the study. The mean concentrations for ^{232}Th, ^{226}Ra and ^{40}K were found to be 41 $\pm$ 8 Bq kg^{-1}, 35 $\pm$ 7 Bq kg^{-1} and 615 $\pm$ 143 Bq kg^{-1} respectively. These values are higher than those of Kaiga, India discussed above. The total annual external gamma radiation dose was 0.38 m Sv which is a low value (dose equivalent less than 1 mSv y^{-1}) implying that there is no potential health hazard associated with the soils.

Far away in the South Pacific, some scientists have also studied the distribution or radionuclides in soils of Southern and Western coasts of Viti Levu, in the Fiji Islands (Garimella and Prasad, 2002). Gamma spectrometry was employed in the study but a NaI(Tl) detector was used to detect the radiation. The average activities of ^{232}Th, ^{238}U and ^{40}K in soils of the region were 2.8 Bq kg^{-1}, 3.6 Bq kg^{-1} and 160 Bq kg^{-1} respectively. The corresponding average absorbed dose rate was estimated to be 10.3 nGy h^{-1}. These values (concentrations and dose) are not very high compared to the world average value of 59 nGy h^{-1} reported for normal background areas (UNSCEAR, 2008).

Closer home, the natural radioactivity in the soil samples of the University of Namibia, Windhoek, have been studied (Oyedele, J.A., 2005). The concentrations were measured using a sensitive γ-ray spectroscopic system consisting of an HPGe detector and associated equipment. ^{40}K was found to have the highest specific concentration varying

between 306.8 ± 15.2 Bq kg^{-1} and 720.8 ± 28.4 Bq kg^{-1} with a mean value of 444.7 ± 101.8 Bq kg^{-1} while, the concentration of ^{232}Th varied between 17.5 ± 2.3 Bq kg^{-1} and 38.1 ± 3.3 Bq kg^{-1} with a mean value of 28.5 ± 4.7 Bq kg^{-1} and the concentration of ^{238}U varied between 14.7 ± 1.5 Bq kg^{-1} and 29.7 ± 2.0 Bq kg^{-1} with a mean value of 20.4 ± 4.0 Bq kg^{-1}. The corresponding annual effective dose obtained from the radionuclides is 0.06 ± 0.01 mSv. These values (concentrations and dose) are not very high and lower than those of the Punjab province of Pakistan. The University of Namibia is therefore in an area of low or normal background radiation.

At the international high-energy stereoscopic system (HESS) project in Namibia, concentrations of the natural radionuclides ^{40}K, ^{238}U, and ^{232}Th in soil samples have been determined using an HPGe detector. They were found to vary from 10.8 ± 1.4 to 26.4 ± 1.8 Bq kg^{-1} for ^{238}U, for ^{232}Th the values varied from 12.8 ± 2.4 – 52.3 ± 3.7 Bq kg^{-1} and from 212.1 ± 12.1– 683.8 ± 27.1 Bq kg^{-1} for ^{40}K. The corresponding annual effective dose is 0.06 ± 0.01 mSv, which is less than the limit of 1.0 mSv recommended for the public by the ICRP (Oyedele, J.A., 2006). The radioactivity in the four major towns in northern Namibia have also been studied (Oyedele, J.A., Sitoka, S., Davids, I., 2008), using gamma-ray spectrometry with the objective of providing baseline data on the radiation level in the region. The average concentrations of radionuclides in the towns vary from 7.5 ± 2.3 to 14.2 ± 3.3 Bq kg^{-1} for ^{238}U, 5.8 ± 2.6 to 24.9 ± 6.1 Bq kg^{-1} for ^{232}Th and 52.1 ± 28.7 to 380.1 ± 112.9 Bq kg^{-1} for ^{40}K. These concentrations were used to calculate the mean absorbed dose rate and the mean annual effective dose in the

region. The low value of 21 ± 16 μSv obtained for the mean annual effective dose indicates that the region has normal background radiation.

The concentrations of primordial radionuclides in soil samples were also carried out in Botswana (Murtya,V.R.K., Karunakara, N., 2008). These measurements were made by gamma spectrometry employing a HPGe detector. The activity of ^{226}Ra was found to vary in the range 6.1 – 97.4 Bq kg^{-1} with a mean value of 34.8 Bq kg^{-1},while for ^{232}Th the values were in the range 7.4 – 110.0 Bq kg^{-1} with a mean value of 41.8 Bq kg^{-1} and ^{40}K varied between 33.5 Bq kg^{-1} and 1085.7 Bq kg^{-1} with a mean value of 432.7 Bq kg^{-1} in surface soils. The mean value of the annual effective dose was 0.07 mSv which is less than the recommended limit of 1.0 mSv.

Studies on the radionuclide distribution and the radiation level of the primordial radionuclides ^{238}U, ^{232}Th and ^{40}K in the soils of the coastal areas of Southern Nigeria have also been carried out. Soil samples were analysed for the radioactivity concentrations of these naturally occurring radionuclides using an HPGe detector. The mean activity of the radionuclides were found to be 283.28, 34.54 and 9.17 kBq kg^{-1} for ^{40}K, ^{226}Ra (a daughter of ^{238}U) and ^{232}Th. The mean absorbed dose rate in air due to these NORM was found to be 33.655 ± 3.409 nGy h^{-1}, which is far less than the world average value of 59 nGy h^{-1} reported for normal background areas (UNSCEAR, 2008).

3.2 Areas of high background radiation

In studies done worldwide (to determine the natural background levels) it has been found that there exist areas in some parts of the world that have very high background radiation levels. The elevated levels of radiation in these areas have been attributed to the geology and geochemical structure of the soil (e.g monazite soil) and in some cases to the radioactive content of hot springs that are flowing into the areas (UNSCEAR, 2000).

A pre-operational survey done at Kalpakkam coast in India indicated elevated gamma background radiation levels in the range of 100 – 400 nGy h^{-1} over the large tracts of the coastal sands due to the presence of pockets of monazite mineral in the beach sands. Gamma spectrometry was employed in the study and an HPGe detector was used to detect the gamma rays. The concentrations of ^{238}U, ^{232}Th and ^{40}K in soil samples were 5 - 71, 15 - 776 and 200 - 854 Bq kg^{-1}, respectively. Also, the total absorbed dose rate in air due to the presence of these primordial radionuclides in the soil samples of Kalpakkam varied between 24 and 556 nGy h^{-1} with a mean of 103 nGy h^{-1} (Kannan, V., Rajan, M.P., Ramesh, R., 2002). These values are clearly higher than the worldwide range of 28 – 120 nGy h^{-1} and the average value of 59 nGy h^{-1} reported for normal background areas (UNSCEAR, 2008).

On the south eastern coast of India at the Chhatrapur beach placer deposit of Orissa state, high natural background radiation levels is reported for the area. This is due to the presence of radiogenic heavy minerals. The average activity concentrations of radioactive elements ^{232}Th, ^{238}U and ^{40}K in bulk sand samples were measured by

gamma-ray spectrometry (using a HPGe detector) and found to be 2500 ± 1850, 230 ± 140 and 120 ± 35 Bq kg^{-1} respectively. The absorbed gamma dose rates in air due to the naturally occurring radionuclides varied from 375 to 5000 nGy h^{-1}, with an average value of 1625 ± 1200 nGy h^{-1}. The external effective dose rate of the region ranged from 0.46 to 6.12 mSv y^{-1} with an average value of 2.0 ± 1.5 mSv y^{-1}. The absorbed gamma dose rate levels of Chhatrapur beach area were similar to those of the monazite sand-bearing high background radiation areas of southern and southwestern coastal tracts of India and other similar areas of the world. The major contributors to the enhanced level of radiation are monazite and zircon sands (Mohanty, A.K., Sengupta, D., Das, S.K., Saha, S.K. and Van, K.V., 2004).

A radiometric assessment around the Mrima Hill in Kenya (Kebwaro, J.M., Rathorel, I.V.S., Hashim, N.O. and Mustapha, A.O., 2011) was performed using a NaI(Tl) detector. This was done to ascertain the level of natural radioactivity due to naturally occurring radionuclides. The average concentrations of ^{238}U, ^{232}Th and ^{40}K were 207.0 $\pm$ 11.3 Bq kg^{-1}, 500.7 $\pm$ 20.0 Bq kg^{-1} and 805.4 $\pm$ 20.0 Bq kg^{-1} respectively. The mean absorbed dose rate in air was found to be 440.7 $\pm$ 16.8 nGy h^{-1} and the annual average effective dose was 1.11 $\pm$ 0.01 mSv, which shows that the area has elevated levels of radioactivity as it is higher than the recommended value of 1 mSv. Several areas of the world are known to have levels of exposure due to natural sources of radiation that are in excess of those considered to be “normal background”.

There are numerous causes for these elevated exposure levels. The monazite sand deposits (which have high levels of thorium) that are found at Guarapari in Brazil, at Yangiang in China and in the states of Kerala and Madras in India are some of the causes for the high exposure levels. Volcanic soils such as in Mineas Gerais in Brazil, Niue Island in the Pacific and in some parts of Italy are also causes of high exposure levels. In the areas of Ramsar and Mahallat in Iran, the elevated levels of radioactivity are due to ^{226}Ra deposited in the area from waters flowing from hot springs (UNSCEAR, 2000).

3.3 Importance of radioactivity measurements

Humans are continuously exposed to ionising radiation from both natural and man-made sources and any hazardous effect (due to radioactivity) depends on the duration of the exposure to the radiation. To quantify the total exposure (due to ionising radiation) to members of the public it is important to determine the magnitude of the exposure to the prevailing natural background radiation. The values for the concentration of the natural radionuclides present (*in the soil, water, vegetation, rocks and air*) in an area is a good measure of their contribution to the ambient dose rate (*or air kerma rate*) and the effective dose that could possibly be harmful to living organisms in that specific area.

Radioactivity and the effects of ionising radiation on living tissues have been studied for many decades and today it is well recognised that an exposure to large doses of ionising radiation may have potentially damaging effects on humans (UNSCEAR, 2008). The need for proper regulation and control of exposure levels for all living beings on earth

has prompted many countries to establish different international organizations that could establish basic principles and procedures to ensure that exposure to ionising radiation is adequately regulated.

One such organisation is the International Commission on Radiological Protection (ICRP). Its purpose is to establish basic principles for and issue recommendations on radiation protection, which today form the basis for international as well as national regulations governing the exposure of radiation workers and members of the public to radiation. The ICRP's recommendations have also been incorporated by the International Atomic Energy Agency (IAEA) into its Basic Safety Standards for Radiation Protection which are published jointly with the World Health Organisation (WHO), the International Labour Organisation (ILO) and the Nuclear Energy Agency (NEA). Today, these standards are used worldwide to ensure radiation safety and protection for workers who may be occupationally exposed to ionising radiation, as well as for members of the general public (VO Consulting, 2012).

In 1955, the General Assembly of the United Nations formed an inter-governmental body known as the United Nations Scientific Committee on the Effects of Atomic Radiation (UNSCEAR). UNSCEAR is tasked to assemble, study and disseminate information on observed levels of ionising radiation and radioactivity (both natural and man-made) in the environment, and on the effects of such radiation on humans and the environment. Many of the UNSCEAR reports are used regularly to guide assessments of exposures to radiation (VO Consulting, 2012).

Many studies of the natural radioactivity in soils due to ionizing radiation have been carried out to ascertain baseline values in different parts of the world (Alatise et.al, 2008, Tahir et. al., 2005, Oyedele et.al, 2006 and Kebwaro et. al., 2011). Therefore, it is important to determine natural radioactivity in the environment especially as it will serve as a significant parameter for public exposure control and as reference for possible future changes in the environment. These baseline values are of utmost importance in areas where human activities such as mining, oil exploration, milling, ore-processing and nuclear power reactors could cause a possible change in the levels of the natural radioactivity in that environment. In the event that there is a radionuclide fallout or nuclear power station disaster as happened recently in Japan (IAEA, 2011) knowledge of the radioactivity levels before the accident would be very useful in accessing the severity of the increase in levels of natural radioactivity. Hence, this study and many others being carried out in other parts of the world are very important.

CHAPTER 4

4. EXPERIMENTAL SET-UP AND MEASUREMENT

4.1 Detector system

The detector system used in this study consists of a high resolution (1.0 keV FWHM at 1.22 keV and 1.9 keV FWHM at 1332 keV) HPGe p-type coaxial detector with 25% relative efficiency (Canberra model GC2519) as shown in Figures 4.1 (a) and (b). The detector was placed inside a Canberra Model 737 lead shield having a thickness of 10 cm. In addition, it has a graded 1.5 mm copper and 1.0 mm tin linning with an outer jacket of 9.5 mm thick low carbon steel. A Model 7915-30 Cyrostat (Base Model 7915-30) was used to supply liquid nitrogen (LN_2) to the detector, with a Model 2002C Pre-amplifier as shown in Figure 4.2. The system also consists of a Model 2100 Bin/Power Supply providing mounting space for a Model 1786 LN_2 monitor and a High Voltage Power Supply (HVPS) Model 9645. It also includes a Model 9660 Digital Signal Processor (housing a Model 2016 Amplifier-TCA, an Analog to Digital Converter (ADC)), an Acquisition Interface Module (AIM 556A) Multichannel Analyser (MCA) as shown in Figure 4.3 (a) and (b). A Genie® 2000 software (version 2.0) was used to analyse the spectra acquired in the measurements (Canberra, 1998).

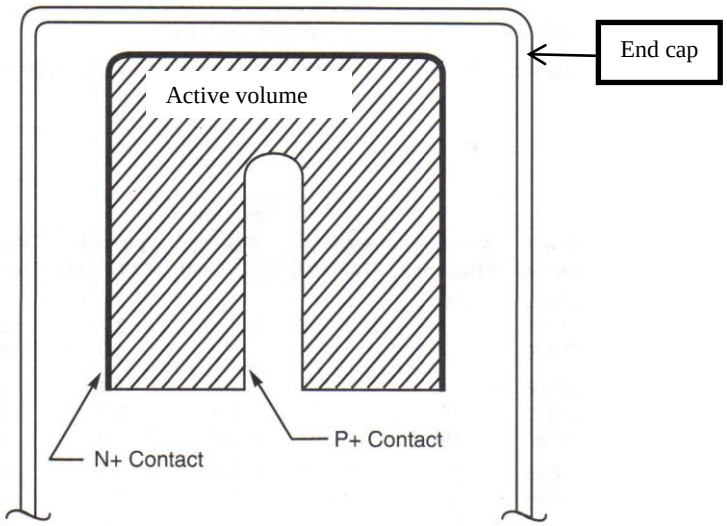

(a)

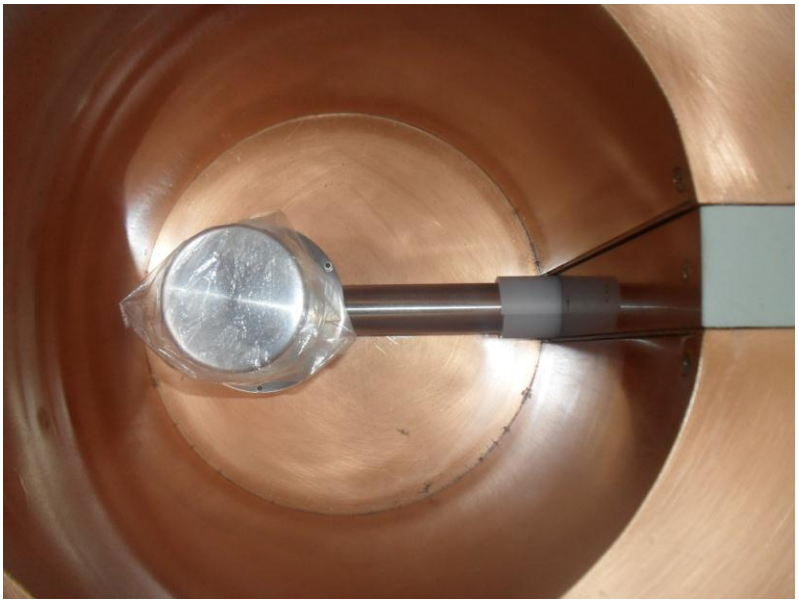

(b)

Figure 4.1: (a) A configuration of the closed end coaxial p-type HPGe detector used in the study and (Canberra Catalogue) (b) a photograph of the top view of the HPGe detector placed inside a lead shield.

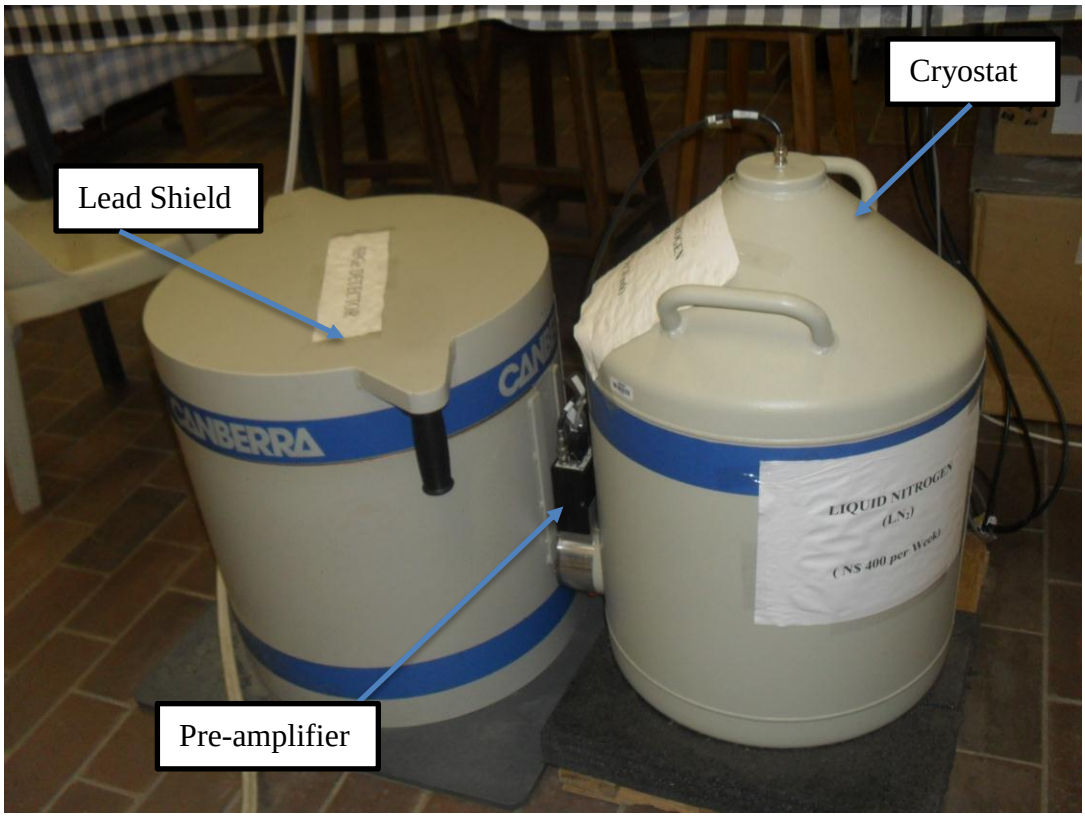

Figure 4.2: The detector configuration used for measurements with a Model 737 Lead Shield, a Pre-amplifier and a Model 7915-30 Cryostat.

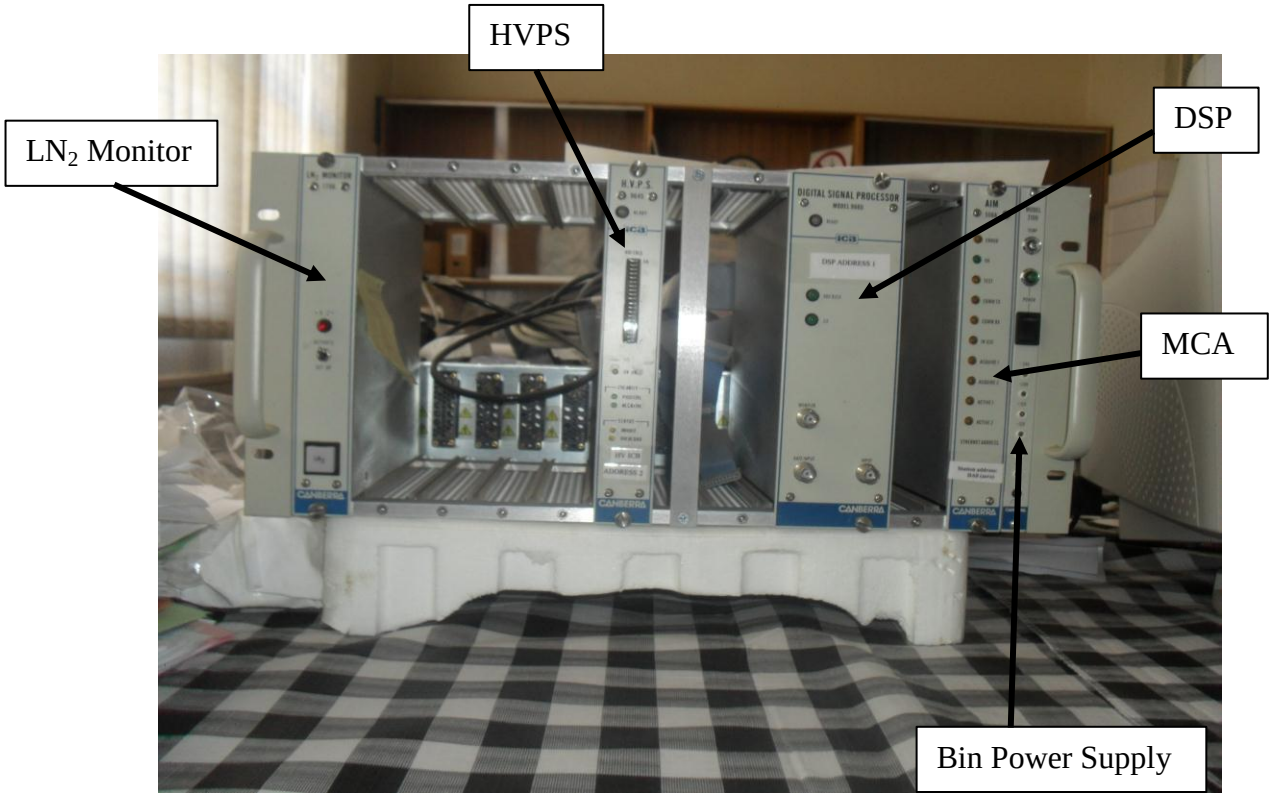

(a)

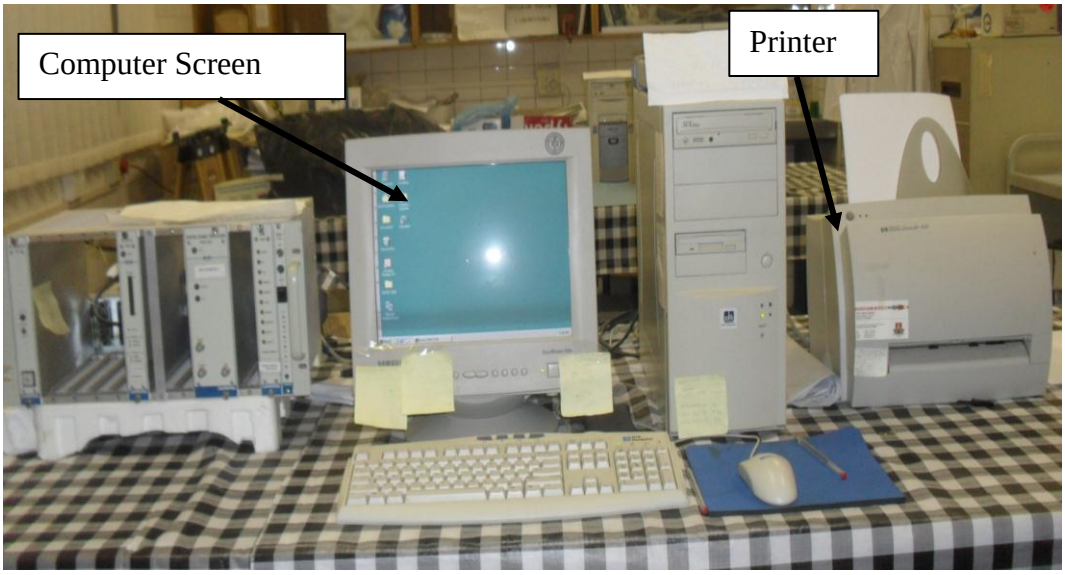

(b)

Figure 4.3: Photographs of the system electronics: (a) the liquid nitrogen (LN_2) monitor, High voltage power supply (HVPS), Digital Signal Processor (DSP), Multi Channel Analyser (MCA) and the Power supply to the components. (b) The computer screen and printer.

High resolution gamma spectroscopy provides fast, accurate and non-destructive analysis of natural radionuclides in environmental samples. The High-purity germanium detector (HPGe) used in this study is basically a cylindrical germanium crystal with an n-type contact on the outer surface, and a p-type contact on the surface of an axial well (Figure 4.1 (a)). The germanium has a net impurity level of around 10^{10} atoms/cc so that with moderate reverse bias, the entire volume between the electrodes is depleted, and an electric field extends across this active region. Photon interaction within this region produces charge carriers which are swept by the electric field (produced by the high voltage supplied over the crystal lattice) to their collecting electrodes, where a charge sensitive preamplifier converts this charge into a voltage pulse proportional to the energy deposited in the detector (Canberra, 1998).

Liquid nitrogen (LN_2) is used to cool the detector to drastically reduce detector thermal noise and to freeze moisture that could be in the system. To prevent the system from warming up, LN_2 is always supplied to it when in operation. The voltage pulse produced by the preamplifier travels a certain distance without much loss of energy to an amplifier that shapes and amplifies the signal. The signals then go to a digital signal processor (DSP) that quantifies the energy from the detector and sends it to a multi-channel analyser (MCA) as shown in Figure 4.4. The MCA can scan a whole energy range and records the number of pulses they count depending on their pulse height (which is proportional to the incident gamma photon energy) the pulses are divided into channels according to their energies and the memory accumulator consists of 4096 individual channels. A histogram of data accumulated in the MCA memory therefore represents a

plot of the number of counts (intensity) versus channel number (γ-photon energy) for all pulses acquired in a specified time interval. Such a histogram or spectrum obtained from a soil sample is shown in Figure 4.5.

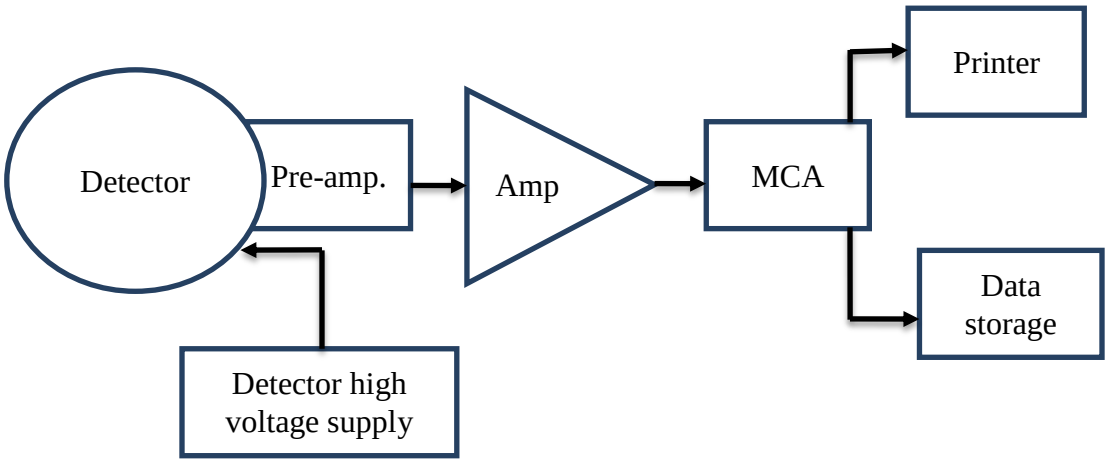

Figure 4.4: Block diagram of a typical gamma spectroscopic system.

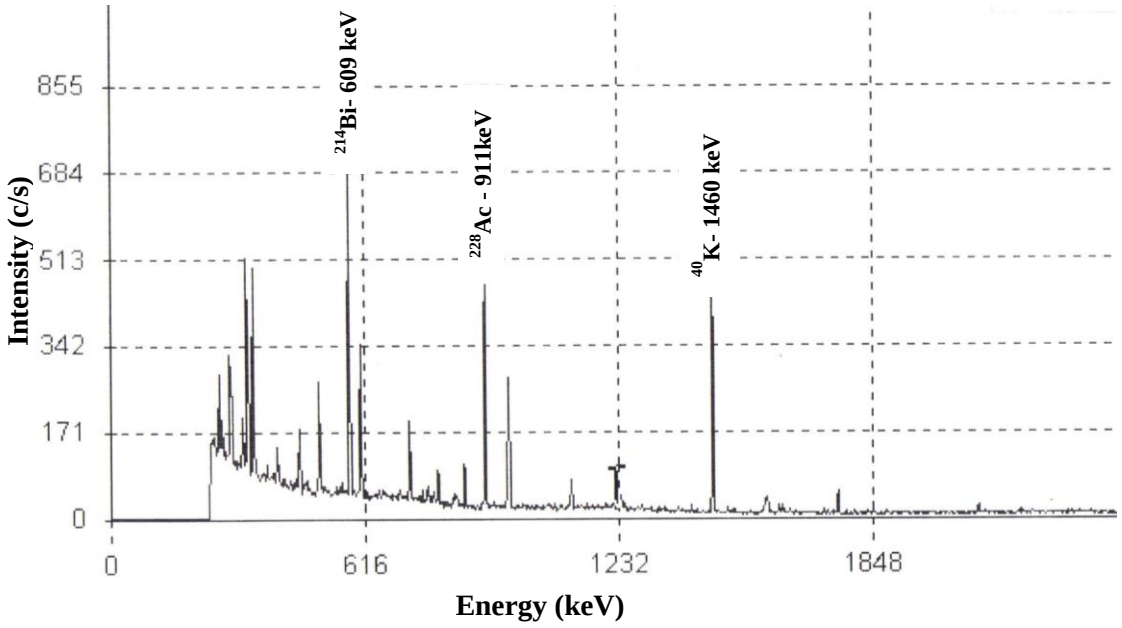

Figure 4.5: A typical spectrum of a soil sample measured with the HPGe detector.

The sensitivity of a HPGe detector system depends largely on several factors, such as detector efficiency, detector resolution, background radiation, sample matrix, sample geometry and the counting time. Background radiation can come either from the sample being counted (Compton-produced) or from the environment, hence the need for a well-shielded detector system as used in this study. Sample geometry is another important aspect that is quite often overlooked, hence for maximum sensitivity the sample is distributed evenly so as to minimize the distance between the sample volume and the detector itself. The resolution of a spectroscopic system is another aspect. It is determined by the width of the peaks produced in the spectrum. A high resolution enables the system to separate two gamma lines which are very close to each other (i.e all peaks in the spectrum are separate and distinct). The most common property of spectroscopic systems that expresses a detector's resolution is the Full Width at Half Maximum (FWHM), which is the width of a gamma ray peak at half of the highest point of the peak.

It may be useful to mention that resolution can be expressed in absolute terms (in eV or keV), or relative terms. The resolution of the detector system used in this study as mentioned earlier is 1.0 keV FWHM at 122 keV and 1.9 keV FWHM at 1332 keV. In relative terms this translates to the FWHM (in keV) divided by the energy of the gamma ray and multiplied by 100. Hence, in relative terms, the resolution of the detector system used is 0.82% at 122 keV and 0.14 % at 1332 keV. This indicates that the system has a high resolution. Figure 4.6 shows the resolution of a gamma ray spectrometer.

The detector system used in this study was donated by the International Atomic Energy Agency (IAEA).

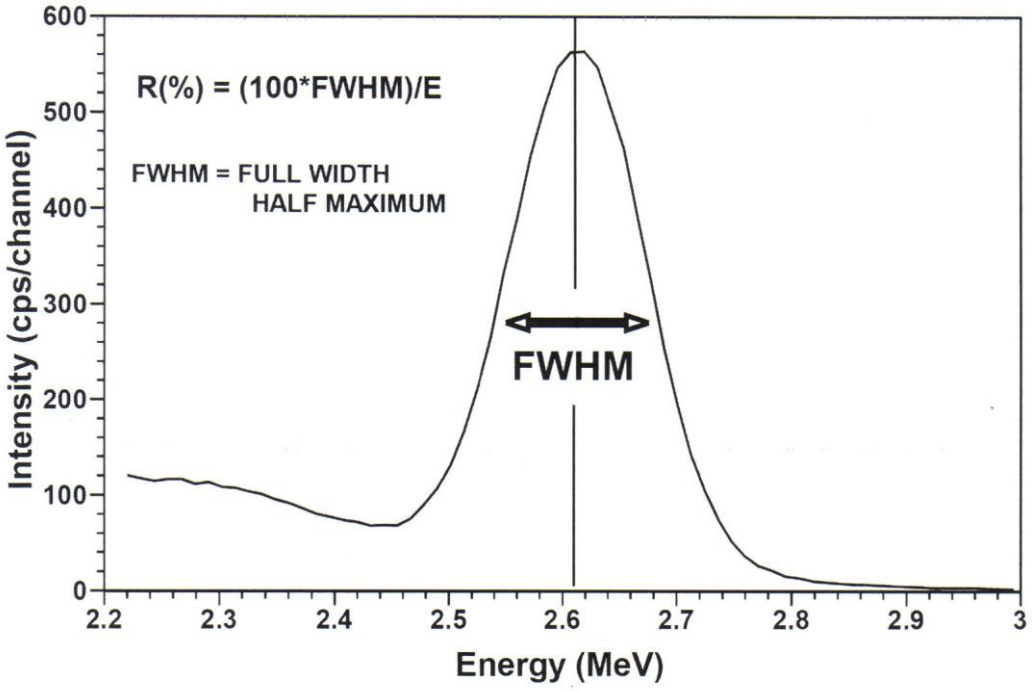

Figure 4.6: Diagram illustrating the energy resolution of a gamma ray spectrometer. The spectrometer energy resolution is defined as the full width of a photopeak at half the maximum amplitude (FWHM) expressed as a precentage of the energy (IAEA, Tec-Doc-1363, 2000).

4.2 Calibration of detector

An essential requirement for gamma-ray spectroscopy is to obtain a relationship between the position of the photo peak in the spectrum and the gamma-ray energy. Identifying the gamma rays within a measured spectrum requires matching the energies of the gamma rays with those emitted by known radionuclides. The energy calibration of the detector system used in this study was done by measuring mixed standard point sources of known radionuclides with well-defined energies within the energy range of interest. In the calibration: ^{22}Na, ^{60}Co and ^{137}Cs point sources were used. Energy calibration was done to obtain a relationship between the peak position in the spectrum and the corresponding gamma-ray energy as shown in Table 4.1. The spectrum of the gamma-ray emitting sources with known specific energy values was acquired long enough to identify the peak energies in the spectra. These point sources were selected to cover a wide energy range over which the spectrometer is to be used. The process involved measuring the spectrum of the point sources (of precisely known energies) and comparing the measured peak position with energy. This involves marking the peaks in the acquired spectrum with their true energies, then using the Genie 2000 software calibration analysis functions to fit the linearity graph as shown in Figure 4.7. The system was also calibrated using reference materials provided by the IAEA namely RGU-1, RGTh-1 and RGK-1. Figure 4.8 is a photograph of the reference materials. The spectra obtained for these reference materials are shown in Figures 4.9 (a), (b) and (c). With this information stored in the memory of the MCA, radionuclides present in the soil samples could easily be identified by comparing their spectra with those of the reference materials.

Table 4.1: Point sources or radionuclides used for Energy - Channel calibration.

Nuclide	Energy (keV)	Channel number
^{137}Cs	661.66	1104
^{60}Co	1173.24	1957
	1332.50	2222
^{22}Na	1274.54	2126

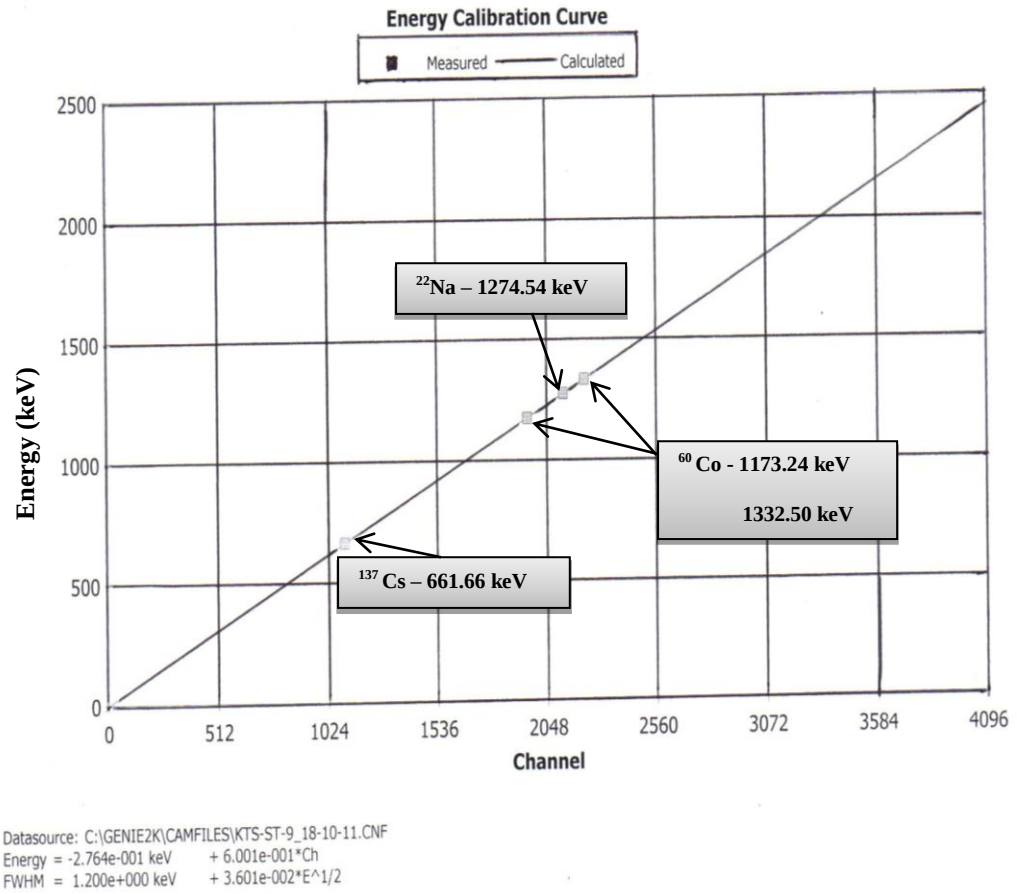

Figure 4.7: The energy calibration curve obtained with the gamma ray spectrometer.

Figure 4.8: Photograph of IAEA reference materials RGU-1, RGTh-1 and RGK-1.

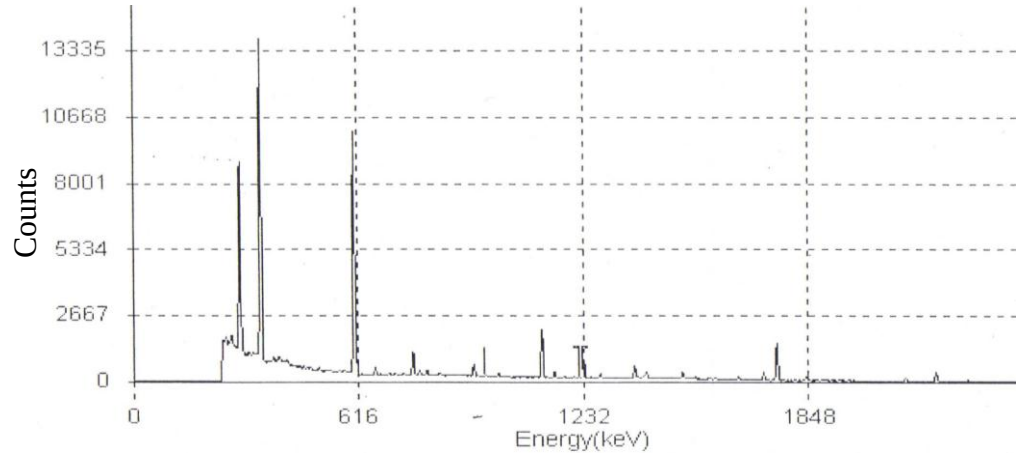

(a)

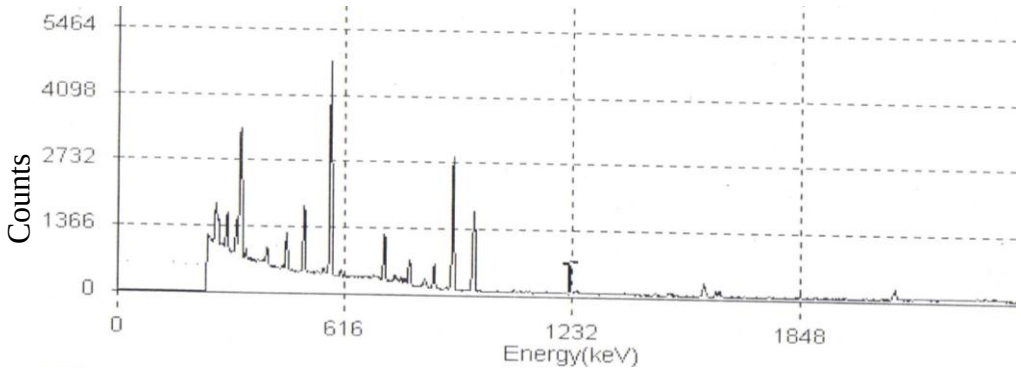

(b)

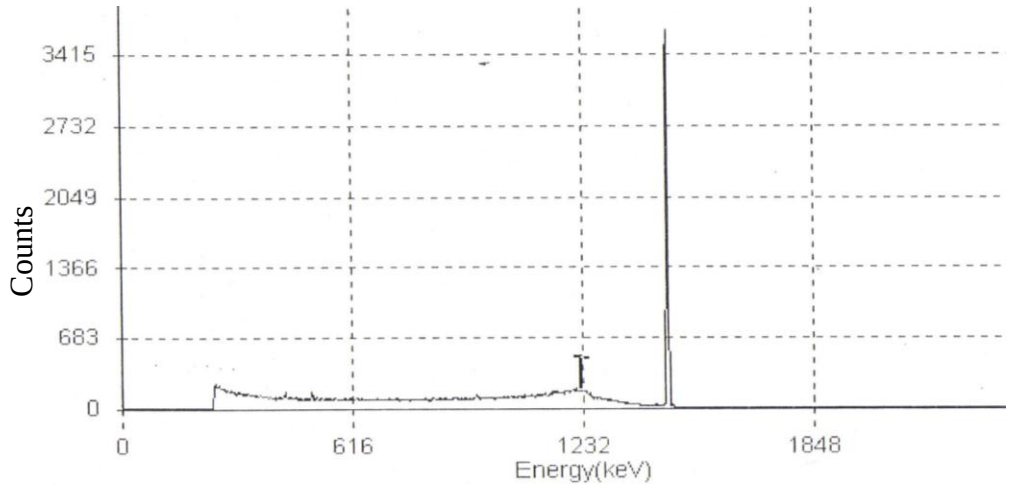

(c)

Figure 4.9: Spectrum of (a) RGU-1, (b) RGTh-1 and (c) RGK-1 reference materials.

4.3 Background counting

The background radiation around the detector was counted for 10800 seconds (3 hours) with an empty polythene bottle having the same dimensions as the soil samples. As discussed earlier (Section 4.1), a well-shielded detector was used in the study and the background spectrum was stored in the MCA. The background radiation was low and there were no peaks at the channels corresponding to the peaks of interest or of the reference materials.

4.4 Sample collection

A total of 305 soil samples were collected from at least ten geographical areas in each of the six towns. At each geographical area in a town, soil samples were collected at five sites across the area. All the sites chosen were away from roads, buildings, railway lines, industrial or agricultural sites and rivers. Soil samples were collected from undisturbed areas with a natural morphology. A 1.0 m^2 area was chosen and samples were taken by first clearing vegetation and other organic matter from the surface. The samples were collected at a depth of about 2cm - 5cm below the soil surface as shown in Figure 4.10. Gloves, dust masks, spades and digging equipment were employed to collect 50 to 55 samples of about 1kg across each town. They were then placed in labelled nylon plastic bags corresponding to the areas and sites where they were collected. All samples were then transported from the site(s) to the Radiation Physics Laboratory in the Department of Physics of the University of Namibia (UNAM) in Windhoek for processing.

4.5 Sample preparation

At the laboratory, the samples were left to dry at room temperature under normal laboratory conditions for about 72 hours (depending on the moisture in the soil at the time of sampling) as shown in Figure 4.11 (a). After removing stone, vegetation and organic matter the dried soil samples were pulverised and sieved through a 2 mm mesh screen as shown in Figure 4.11 (b). 500 g of each sample were carefully weighed and placed in 500 ml polythene bottle similar to those of the reference materials as shown in Figure 4.12 (a) and (b). The air tight bottles (Figure 4.12 (b)) were then stored for about four weeks to ensure radioactive equilibrium between ^{226}Ra and ^{232}Th and their progeny before they were counted in the gamma spectrometry detector system.

Figure 4.10: Collection of soil samples at Arandis.

(a)

(b)

Figure 4.11: (a) Drying soil samples under laboratory condition and (b) pulverising and sieving soil samples.

(a)

(b)

Figure 4.12: (a) Filling bottles with soil samples and (b) storing samples in airtight bottles.

4.6 Detection and counting of radiation

After the isolation period, the soil samples were counted using the high-resolution gamma-ray spectrometer as discussed in Section 4.1. The detector system used was first set to its normal operating conditions before counting commenced. The calibration of the detector and the background measurements were done as discussed in Sections 4.2 and 4.3. The radiation emitted by each of the certified reference materials obtained from the IAEA (RGU-1, RGTh-1 and RGK-1) was counted for 10800s. This was done by placing the materials, one at a time, directly on the detector and counting the radiation as shown in Figure 4.13. All the collected and processed samples from the different areas or towns were then counted with periodic background measurements, and all the spectra were stored in a computer. The radioactivity of each sample was determined from the activity concentrations of ^{238}U, ^{232}Th and ^{40}K. Each sample was placed at the same position on the detector and counted for 10 800 s. The uranium and thorium contents of the samples were determined by measurements of the photo peaks of gamma rays from ^{214}Bi (609.31 keV) and ^{228}Ac (911.21 keV), respectively. Similarly, the potassium content in the samples were determined from the 1460.81 keV gamma ray.

Figure 4.13: Reference material (RGU-1) placed on the HPGe detector inside a lead shield.

CHAPTER 5

5. RESULTS AND DISCUSSION

5.1 Determination of activity concentrations for ^{238}U, ^{232}Th and ^{40}K

The activity concentrations of the radionuclides ^{238}U, ^{232}Th and ^{40}K in the soil samples and reference materials were determined using gamma spectrometry. The height of a particular peak in the gamma ray spectrum is directly proportional to the energy of the gamma ray producing it. Also the area A under a photopeak depends on the concentration of the radionuclides in a sample and the sensitivity of the measuring system (Beck, H.L., Decompo, J. and Gologak, J., 1972). The activity concentration of ^{238}U was evaluated from the intensity of 609 keV gamma transition line of ^{214}Bi while the activity concentration of ^{232}Th was determined using the 911 keV gamma line of ^{228}Ac and the activity concentration of ^{40}K was determined directly from its characteristic 1460 keV gamma ray energy peak. As usual, the soil samples and reference materials studied in this work were counted under identical conditions of sample-detector geometry and counting time (Senthilkumar et al., 2010, Alatise, 2007). Since a fixed geometry was maintained and the sensitivity of the detector was kept constant, then the net peak area, A, is directly proportional to the concentration, C of the radionuclides in the soil sample. That is,

$$A \propto C \quad \text{or } A = KC$$

$$\therefore K = A/C \tag{5.1}$$

where K is a constant of proportionality and is referred to as the area under the photo-peak per unit concentration.

The activity concentrations of the soil samples were determined by comparing the full energy absorption peak areas observed for the samples with the corresponding peak areas observed for the reference materials or standards under the same condition. The unknown activity concentrations of the radionuclides in each of the samples were calculated using the relation

$$D_u = (A_u / A_k) D_k \quad (5.2)$$

where D_k and A_k are respectively the known activity concentration in the standard and the area under the corresponding photopeak in the gamma ray spectrum obtained for the standard. Similarly, D_u and A_u are respectively the activity concentration (unknown) in the sample and the area under the corresponding photopeak in the spectrum obtained for the sample. From equations 5.1 and 5.2, the concentration, C of a radionuclide in a soil sample is

$$C = D_u / \text{Mass of the sample} \quad (5.3)$$

Equation 5.3 was used to determine the concentrations of different radionuclides in all the samples. The results obtained were used to calculate the average concentration of a given radionuclide in a given geographical area for a given town. Tables 5.1 – 5.6 (columns 2 - 4) show the range (in parenthesis) of the concentrations of different radionuclides in the different geographical areas and the corresponding average concentration for each area.

5.2 Absorbed Dose Rate

The activity concentrations of the radionuclides ^{40}K, ^{232}Th and ^{238}U only provide information on the quantity of the radionuclides in the soil. A measure of the effect of the quantity of these radionuclides on living organisms in the area is the absorbed dose.

More specifically, absorbed dose is a measure of the energy absorbed per unit mass and the unit is Gray. In calculating the absorbed dose rate the conversion factors 0.0417 nGy h^{-1} per Bq kg^{-1} for ^{40}K, 0.462 nGy h^{-1} per Bq kg^{-1} for ^{238}U and 0.604 nGy h^{-1} per Bq kg^{-1} for ^{232}Th was adopted (UNSCEAR, 2000; Harb, 2008; Oyedele, 2008; Antovic, N.M., Svrokota, N. and Antovic, I., 2011; Murty, V.R.K. and Karunakara, N., 2008) That is, the absorbed dose rate was calculated using the equation

$$D = 0.0417A_K + 0.462A_U + 0.604A_{Th} \quad (5.4)$$

where D is the dose rate (nGy h^{-1}) at 1m above the ground due to ^{238}U, ^{232}Th and ^{40}K in the soil. A_U, A_{Th} and A_K are the activity concentrations of ^{238}U, ^{232}Th and ^{40}K (in Bq kg^{-1}) respectively. The absorbed dose rate at each site where the samples were collected and for each geographical area were calculated. The results obtained are shown in Tables 5.1 – 5.6 (column 5).

5.3 Annual Effective Dose

The absorbed dose rate discussed in the last section is a very useful physical concept. However, the same degree of damage is not necessarily produced by the same absorbed dose of different radiation in a given organ of a biological system. Therefore, there is a need to introduce a quantity that takes into account, the biological damage caused by different radiation UNSCEAR in its report suggest a quantity referred to as the effective dose (UNSCEAR, 2000). In estimating the effective dose in any environment, the two factors of importance are the conversion coefficient from Gy h^{-1} to Sv h^{-1} and the occupancy factor (Senthilkumar et al., 2010). The conversion factor of 0.7 Sv Gy^{-1} is applied to convert absorbed dose rate in air to human effective dose. In addition, the

outdoor occupancy factor of 0.2 which assumes that an average individual stays outdoors for about 4.8 hours a day is recommended (UNSCEAR, 2000). The annual effective dose for each of the sites where samples were calculated was calculated (in units of mSv) using the following relation,

$$H_E = D \times T \times F \tag{5.5}$$

where D is the calculated dose rate in (Gy h^{-1}), T is the outdoor occupancy time (24 h × 365.25 days × 0.2 = 1753 h y^{-1}) and F is the conversion factor (0.7 Sv Gy^{-1}). The results obtained were used to calculate the average effective dose rate for each geographical area and for each town. Tables 5.1 – 5.6 (column 6) shows the range (in parenthesis) of the effective dose rate in each geographical area and the average effective dose rate in each area. All the calculations of radionuclide concentrations, absorbed dose rates and annual effective doses for all the towns were done using a MatLab software and an algorithm written by the author (Appendix A).

5.4 Radioactivity in towns

5.4.1 Natural radioactivity in Usakos

The ten geographical areas where soil samples were collected in the town of Usakos are shown in Figure 5.1. The range and mean of activity concentrations of the radionuclides ^{40}K, ^{232}Th and ^{238}U in the soil samples collected from the ten geographical areas of Usakos are presented in Table 5.1 (columns 2-4) and shown in Figure 5.2. Of the three radionuclides, ^{40}K has the highest concentration in all the ten areas of Usakos as could be seen in Figure 5.2. It's concentration Table 5.1 (column 2) varies from a minimum of 615.8 ± 26.4 Bq kg^{-1} (at HK) to a maximum of 1477.0 ± 51.4 Bq kg^{-1} (at HA) with an overall average value of 959.5 ± 194.7 Bq kg^{-1} for the town. It should be mentioned that the highest concentration of ^{40}K was in the Hakaseb area which is mainly occupied by the middle to lower income population groups of the community of Usakos. There exist no agricultural or mining activities in this area, as it is just a municipal residential area with houses, schools, a community centre and church. Hence the high concentration of ^{40}K in this area could be attributed to its natural abundance in the soil of the area. The mean concentration of ^{40}K for the town was found to be 2.3 times the world average value of 412 Bq kg^{-1} (UNSCEAR, 2008). This high concentration of ^{40}K has also been observed in other parts of Africa (Murty et al, 2010, Alatise et al, 2008 and Harb, 2008).

^{232}Th has the second highest concentration in the town as could be seen in Figure 5.2. The concentration ranged from 41.8 ± 4.1 Bq kg^{-1} (at HK) to 173.4 ± 8.1 Bq kg^{-1} (at RS) with an overall mean value of 74.8 ± 30.2 Bq kg^{-1}(Table 5.1 column 3). As could be observed in Figure 5.2 the average concentration of ^{232}Th did not vary widely from one

area to another. This is an indication that the distribution of ^{232}Th in the soils of Usakos is fairly uniform. The mean activity concentration for ^{232}Th was however observed to be higher than the world average value of 45 Bq kg^{-1} for this radionuclide (UNSCEAR, 2008).

^{238}U has the lowest activity concentration in all the areas as could be observed in Figure 5.2. The concentration ranged from a minimum of 26.6 $\pm$ 2.5 Bq kg^{-1} (at HA) to a maximum of 85.3 $\pm$ 3.4 Bq kg^{-1} (at HA) with a mean of 44.2 $\pm$ 9.7 Bq kg^{-1} (Table 5.1 column 4). The mean concentration of 44.2 $\pm$ 9.7 Bq kg^{-1} is comparable to the world average value of 33 Bq kg^{-1} for ^{238}U (UNSCEAR, 2008).

The absorbed dose rate calculated for each site in the town varies from 76.5 $\pm$ 3.1 nGy h^{-1} (at HK) to 179.7 $\pm$ 5.5 nGy h^{-1} (at HA) with an average of 105.7 $\pm$ 23.9 nGy h^{-1} (Table 5.1 column 5). Figure 5.3 shows the average absorbed dose rates for the different geographical areas. As could be expected, the average absorbed dose rate varies from one area to another with the highest value at the Hakaseb (HA) area. It may be useful to mention that for each geographical area in the town the largest contribution to the dose rate comes from ^{40}K.

Using the values of the absorbed dose rates obtained for the different sites in the town and a conversion factor of 0.7 Sv Gy^{-1} with an outdoor occupancy factor of 20% (equation 5.5), the annual effective dose for each site was calculated. The results obtained are shown in Table 5.1 (column 6) and Figure 5.4. The annual effective dose

varies from 0.09 mSv (in area HK and KS) to 0.18 mSv (at HA) with a mean of 0.13± 0.03 mSv (Table 5.1). The individual values of the annual effective dose due to external exposure of natural terrestrial sources in the soil for the town varied from one area to another. A comparison of the effective dose for the ten geographical areas of the town is shown in Figure 5.4. As could be seen in the figure, the average annual effective dose is fairly the same across the different geographical areas except for the Hakaseb (HA) and the Usakos Municipality (UM) areas. The average value of 0.13 mSv obtained for the town is far below the 0.48 mSv value estimated as the world average by the United Nations Scientific Committee on the Effects of Atomic Radiation. Also, the average value is less than the annual maximum permissible dose of 1.0 mSv recommended for the public by the International Commission on Radiological Protection (ICRP). It can therefore be concluded that the town of Usakos has a normal background radiation.

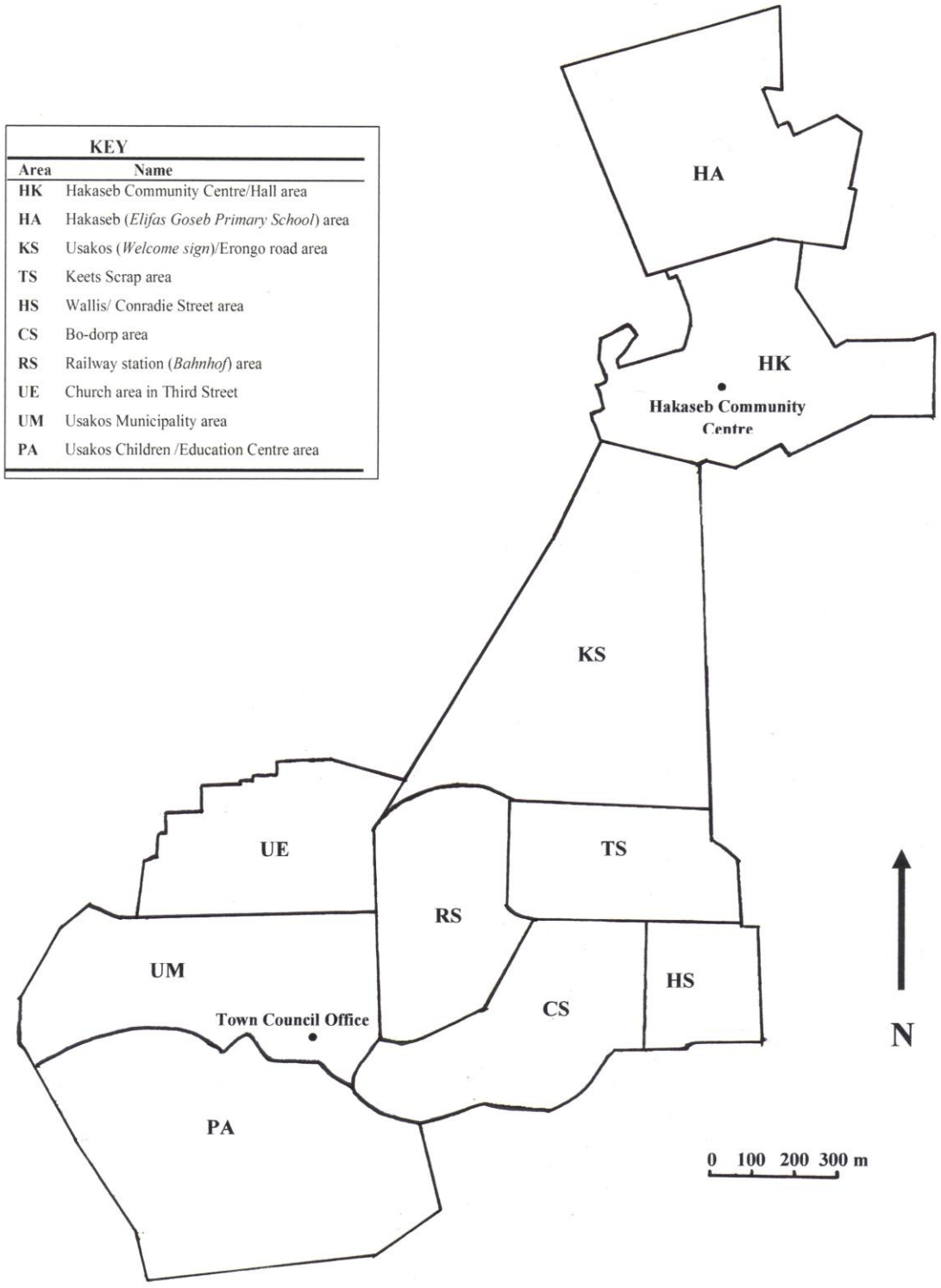

Figure 5.1: Map showing the ten geographical areas where soil samples were collected in Usakos.

Table 5.1: Average (± standard deviation) radionuclide concentrations, absorbed dose rates and annual effective doses in ten geographical areas of Usakos. The corresponding range of values is given in parentheses.

Area	Radionuclide concentration (Bq kg^{-1})			Absorbed dose rate (nGy h^{-1})	Annual effect. dose (mSv)
	^{40}K	^{232}Th	^{238}U		
HK	774.6 ± 127.4	45.7 ± 3.9	52.9 ± 18.6	84.4 ± 6.3	0.10 ± 0.01
	(615.8 – 894.9)	*(41.8 – 51.7)*	*(39.9 – 85.3)*	*(76.7 – 92.6)*	*(0.09 – 0.11)*
HA	1336.5 ± 142.0	118.9 ± 37.5	33.1 ± 3.8	142.8 ± 26.6	0.18 ± 0.03
	(1145.0 – 1477.0)	*(78.6 – 167.6)*	*(26.6 – 35.9)*	*(111.8 – 178.3)*	*(0.14 – 0.22)*
KS	790.9 ± 118.5	50.8 ± 5.1	45.3 ± 3.4	84.6 ± 6.4	0.10 ± 0.01
	(654.3 – 976.6)	*(42.6 – 54.8)*	*(42.2 – 50.8)*	*(76.5 – 93.3)*	*(0.09 – 0. 11)*
TS	1068.0 ± 47.4	63.7 ± 4.5	39.7 ± 4.9	101.3 ± 5.0	0.12 ± 0.01
	(986.3 – 1106.5)	*(59.0 – 70.5)*	*(33.2 – 46.5)*	*(97.1 – 109.6)*	*(0.12 – 0. 13)*
HS	946.8 ± 88.7	74.4 ± 11.9	40.6 ± 13.5	103.1 ± 15.4	0.13 ± 0.02
	(841.9 – 1048.8)	*(57.0 – 86.6)*	*(30.1 – 63.4)*	*(83.4 – 120.3)*	*(0.10 – 0.15)*
CS	868.9 ± 183.8	68.3 ± 25.5	47.6 ± 4.1	99.5 ± 21.1	0.12 ± 0.03
	(697.6 – 1178.7)	*(42.9 – 109.7)*	*(40.6 – 50.5)*	*(78.3 – 134.2)*	*(0.10 – 0.17)*
RS	1003.6 ± 185.5	90.1 ± 47.3	42.1 ± 9.3	115.7 ± 37.0	0.14 ± 0.05
	(822.7 – 1308.6)	*(58.6 – 173.4)*	*(28.7 – 54.2)*	*(91.0 – 179.7)*	*(0.11 – 0.22)*
UE	891.0 ± 52.0	66.5 ± 18.6	45.2 ± 4.7	98.2 ± 10.6	0.12 ± 0.01
	(808.3 – 943.0)	*(49.8 – 96.8)*	*(41.8 – 52.8)*	*(88.7 – 115.3)*	*(0.11 – 0.14)*
UM	1045.0 ± 90.5	101.9 ± 23.3	46.8 ± 6.9	126.8 ± 17.7	0.16 ± 0.02
	(909.3 – 1130.6)	*(78.6 – 126.2)*	*(34.8 – 51.6)*	*(107.1 – 147.2)*	*(0.13 – 0.18)*
PA	869.8 ± 127.3	68.1 ± 4.7	49.0 ± 7.3	100.0 ± 0.4	0.12 ± 0.00
	(726.5 – 1010.3)	*(63.0 – 75.8)*	*(40.9 – 59.9)*	*(99.4 – 100.4)*	*(0.12 – 0.12)*
All samples	**959.5 ± 194.7**	**74.8 ± 30.2**	**44.2 ± 9.7**	**105.7 ± 23.9**	**0.13 ± 0.03**
	(*615.8 - 1477.0*)	**(*41.8 - 173.4*)**	**(*26.6 - 85.3*)**	**(*76.5 - 179.7*)**	**(*0.09 - 0.22*)**

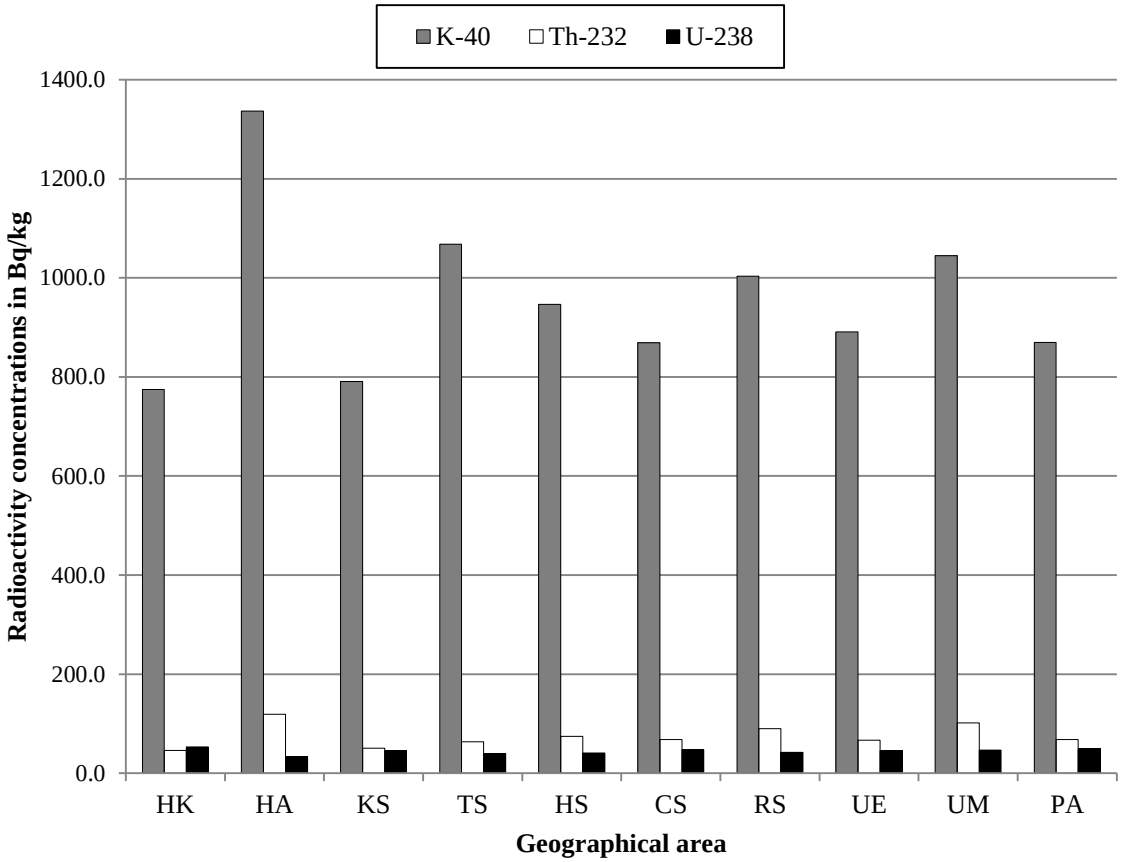

Figure 5.2: Comparison of mean activity concentrations of ^{40}K, ^{232}Th and ^{238}U for the ten geographical areas of Usakos.

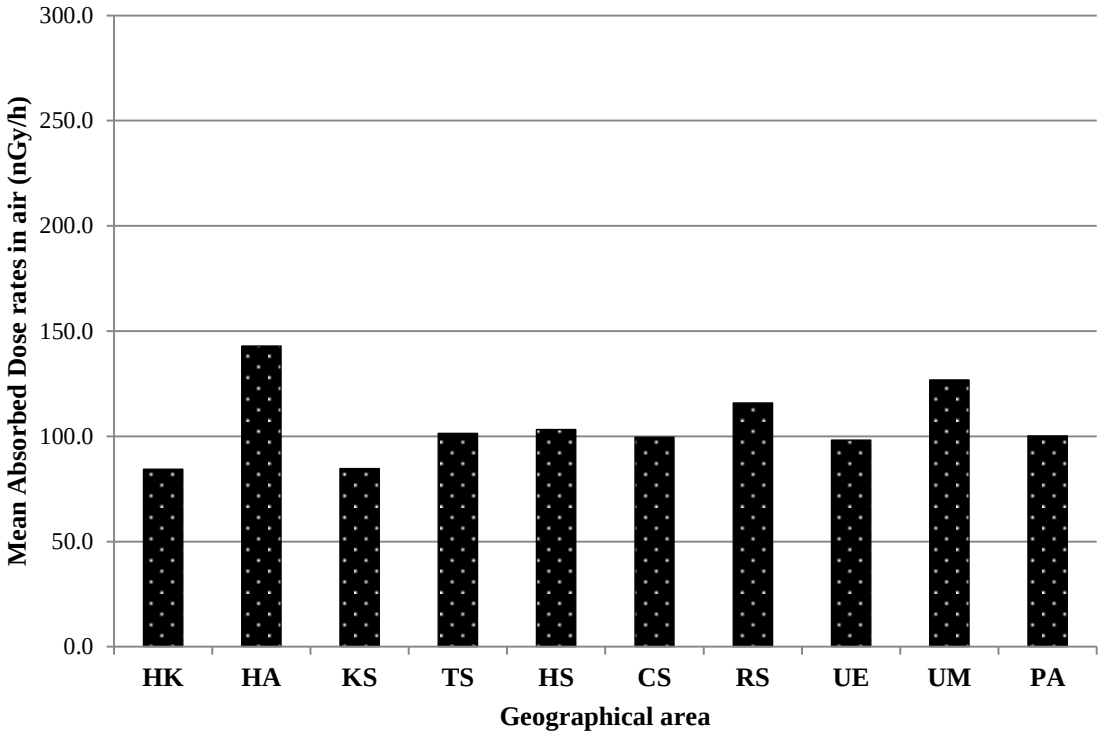

Figure 5.3: Comparison of mean absorbed dose rates for ten geographical areas of Usakos.

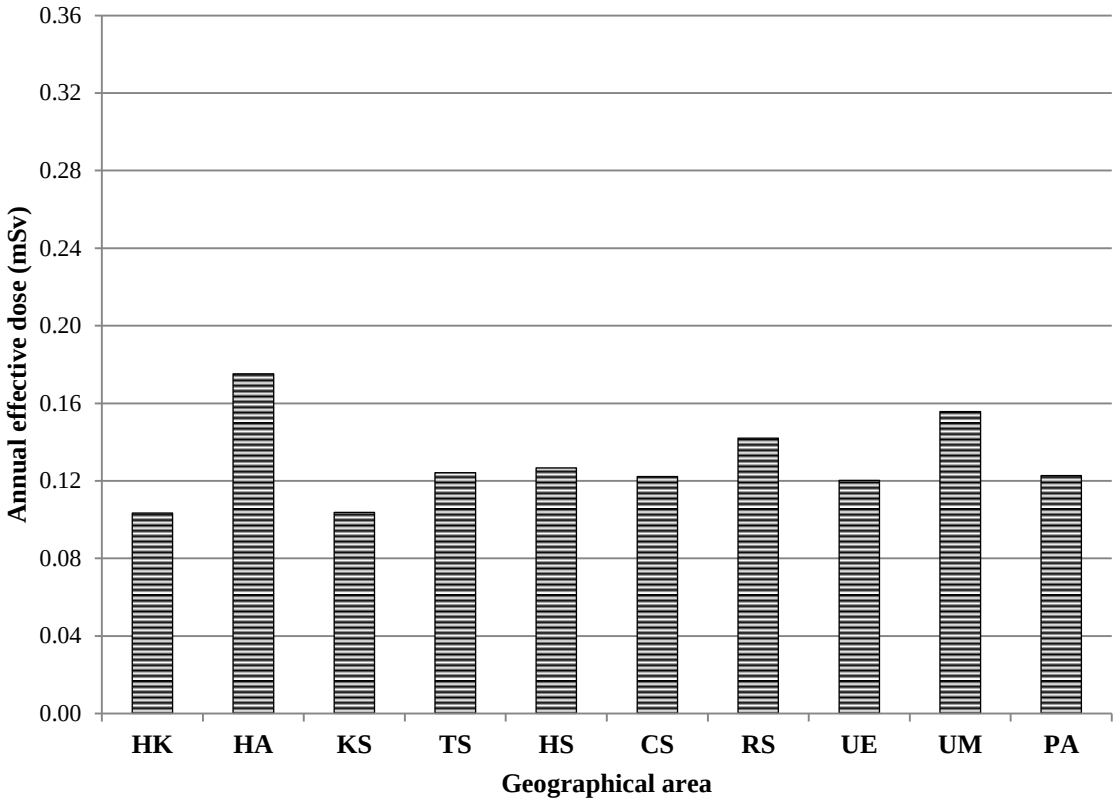

Figure 5.4: Comparison of mean annual effective dose for ten geographical areas of Usakos**.**

5.4.2 Natural radioactivity in Arandis

A total of fifty-five soil samples were collected from eleven geographical areas (five samples per area) of Arandis and studied. The geographical areas are shown in Figure 5.5 while the results obtained are presented in Table 5.2 and shown in Figure 5.6. As observed in Usakos, the concentration of ^{40}K is much higher than those of ^{232}Th and ^{238}U in all areas as could be seen in Figure 5.6. The concentration of ^{40}K varies from 740.3 $\pm$ 29.2 Bq kg^{-1} (at HA) to 1053.6 $\pm$ 39.4 Bq kg^{-1} (at PP) with an average of 899.7 $\pm$ 65.8 Bq kg^{-1} as shown in Table 5.2 (column 2). This average value is about two times higher than the world average of 412 Bq kg^{-1} (UNSCEAR, 2008).

For ^{232}Th, the activity concentration varies from 105.3 $\pm$ 6.1 Bq kg^{-1} (at WL) to 421.9 $\pm$ 14.9 Bq kg^{-1} (at ST) with an average value of 245.7 $\pm$ 87.4 Bq kg^{-1} for the town as shown in Table 5.2 (column 3). This average value is less than half of the average concentration of ^{40}K but than double that of ^{238}U as could be seen in Table 5.2. Also, the average value is higher than the world's average value of 45 Bq kg^{-1}.

Of the three radionuclides, ^{238}U has the lowest concentration in all the geographical areas as could be observed in Figure 5.6. The concentration varies from a low 45.9 $\pm$ 2.7 Bq kg^{-1} (at PK) to 101.8 $\pm$ 4.8 Bq kg^{-1} (at ST) with an average of 72.4 $\pm$ 13.5 Bq kg^{-1} as shown in Table 5.2 (column 4). These relatively low values for ^{238}U are an indication that there exist no large deposits of uranium in the town, although it is close to one of the world's largest open-pit uranium mine, Rössing Uranium Mine. However, the average activity concentration of ^{238}U is much higher than the world's average of 33 Bq kg^{-1}.

The measured concentrations of ^{40}K, ^{232}Th and ^{238}U were used to calculate the absorbed dose rate (in air 1m above the ground) at each of the sites where samples were collected. The dose varies from 119.1 $\pm$ 4.1 nGy h^{-1} (at WL) to 342.0 $\pm$ 9.4 nGy h^{-1} (at ST) with an average of 219.4 $\pm$ 58.5 nGy h^{-1} for the town as shown in Table 5.2 (column 5) and Figure 5.7. As could be observed in Figure 5.7, the absorbed dose varies from slightly from area to area. The mean value of the absorbed dose for the town (219.4 $\pm$ 58.5 nGy h^{-1}) is about four times the world's average value of 58 nGy h^{-1}.

All the values obtained for the absorbed dose rate were used to calculate the annual effective dose for the different sites using equation 5.5. The effective dose varies from 0.15 mSv (at WL) to 0.42 mSv (at ST) with an average of 0.27 mSv as shown in Table 5.2 (column 6) and Figure 5.8. As in the case of the absorbed dose, the annual effective dose vary slightly from area to area as could be observed in Figure 5.8. The average value of 0.27 mSv obtained for the town is far less than the maximum permissible annual dose of 1.0 mSv recommended for the public by the ICRP. Therefore the town of Arandis can be regarded as having normal background radiation.

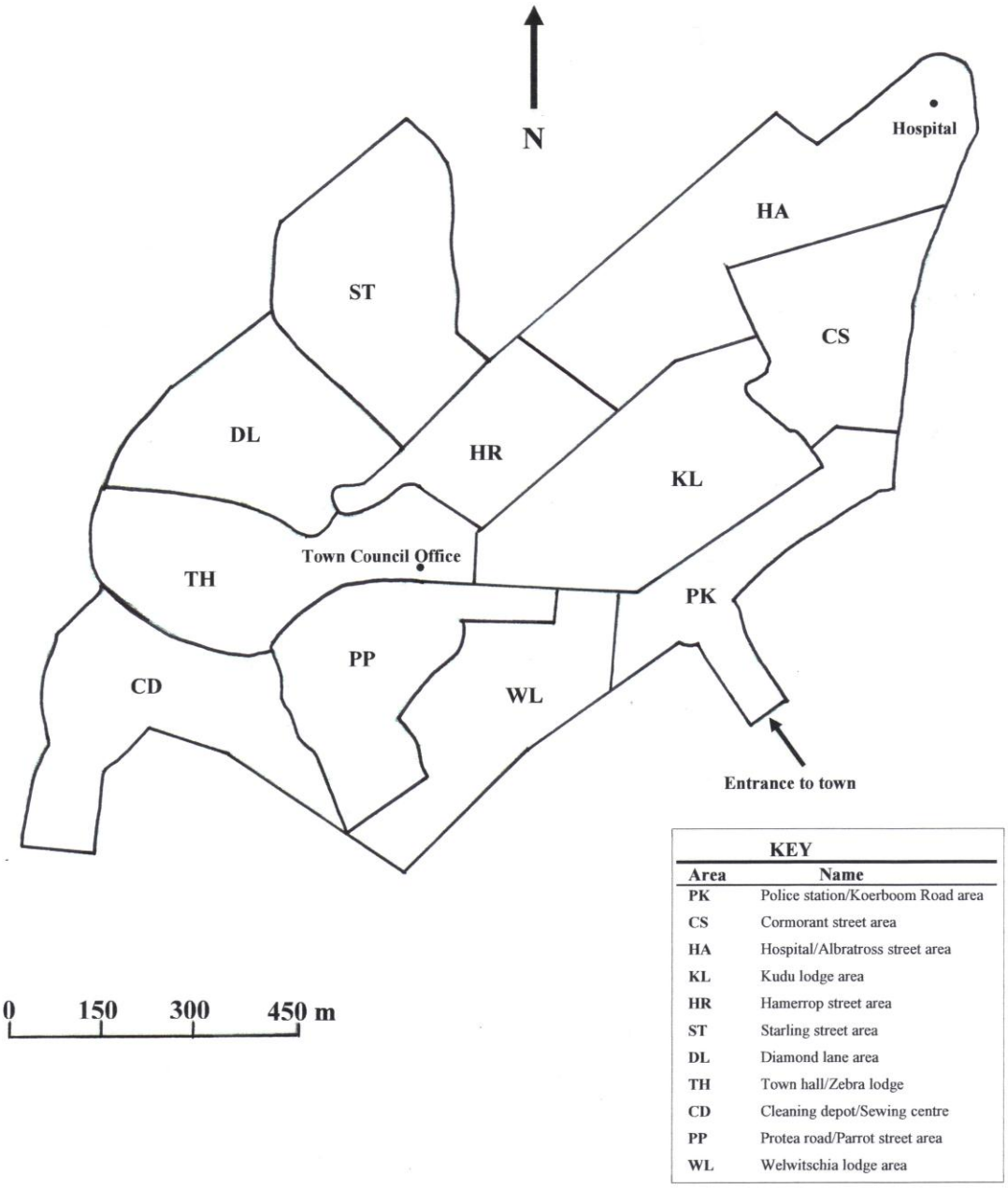

Figure 5.5: Map showing the ten geographical areas where soil samples were collected in Arandis.

Table 5.2: Average (± standard deviation) radionuclide concentrations, absorbed dose rates and annual effective doses in eleven geographical areas of Arandis. The corresponding range of values is given in parentheses.

Area	Radionuclide concentration (Bq kg^{-1})			Absorbed dose rate (nGy h^{-1})	Annual effect. dose (mSv)
	^{40}K	^{232}Th	^{238}U		
PK	893.2 ± 68.8	191.3 ± 55.7	65.5 ± 14.4	183.1 ± 34.4	0.23 ± 0.04
	(816.3 – 987.1)	*(134.1 – 253.7)*	*(45.9 – 85.7)*	*(154.5 – 220.7)*	*(0.19 – 0. 27)*
CS	954.9 ± 65.8	238.1 ± 97.3	68.6 ± 14.8	215.3 ± 63.1	0.26 ± 0.08
	(849.5 –1020.3)	*(175.3 – 410.5)*	*(58.2–94.7)*	*(173.4 – 327.1)*	*(0.21 – 0.40)*
HA	884.6 ± 82.0	213.3 ± 66.8	73.7 ± 6.0	199.7 ± 44.3	0.25 ± 0.05
	(740.3 – 939.7)	*(142.5 – 313.6)*	*(65.7 – 80.5)*	*(154.4 – 264.5)*	*(0.19 – 0.32)*
KL	938.7 ± 45.9	281.7 ± 86.6	79.6 ± 10.9	246.1 ± 56.8	0.30 ± 0.07
	(868.5 – 987.1)	*(186.7 – 379.2)*	*(67.6 – 97.3)*	*(183.5 – 314.1)*	*(0.23 – 0.39)*
HR	880.8 ± 27.2	296.8 ± 76.2	79.7 ± 18.1	252.8 ± 53.3	0.31 ± 0.07
	(844.8 – 920.7)	*(183.9 – 392.0)*	*(49.9 – 98.5)*	*(172.5 – 319.1)*	*(0.21 – 0.39)*
ST	917.8 ± 61.0	334.4 ± 86.9	88.2 ± 10.0	281.0 ± 58.4	0.35 ± 0.07
	(830.5 – 987.1)	*(235.2 – 421.9)*	*(78.6 – 101.8)*	*(216.0 – 342.0)*	*(0.27 – 0.42)*
DL	862.8 ± 92.2	271.4 ± 65.4	70.2 ± 4.3	232.3 ± 38.8	0.29 ± 0.05
	(759.3 – 977.6)	*(203.8 – 347.8)*	*(63.7 – 74.7)*	*(196.0 – 274.2)*	*(0.24 – 0.34)*
TH	914.0 ± 34.2	261.5 ± 81.0	69.7 ± 11.1	228.3 ± 54.8	0.28 ± 0.07
	(873.2 – 963.4)	*(138.4 – 356.4)*	*(52.4 – 83.1)*	*(145.4 – 293.8)*	*(0.18 – 0.36)*
CD	864.7 ± 18.2	223.0 ± 91.1	66.7 ± 16.8	201.5 ± 62.5	0.25 ± 0.08
	(840.0 – 887.5)	*(134.1 – 359.2)*	*(46.2 – 90.8)*	*(144.1 – 295.3)*	*(0.18 – 0.36)*
PP	878.9 ± 72.9	207.9 ± 81.9	77.3 ± 8.3	233.3 ± 54.0	0.29 ± 0.07
	(859.0 –1053.6)	*(173.9 – 349.2)*	*(65.7 – 84.4)*	*(173.4 – 293.9)*	*(0.21 – 0. 36)*
WL	841.9 ± 62.2	128.9 ± 18.2	57.5 ± 7.7	139.5 ± 14.8	0.17 ± 0.02
	(749.8 – 892.2)	*(105.3 – 152.5)*	*(50.2 – 68.9)*	*(119.1 – 157.8)*	*(0.15 – 0. 19)*
All samples	**899.7 ± 65.8**	**245.7 ± 87.4**	**72.4 ± 13.5**	**219.4 ± 58.5**	**0.27 ± 0.07**
	(*740.3 – 1053.6*)	**(*105.3 – 421.9*)**	**(*45.9 – 101.8*)**	**(*119.1 – 342.0*)**	**(*0.15 - 0.42*)**

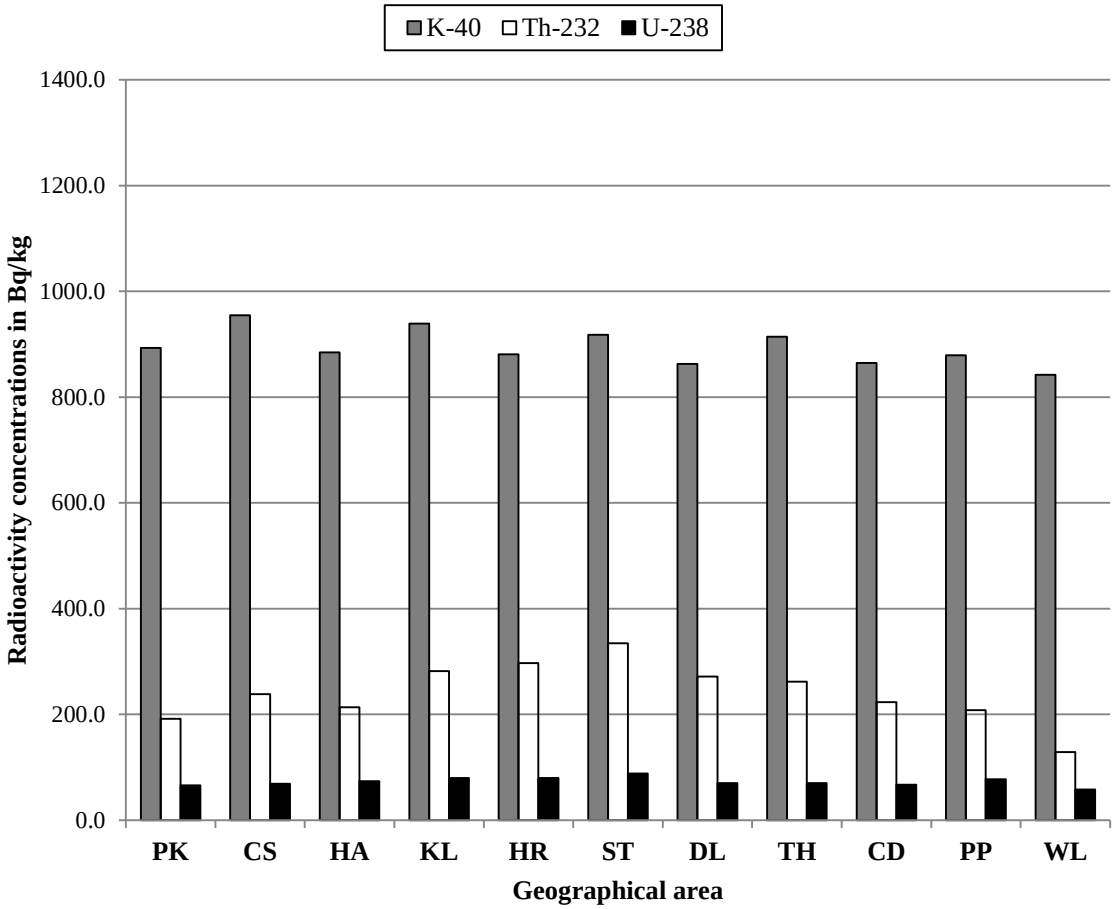

Figure 5.6: Comparison of mean activity concentrations of ^{40}K, ^{232}Th and ^{238}U for eleven geographical areas of Arandis.

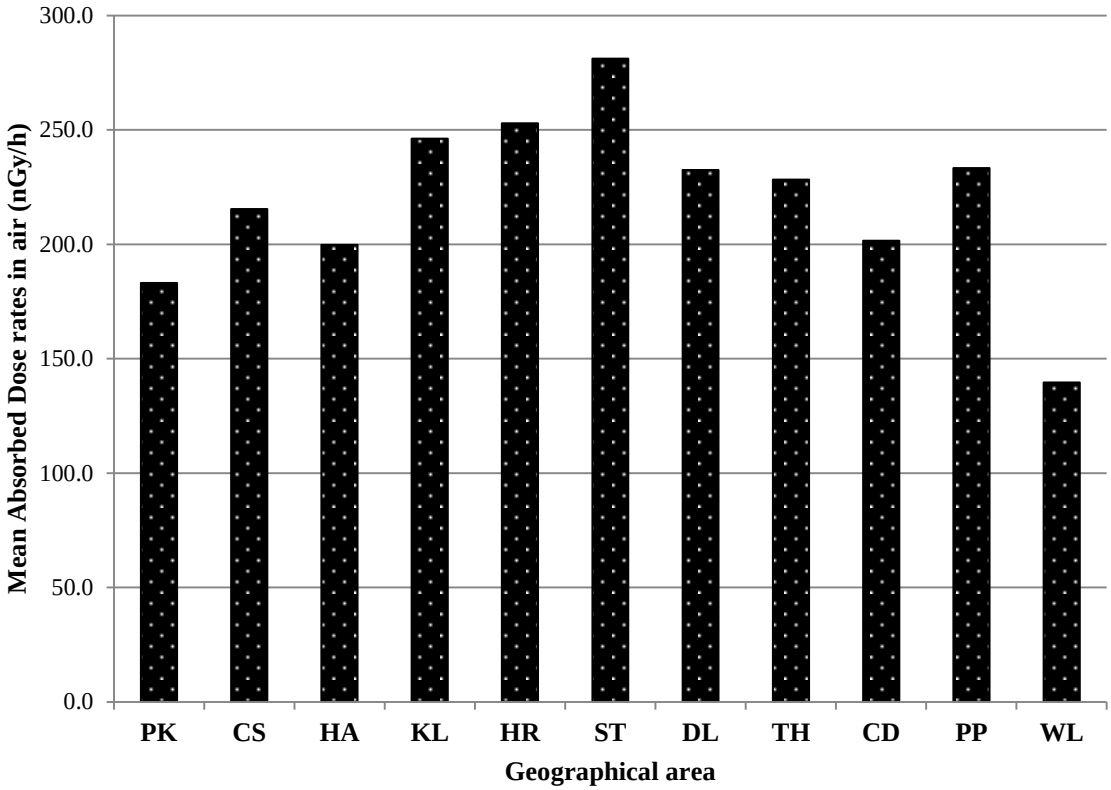

Figure 5.7: Comparison of mean absorbed dose rates for eleven geographical areas of Arandis.

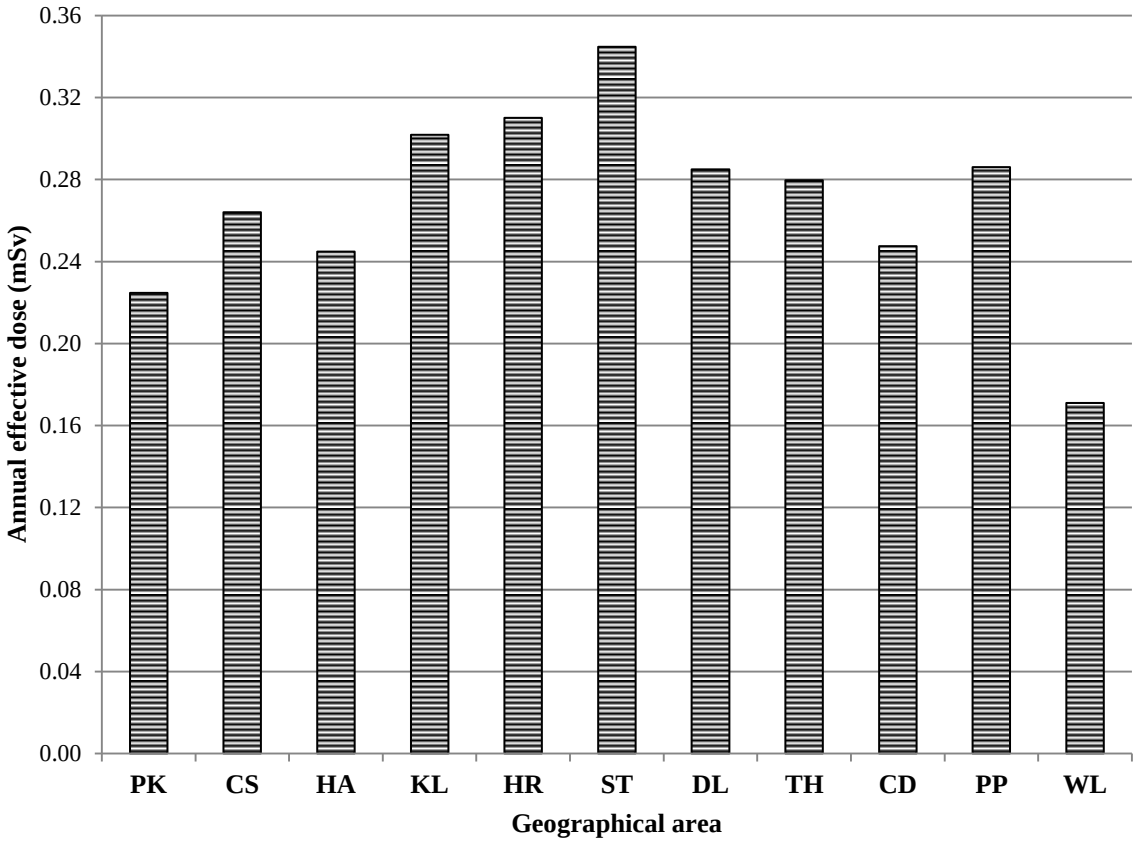

Figure 5.8: Comparison of mean annual effective dose for eleven geographical areas of Arandis.

5.4.3 Natural Radioactivity in Swakopmund

At the coastal town of Swakopmund soil samples were collected from ten geographical areas as shown in Figure 5.9. The activity concentrations of ^{40}K, ^{232}Th and ^{238}U in the soil samples are presented in Table 5.3 (columns 2-4). As observed in Usakos and Arandis, ^{40}K has the highest activity concentration (out of the three radionuclides) in each area of the town with values varying from 447.0 $\pm$ 20.7 Bq kg^{-1} (area JT) to 823.0 $\pm$ 32.0 Bq kg^{-1} (area HH) with a mean of 645.5 $\pm$ 69.5 Bq kg^{-1} (Table 5.3 column 2). As could be observed from Figure 5.10, the concentration of ^{40}K varies slightly from one area to another with the highest value observed at the Hage Heights (HH) area. There are no agricultural activities in the town, hence the high value of ^{40}K is attributed to it's natural abundance in the soil.

The activity concentration of ^{232}Th was found to be the second highest in the town and varied from 26.8 $\pm$ 3.2 Bq kg^{-1} (area VT) to 213.3 $\pm$ 9.1 Bq kg^{-1} (area DR) with a mean of 91.1 $\pm$ 41.0 Bq kg^{-1} (Table 5.3 column 3 and Figure 5.10). As could be observed in Figure 5.10, the highest concentration for ^{232}Th was at the DRC informal settlement area (DR). However, there exists no significant variation in the concentration of ^{232}Th from one geographical area to another.

The concentration of ^{238}U was observed to vary from a minimum of 22.2 $\pm$ 1.8 Bq kg^{-1} (area VT) to a maximum 79.8 $\pm$ 3.8 Bq kg^{-1} (area DR) with a mean of 46.4 $\pm$ 14.2 Bq kg^{-1} as shown in Table 5.3 (column 4). As could be observed in Figure 5.10, there exist no variation of the average values of ^{238}U in the different geographical areas of

Swakopmund. The activity concentrations for the three radionuclides in the soil of Swakopmund are far less than those obtained for the coastal areas of Nigeria, where the total mean concentrations of ^{238}U, ^{232}Th and ^{40}K were reported as 34.95 kBq kg^{-1}, 9.16 kBq kg^{-1} and 283.3 kBq kg^{-1} respectively (Alatise, O.O., Babalola, A.I., Olowofela, J.A.,2008).

The absorbed dose rate was calculated (using equation 5.4) for each of the sites where samples were collected. It was found that the absorbed dose rate varies from a minimum of 49.3 $\pm$ 2.3 nGy h^{-1} (area VT) to a maximum of 192.3 $\pm$ 5.9 nGy h^{-1} (area DR) with an average of 103.4 $\pm$ 30.9 nGy h^{-1} as shown in Table 5.3 (column 5). Also, the absorbed dose rate in the DRC informal settlement (DR) area is the highest among the dose rates in the ten geographical areas of the town as could be observed in Figure 5.11. The values of the absorbed dose rates vary slightly from one area to another (Figure 5.11). These values are within the world range of 28 – 120 nGy h^{-1} but higher than the average value of 56 nGy h^{-1} reported for normal background areas (UNSCEAR, 1993).

The annual effective dose for each site was calculated from the corresponding absorbed dose rate using equation 5.5. The range and mean values of the annual effective dose in the different areas of Swakopmund are presented in Table 5.3 (column 6). The annual effective dose ranged from a low of 0.09 mSv (area VT) to a high of 0.20 mSv (area DR) with a mean of 0.13 mSv $\pm$ 0.04 (Table 5.3 column 6). A comparison of mean annual effective dose for ten geographical areas of Swakopmund is shown in Figure 5.12. As could be observed in the figure, the highest value is found at the DRC informal

settlement (DR) area. The average value of 0.13 mSv obtained for the annual effective dose in the town is the same as that obtained for Usakos and is below the range for annual external dose rate of 0.3-1.0 mSv estimated for the public (UNSCEAR, 2008). This baseline value obtained indicates that the town of Swakopmund has normal background radiation.

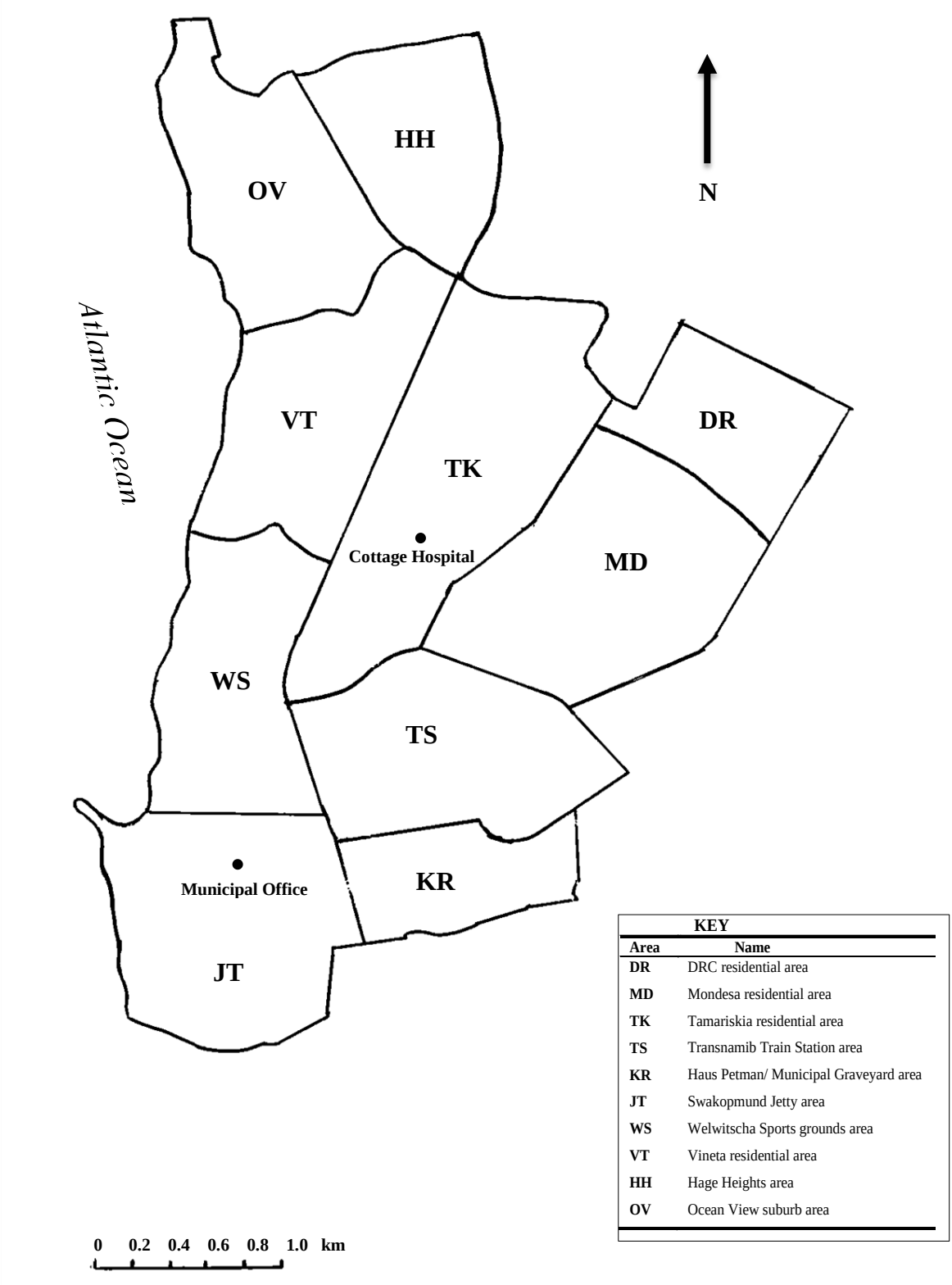

Figure 5.9: Map showing the ten geographical areas where soil samples were collected in Swakopmund.

Table 5.3: Average (± standard deviation) radionuclide concentrations, absorbed dose rates and annual effective doses in ten geographical areas of Swakopmund. The corresponding range of values is given in parentheses.

Area	Radionuclide concentration (Bq kg^{-1})			Absorbed dose rate (nGy h^{-1})	Annual effect. dose (mSv)
	^{40}K	^{232}Th	^{238}U		
DR	661.2 ± 36.2	167.6 ± 32.4	68.1 ± 13.2	160.3 ± 24.6	0.20 ± 0.03
	(610.1 – 695.3)	*(125.5 – 213.3)*	*(48.0 – 79.8)*	*(126.0 – 192.3)*	*(0.16 – 0.24)*
MD	672.6 ± 52.0	107.3 ± 42.6	52.3 ± 16.8	117.0 ± 31.6	0.14 ± 0.04
	(610.1 – 733.1)	*(68.8 – 174.1)*	*(36.5 – 75.4)*	*(88.3 – 165.5)*	*(0.11 – 0.20)*
TK	651.8 ± 20.5	84.1 ± 20.8	45.4 ± 5.4	98.9 ± 14.8	0.12 ± 0.02
	(633.8 – 685.8)	*(60.2 – 114.2)*	*(40.0 – 54.4)*	*(81.9 – 120.7)*	*(0.10 – 0.15)*
TS	640.4 ± 42.9	70.7 ± 13.1	41.9 ± 7.4	88.8 ± 11.9	0.11 ± 0.01
	(591.2 – 690.5)	*(51.9 – 88.2)*	*(28.9 – 46.5)*	*(69.8 – 102.5)*	*(0.09 – 0.13)*
KR	613.0 ± 54.0	59.8 ± 22.8	35.3 ± 9.6	78.0 ± 19.0	0.10 ± 0.02
	(525.0 – 662.2)	*(32.1 – 87.5)*	*(25.6 – 46.4)*	*(53.1 – 99.3)*	*(0.07 – 0.12)*
JT	572.0 ± 106.6	91.7 ± 32.8	45.6 ± 13.5	100.3 ± 21.9	0.12 ± 0.03
	(447.0 – 657.4)	*(58.5 – 135.1)*	*(31.0 – 63.5)*	*(76.3 – 129.6)*	*(0.09 – 0.16)*
WS	651.8 ± 55.9	65.2 ± 16.3	36.4 ± 6.2	83.4 ± 14.4	0.10 ± 0.02
	(591.2 – 704.7)	*(48.0 – 84.4)*	*(31.1 – 45.8)*	*(68.0 – 101.6)*	*(0.08 – 0.13)*
VT	648.9 ± 61.2	55.0 ± 17.9	34.9 ± 8.3	76.4 ± 16.4	0.09 ± 0.02
	(548.7 – 704.7)	*(26.8 – 71.7)*	*(22.2 – 42.1)*	*(49.3 – 90.4)*	*(0.06 – 0.11)*
HH	747.3 ± 55.5	91.7 ± 28.2	47.2 ± 12.5	108.3 ± 21.4	0.13 ± 0.03
	(685.8 – 823.0)	*(51.2 – 130.0)*	*(32.5 – 66.6)*	*(77.9 – 137.9)*	*(0.10 – 0.17)*
OV	596.0 ± 56.8	118.1 ± 36.2	57.2 ± 12.2	122.6 ± 25.2	0.15 ± 0.03
	(525.0 – 657.4)	*(74.9 – 149.4)*	*(42.0 – 71.0)*	*(91.4 – 143.5)*	*(0.11 – 0.18)*
All samples	**645.5 ± 69.5**	**91.1 ± 39.6**	**46.4 ± 14.2**	**103.4 ± 30.9**	**0.13 ± 0.04**
	(447.*0* – *823.0*)	**(26.*8* – *213.3*)**	**(22.*2* – *79.8*)**	**(49.*3* – *192.3*)**	**(*0.06* – *0.24*)**

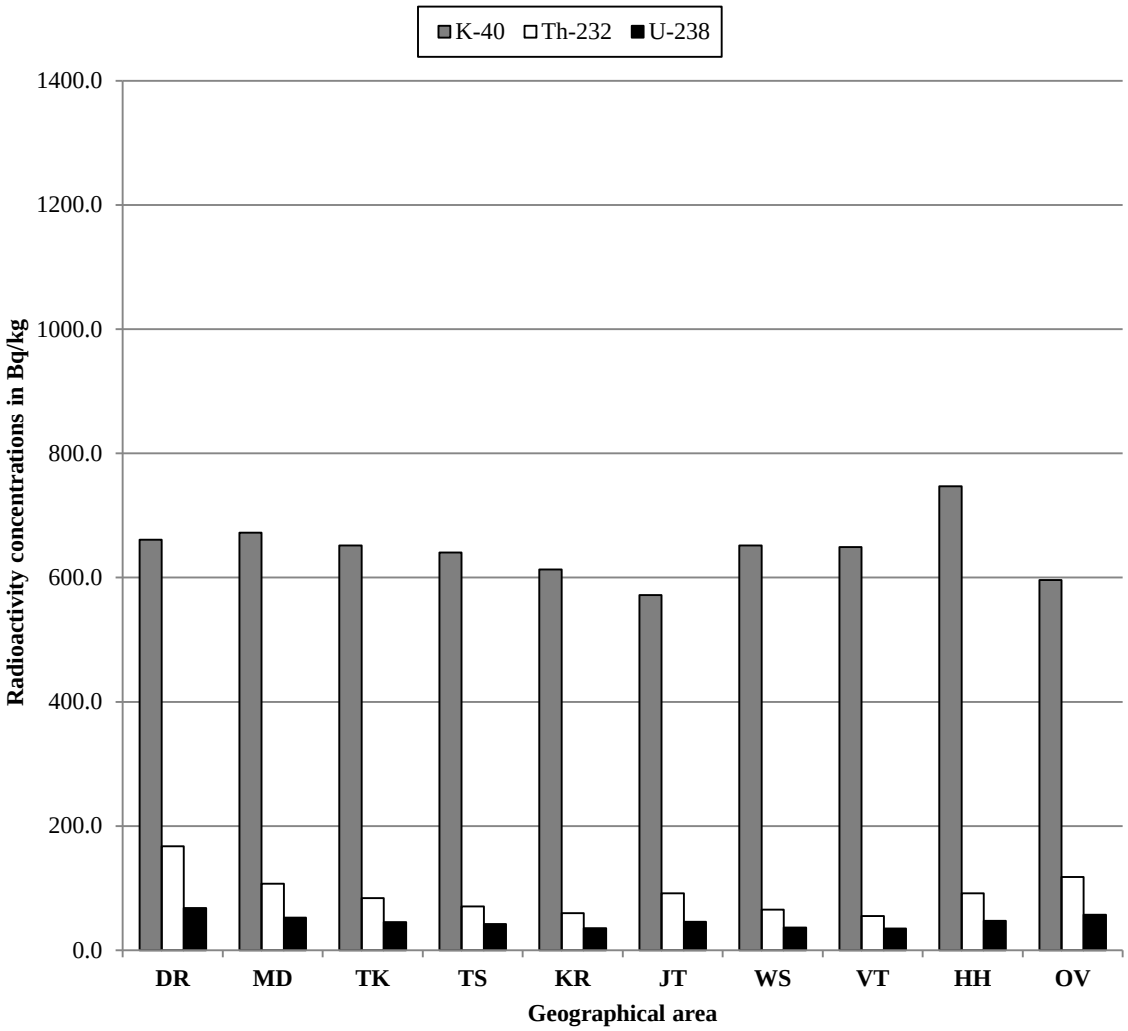

Figure 5.10: Comparison of mean activity concentrations of ^{40}K, ^{232}Th and ^{238}U for the ten geographical areas of Swakopmund.

.

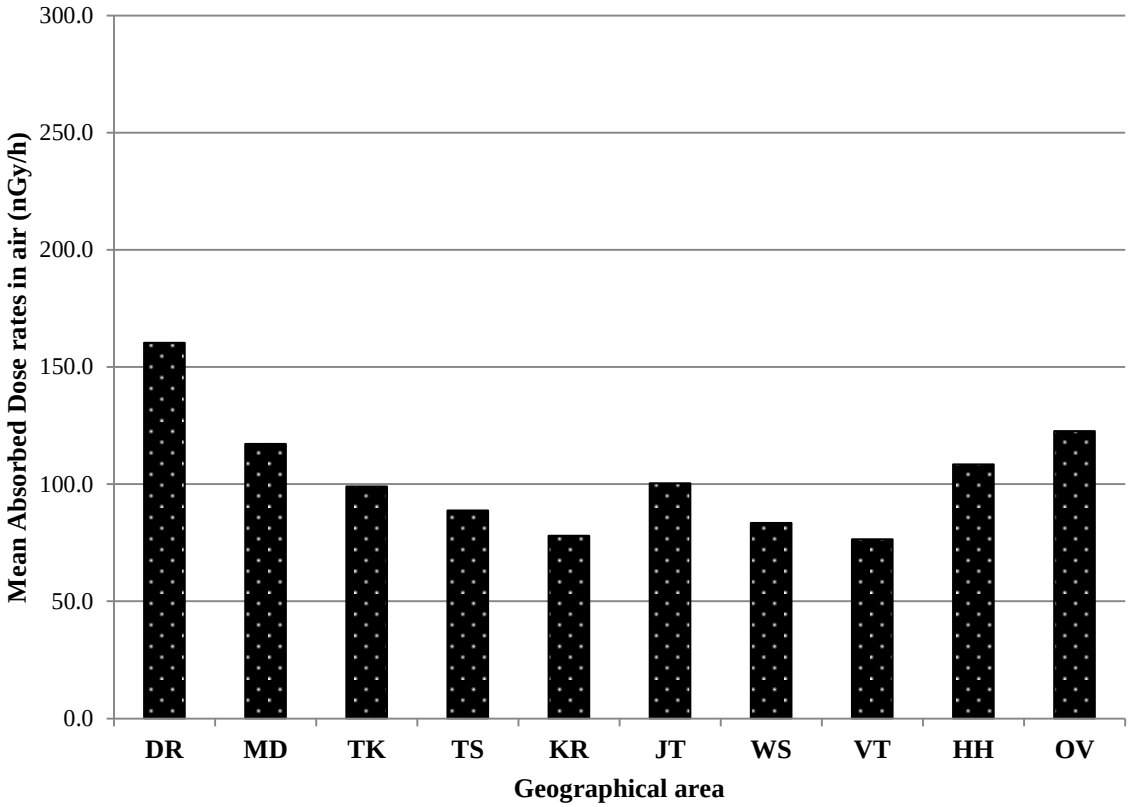

Figure 5.11: Comparison of mean absorbed dose rates for ten geographical areas of Swakopmund.

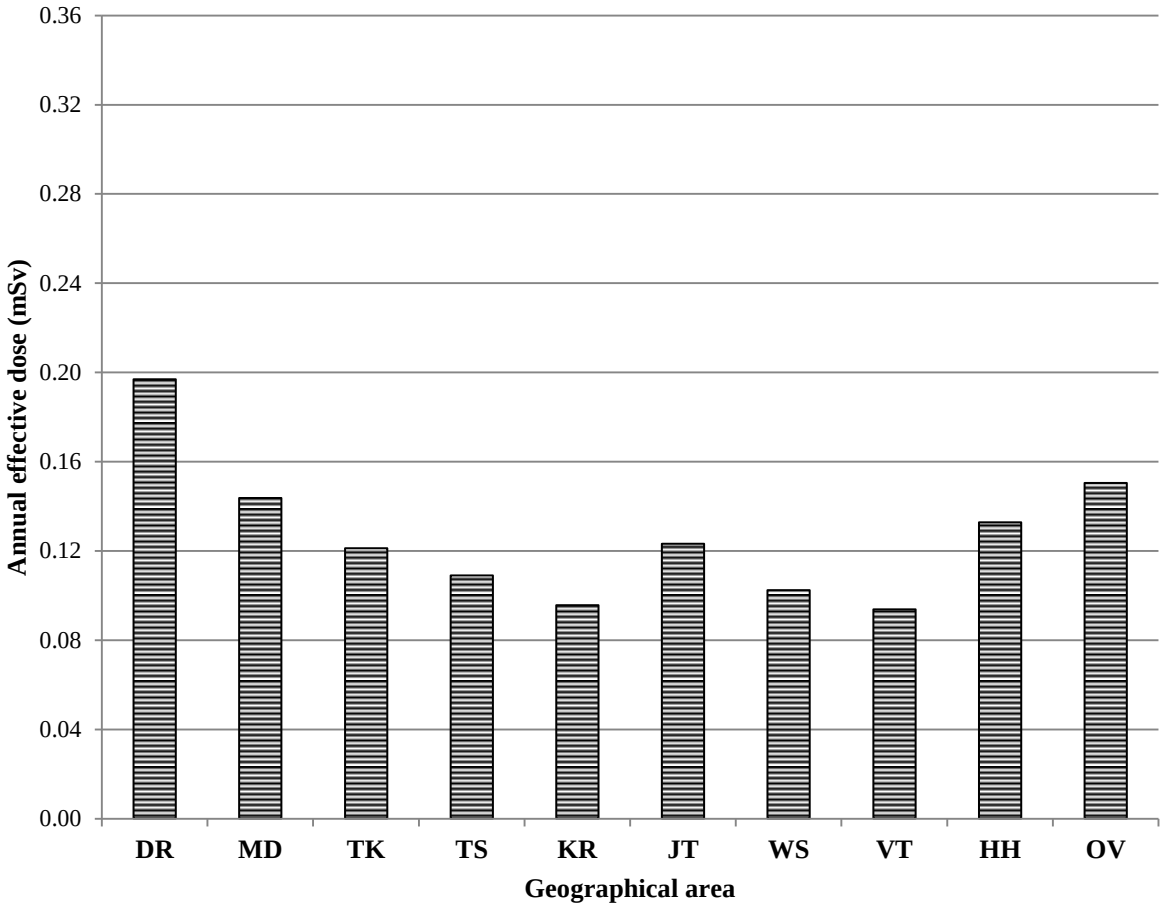

Figure 5.12: Comparison of mean annual effective dose for ten geographical areas of Swakopmund**.**

5.4.4 Natural radioactivity in Walvis Bay

The ten geographical areas where samples were collected in Walvis Bay are shown in Figure 5.13. The range and mean of activity concentrations of the radionuclides ^{40}K, ^{232}Th and ^{238}U in the soil samples collected from the ten geographical areas of Walvis Bay are presented in Table 5.4 (columns 2-4) and shown in Figure 5.14. The activity concentration for ^{40}K was observed to be the highest and range from a minimum of 317.5 ± 15.9 Bq kg^{-1} (at MM) to a maximum of 663.9 ± 27.0 Bq kg^{-1} (at NR) with a mean of 460.3 ± 76.2 Bq kg^{-1} (Table 5.4 column 2). Figure 5.14 shows a comparison of mean activity concentrations of ^{40}K for the ten geographical areas of Walvis Bay. These values indicate no significant variation from area to area.

^{232}Th was found to have the second highest concentration and the values varied from a minimum of 12.7 ± 2.4 Bq kg^{-1} (at MM) to a maximum of 52.1 ± 4.0 Bq kg^{-1} (at NR) with a mean of 23.8 ± 8.4 Bq kg^{-1} (Table 5.4 column 3). This average concentration is much lower than that of ^{40}K as could be seen in Figure 5.14. There was almost no variation of the mean values of ^{232}Th from one geographical area to another. These values are also much lower than those obtained for Usakos, Arandis and Swakopmund.

For ^{238}U, the activity concentration ranged from 11.4 ± 1.5 Bq kg^{-1} (at PK) to 29.5 ± 2.3 Bq kg^{-1} (at NR) with a mean of 18.6 ± 4.6 Bq kg^{-1} as shown in Table 5.4 (column 4). The average concentration of ^{238}U did not show much variation from one area to another as could be observed in Figure 5.14. However, the values of the average concentrations

are lower than those of Usakos, Arandis and Swakopmund. The average concentration of the radionuclides ^{40}K, ^{232}Th and ^{238}U are comparable to the corresponding worldwide average values (UNSCEAR, 2008).

Using the values obtained for the activity concentrations of ^{40}K, ^{232}Th and ^{238}U in the samples, the absorbed dose rates for all the sites were calculated. The absorbed dose rate varies from 28.0 $\pm$ 2.9 nGy h^{-1} (at MM) to 71.7 $\pm$ 2.9 nGy h^{-1} (at NR) with a mean value of 42.1 $\pm$ 9.2 nGy h^{-1} as shown in Table 5.4 (column 5). Figure 5.15 shows a comparison of mean absorbed dose rates for the ten geographical areas of Walvis Bay. As could be observed in the figure, all the mean dose rates, with the exception of one, are less than 50 nGy h^{-1}. The average value of the absorbed dose rates is very low and showed no specific trend from area to area. These values are far less than the world average outdoor value of 58 nGy h^{-1} reported for normal background areas (UNSCEAR, 1993).

The annual effective dose for each site in the town was calculated from the corresponding absorbed dose rate and found to vary from 0.03 mSv (at MM) to 0.09 mSv (at NR) with a mean of 0.05 mSv (Table 5.4 column 6). Figure 5.16 shows a comparison of the mean effective dose rate for the different areas. As could be observed in the figure, the annual effective dose does not vary widely from one area to another. Also, the mean values of the effective dose rate are below the maximum permissible annual dose of 1.0 mSv recommended by the ICRP. Hence, it can be concluded that Walvis Bay has normal background radiation.

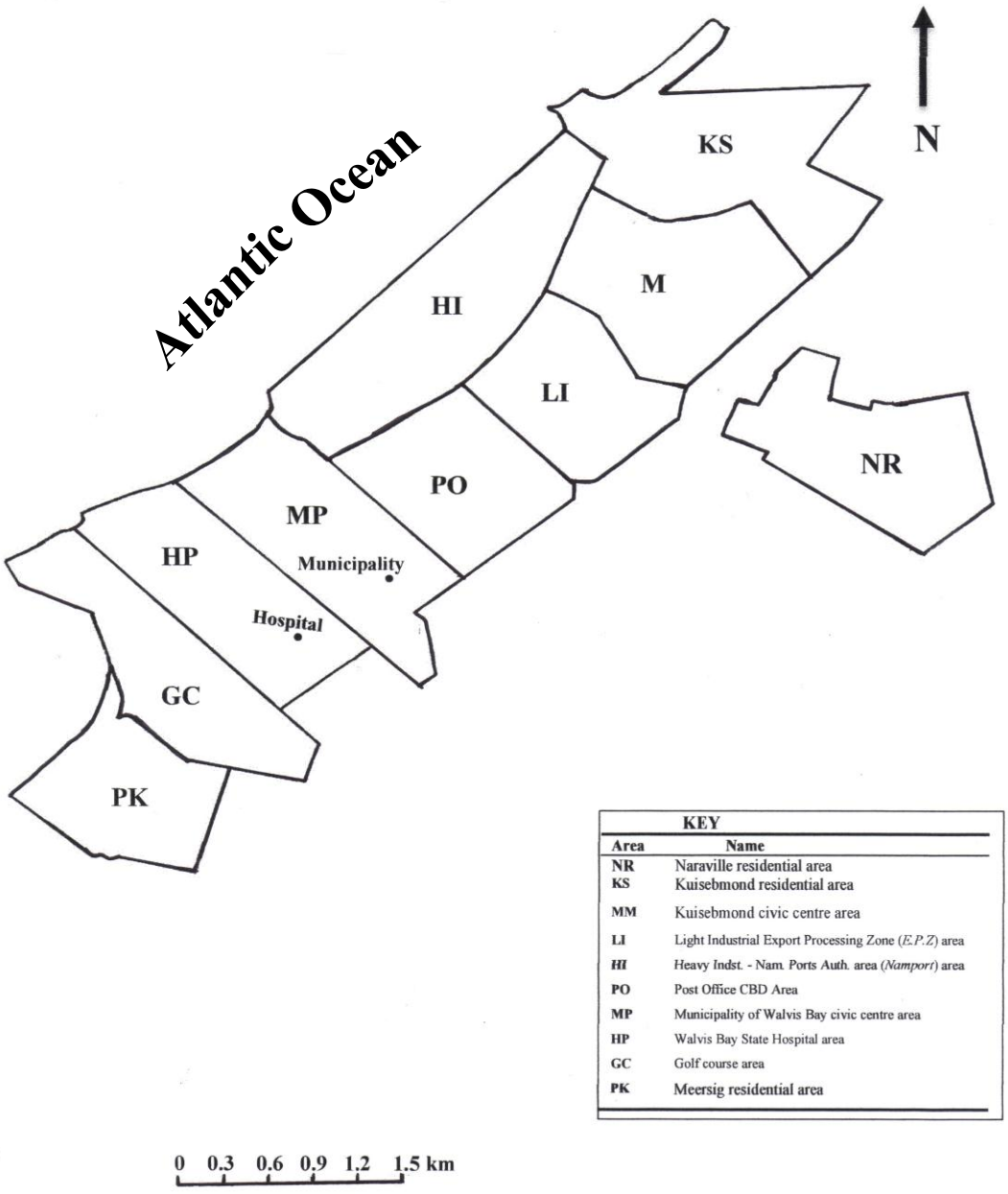

Figure 5.13: Map showing the ten geographical areas where soil samples were collected in Walvis Bay.

Table 5.4: Average (± standard deviation) radionuclide concentrations, absorbed dose rates and annual effective doses in ten geographical areas of Walvis Bay. The corresponding range of values is given in parentheses.

Area	Radionuclide concentration (Bq kg^{-1})			Absorbed dose rate (nGy h^{-1})	Annual effect. dose (mSv)
	^{40}K	^{232}Th	^{238}U		
NR	586.9 ± 44.8	39.7 ± 7.2	27.2 ± 1.8	61.0 ± 6.2	0.08 ± 0.01
	(548.5 – 663.9)	*(33.9 – 52.1)*	*(24.5 – 29.5)*	*(56.1 – 71.7)*	*(0.07 – 0.09)*
KS	383.2 ± 41.3	20.5 ± 9.6	17.0 ± 5.7	36.2 ± 9.9	0.05 ± 0.01
	(348.8 – 449.4)	*(12.8 – 37.2)*	*(11.9 – 26.6)*	*(30.1 – 53.5)*	*(0.04 – 0.07)*
MM	363.2 ± 50.8	18.0 ± 3.0	14.5 ± 2.5	32.7 ± 4.0	0.04 ± 0.01
	(317.5 – 427.2)	*(12.7 – 19.6)*	*(11.8 – 17.7)*	*(28.0 – 36.9)*	*(0.03 – 0.05)*
LI	451.1 ± 19.3	22.5 ± 3.6	17.0 ± 2.3	40.2 ± 3.0	0.05 ± 0.004
	(421.0 – 468.1)	*(18.7 – 27.6)*	*(14.5 – 20.3)*	*(36.2 – 44.5)*	*(0.04 – 0.06)*
HI	457.8 ± 26.7	23.3 ± 4.9	17.9 ± 3.0	41.4 ± 4.2	0.05 ± 0.01
	(434.9 – 500.3)	*(19.8 – 31.8)*	*(15.7 – 23.2)*	*(38.0 – 48.5)*	*(0.05 – 0.06)*
PO	530.4 ± 82.8	21.2 ± 3.2	19.3 ± 1.6	43.8 ± 4.5	0.05 ± 0.01
	(447.4 – 654.3)	*(18.1 – 25.6)*	*(17.4 – 21.3)*	*(38.3 – 48.5)*	*(0.05 – 0.06)*
MP	467.0 ± 43.0	29.4 ± 10.1	19.7 ± 4.9	46.4 ± 9.2	0.06 ± 0.01
	(404.6 – 500.3)	*(17.7 – 45.1)*	*(13.6 – 24.7)*	*(35.3 – 59.2)*	*(0.04 – 0.07)*
HP	457.1 ± 37.1	24.4 ± 3.3	18.8 ± 1.6	42.5 ± 3.6	0.05 ± 0.00
	(404.6 – 505.2)	*(19.9 – 28.1)*	*(17.0 – 20.7)*	*(38.3 – 47.6)*	*(0.05 – 0.06)*
G C	416.1 ± 59.5	20.7 ± 6.8	18.0 ± 4.5	38.2 ± 7.1	0.05 ± 0.01
	(330.0 – 485.9)	*(15.7 – 32.5)*	*(12.4 – 23.3)*	*(31.5 – 48.0)*	*(0.04 – 0.06)*
PK	490.4 ± 31.4	18.3 ± 5.5	16.1 ± 4.3	38.9 ± 5.8	0.05 ± 0.01
	(436.4 – 514.8)	*(14.1 – 27.7)*	*(11.4 – 23.2)*	*(32.3 – 48.1)*	*(0.04 – 0.06)*
All samples	**460.3 ± 76.2**	**23.8 ± 8.4**	**18.6 ± 4.6**	**42.1 ± 9.2**	**0.05 ± 0.01**
	(317.5 – 663.9)	***(12.7 – 52.1)***	***(11.4 – 29.5)***	***(28.0 – 71.7)***	***(0.03 – 0.09)***

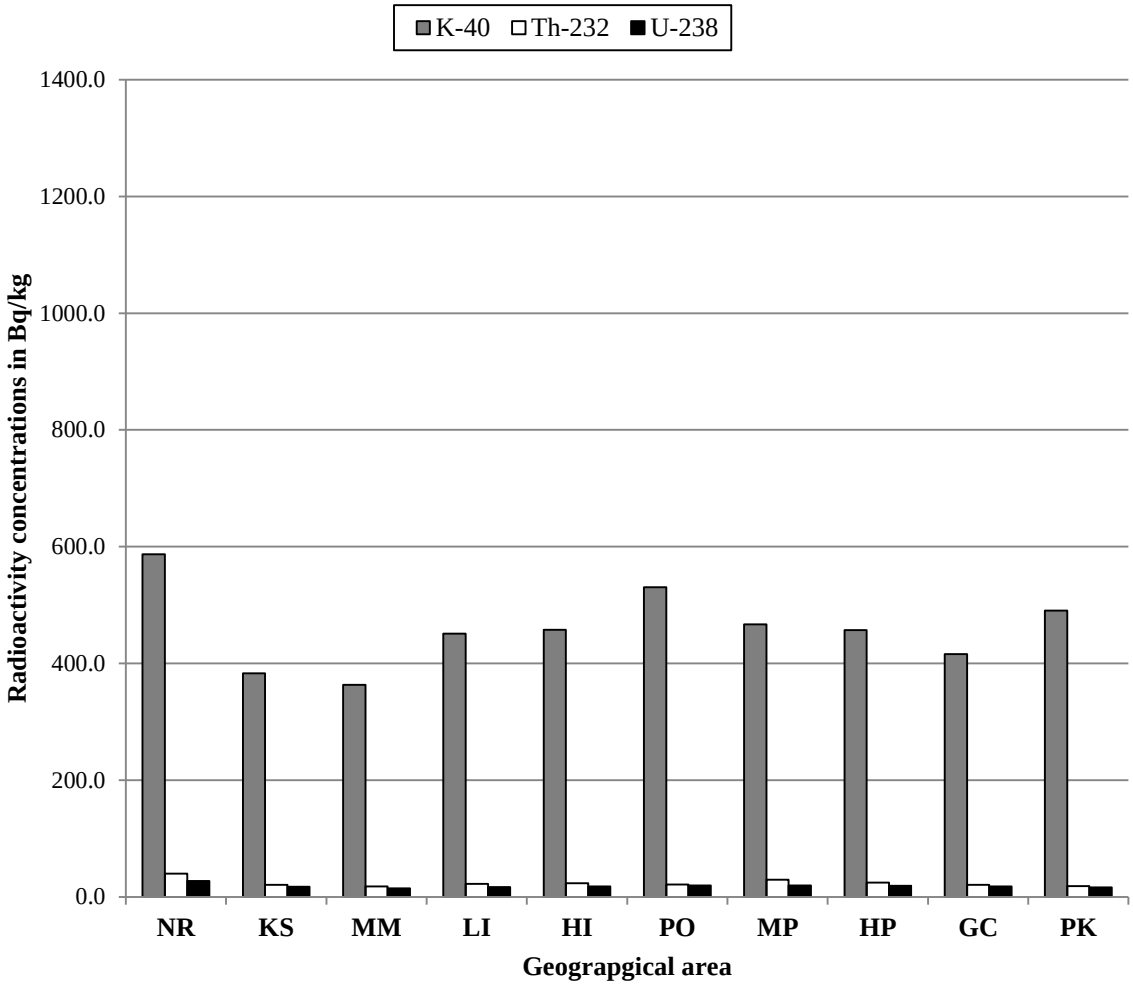

Figure 5.14: Comparison of mean activity concentrations of ^{40}K, ^{232}Th and ^{238}U for the ten geographical areas of Walvis Bay.

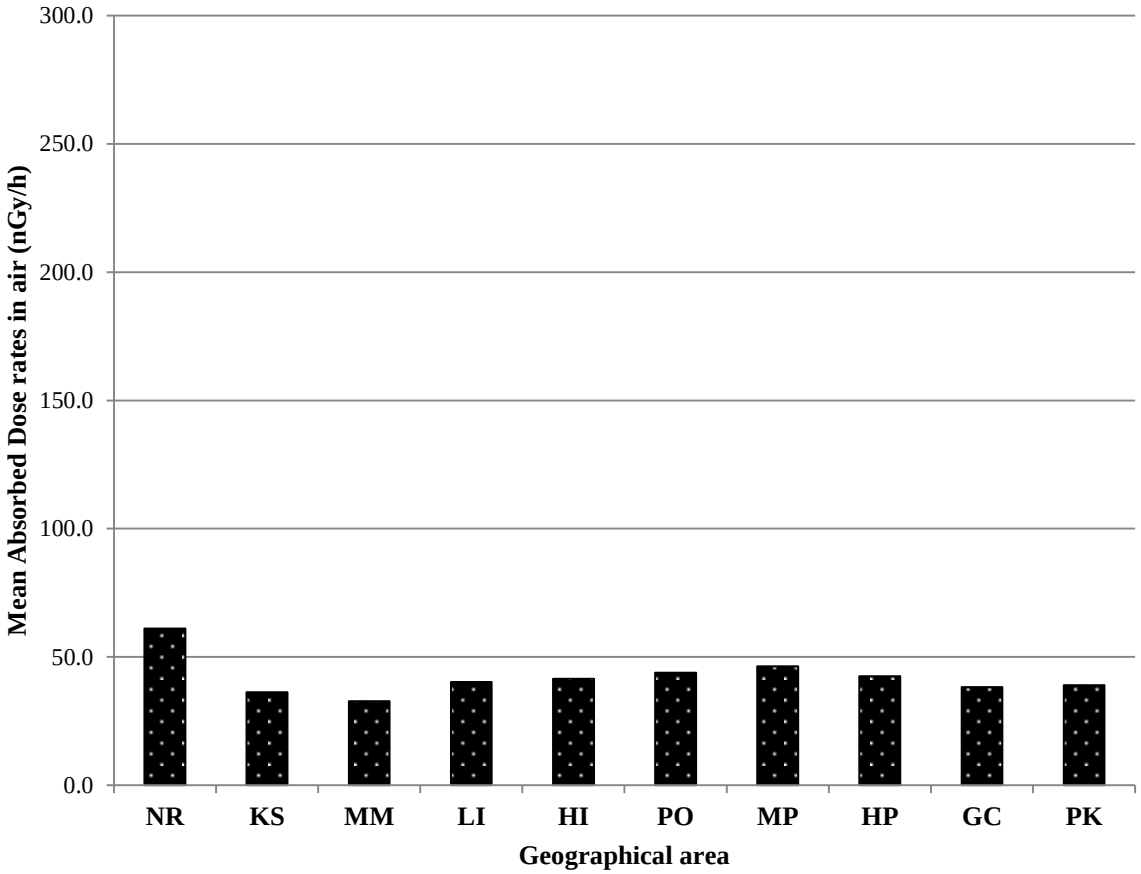

Figure 5.15: Comparison of mean absorbed dose rates for ten geographical areas for Walvis Bay**.**

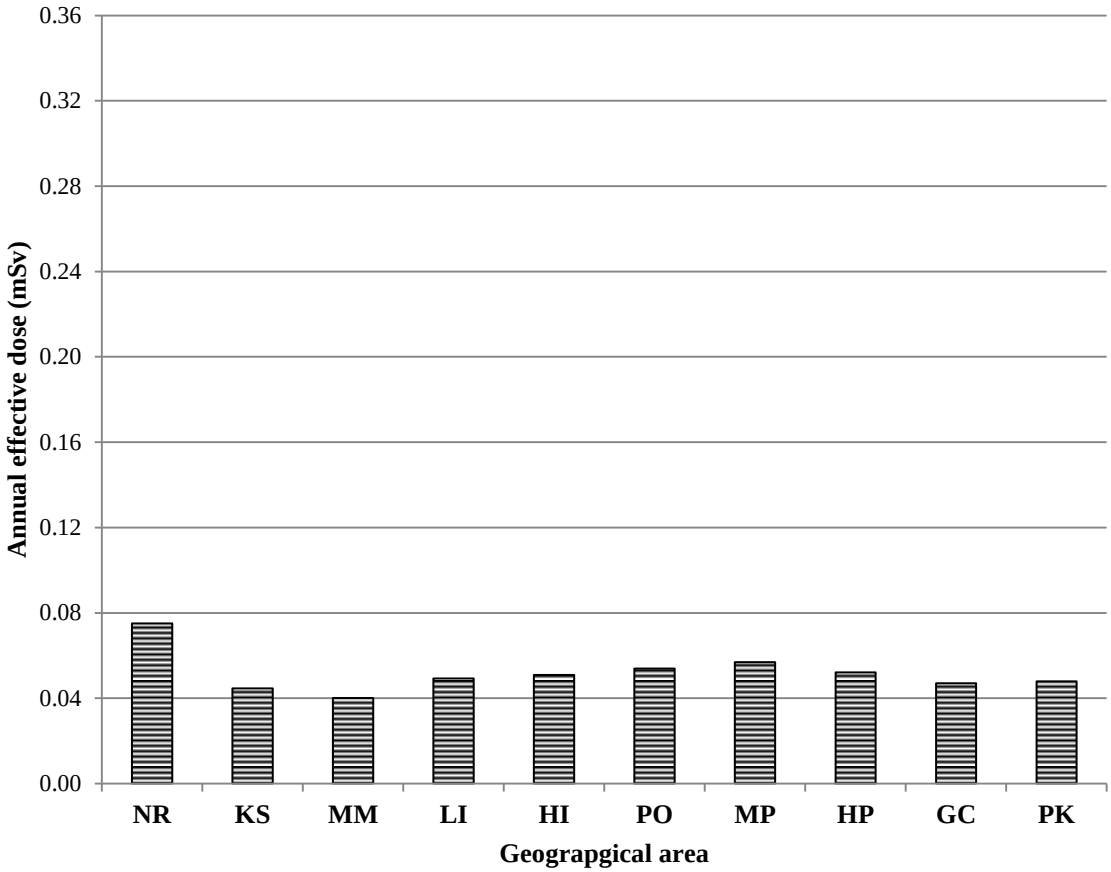

Figure 5.16: Comparison of mean annual effective dose for ten geographical areas of Walvis Bay.

5.4.5 Natural radioactivity in Wlotzkasbaken

Wlotzkasbaken is a small settlement situated at the Namibian coastline on the road from Swakopmund to Hentiesbay. Also, the ten geographical areas where soil samples were collected (five samples per area) are shown in Figure 5.17. The range and mean of the radionuclides ^{40}K, ^{232}Th and ^{238}U in the soil samples collected from the ten geographical areas of Wlotzkasbaken are presented in Table 5.5 (column 2-4) and shown in Figure 5.18. The concentration of ^{40}K in the soil of the settlement varied from 385.4 $\pm$ 4.1 Bq kg^{-1} (at AA) to 832.3 $\pm$ 32.2 Bq kg^{-1} (at FF) with a mean of 759.2 $\pm$ 68.4 Bq kg^{-1} (Table 5.5 column 2). Again, the mean concentration of ^{40}K was observed to be the highest (out of the three radionuclides) for the settlement. However, these values are still less than those obtained for Usakos and Arandis (as discussed in section 5.4.1 & 5.4.2). As could be observed in Figure 5.18, there is a slight variation of the average concentration of ^{40}K from one area to another but all the values are comparable to the worldwide average value of 412 Bq kg^{-1} (UNSCEAR, 2008).

The concentrations of ^{232}Th for all the sites where samples were collected at the settlement ranged from 26.8 $\pm$ 3.3 Bq kg^{-1} (at AA) to 223.5 $\pm$ 9.6 Bq kg^{-1} (at BB and CC) with a mean of 79.5 $\pm$ 44.1 Bq kg^{-1} (Table 5.5 column 3). As could be observed in Figure 5.18, the average concentration values of ^{232}Th vary from area to area. These values are comparable to those obtained for Usakos (Table 5.1 column 3) and hence they are also higher than the worldwide average value of 45 Bq kg^{-1} (UNSCEAR, 2008).

^{238}U has the lowest activity concentration (among the three radionuclides) in all the areas as could be observed in Figure 5.18. The concentration ranged from 30.9 $\pm$ 2.2 Bq kg^{-1} (at JJ) to 153.7 $\pm$ 5.4 Bq kg^{-1} (at CC) with a mean of 69.6 $\pm$ 26.3 Bq kg^{-1} (Table 5.5 column 4). As could be observed in Figure 5.18, the mean activity concentration of ^{238}U and ^{232}Th were almost similar for all the geographical areas. The low values for ^{238}U is also an indication that no large deposits of uranium exist at the settlement.

The corresponding absorbed dose rate values for the sites where samples were collected were calculated using the concentrations of ^{40}K, ^{232}Th and ^{238}U and equation 5.4. The absorbed dose rate values are presented in Table 5.5 (column 5) and shown in Figure 5.19. These values vary from a low of 31.1 $\pm$ 2.9 nGy h^{-1} (at FF) to 236.7 $\pm$ 6.4 nGy h^{-1} (at BB and CC) with a mean of 110.8 $\pm$ 40.3 nGy h^{-1} (Table 5.5). As could be observed in Figure 5.19, the absorbed dose rate does not vary widely from one area to another. It should be noted that the overall mean value of the absorbed dose is almost twice the worldwide average value of 58 nGy h^{-1} reported for normal background areas (UNSCEAR, 2008).

All the values obtained for the absorbed dose rate were used to calculate the corresponding annual effective dose rate values for the different sites (using equation 5.5). The annual effective dose values for the settlement was found to range from a minimum value of 0.06 mSv (at AA and FF) to a maximum of 0.29 mSv (at BB and CC) with a mean of 0.14 $\pm$ 0.05 mSv (Table 5.5 column 6). Figure 5.20 shows a comparison of the average annual effective dose for the ten geographical areas where samples were

collected at Wlotzkasbaken. As could be seen in the figure, the mean annual effective dose varies only slightly from one area to another, with the highest values observed for areas to the north of the Wlotzkasbaken (close to the entrance to the settlement). The average value of 0.14 mSv obtained for the annual effective dose rate represents only 29.2% of the reported worldwide average value of 0.48 mSv (UNSCEAR, 2000). This baseline value indicates that Wlotzkasbaken has a normal background radiation.

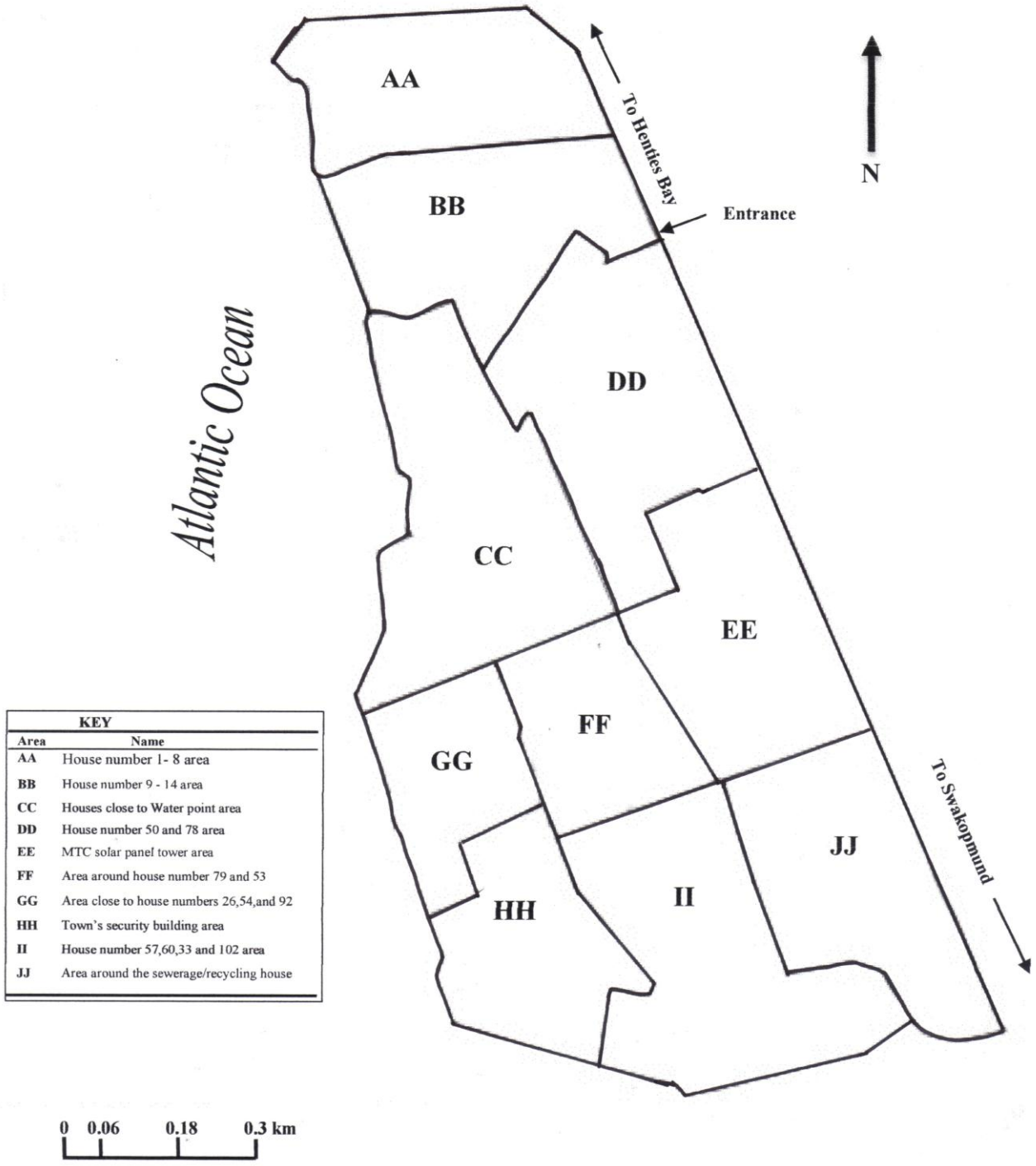

Figure 5.17: Map showing the ten geographical areas where soil samples were collected in Wlotzkasbaken.

Table 5.5: Average (± standard deviation) radionuclide concentrations, absorbed dose rates and annual effective doses in ten geographical areas of Wlotzkasbaken. The corresponding range of values is given in parentheses.

Area	Radionuclide concentration (Bq kg^{-1})			Absorbed dose rate (nGy h^{-1})	Annual effect. dose (mSv)
	^{40}K	^{232}Th	^{238}U		
A A	659.2 ± 164.2	102.5 ± 48.1	82.9 ± 30.8	127.7 ± 50.0	0.16 ± 0.06
	(385.4 – 798.6)	*(26.8 – 154.4)*	*(34.7 – 117.1)*	*(48.3 – 180.7)*	*(0.06 – 0. 22)*
BB	754.4 ± 12.9	133.2 ± 51.2	104.1 ± 28.1	160.0 ± 43.4	0.20 ± 0.05
	(736.1 – 765.0)	*(100.9 – 223.5)*	*(84.3– 153.7)*	*(131.8 – 236.7)*	*(0.16 – 0.29)*
CC	759.1 ± 26.2	126.9 ± 57.3	97.9 ± 33.0	153.5 ± 49.1	0.19 ± 0.06
	(736.1 – 793.8)	*(80.7 – 223.5)*	*(75.9 – 153.7)*	*(117.5 – 236.7)*	*(0.14 – 0.29)*
D D	781.3 ± 18.5	75.9 ± 37.0	66.2 ± 20.6	109.0 ± 31.7	0.13 ± 0.04
	(755.3 – 803.4)	*(37.9 – 128.5)*	*(43.5 – 92.0)*	*(75.5 – 152.4)*	*(0.09 – 0.19)*
EE	774.6 ± 21.3	62.8 ± 18.7	59.4 ± 8.8	97.7 ± 15.1	0.12 ± 0.02
	(745.7 – 803.4)	*(40.4 – 91.0)*	*(46.9 – 67.5)*	*(78.6 – 118.1)*	*(0.10 – 0.15)*
FF	783.2 ± 52.5	54.4 ± 19.0	56.0 ± 10.1	81.0 ± 31.4	0.10 ± 0.03
	(707.2 – 832.3)	*(40.2 – 86.2)*	*(46.7 – 72.0)*	*(31.1 – 116.8)*	*(0.06 – 0.14)*
GG	755.3 ± 54.1	55.4 ± 23.3	55.3 ± 13.9	90.5 ± 18.3	0.11 ± 0.02
	(673.5 – 798.6)	*(32.9 – 84.0)*	*(41.6 – 70.1)*	*(73.0 – 110.9)*	*(0.09 – 0.14)*
H H	772.7 ± 41.8	53.6 ± 10.2	51.5 ± 6.2	88.4 ± 8.0	0.11 ± 0.01
	(726.5 – 817.9)	*(38.5 – 64.9)*	*(45.5 – 61.4)*	*(77.8 – 97.8)*	*(0.10 – 0.12)*
II	810.2 ± 23.7	73.0 ± 36.4	69.3 ± 16.5	109.9 ± 29.6	0.13 ± 0.04
	(769.8 – 827.5)	*(42.9 – 135.7)*	*(55.8 – 97.1)*	*(87.2 – 161.2)*	*(0.11 – 0.20)*
J J	741.9 ± 52.2	56.8 ± 32.7	53.3 ± 21.6	89.9 ± 30.9	0.11 ± 0.04
	(659.1 – 789.0)	*(27.7 – 103.7)*	*(30.9 – 84.9)*	*(58.5 – 134.8)*	*(0.07 –0. 17)*
All samples	**759.2 ± 68.4**	**79.5 ± 44.1**	**69.6 ± 26.3**	**110.8 ± 40.3**	**0.14 ± 0.05**
	(385.4 – 832.3)	***(26.8 – 223.5)***	***(30.9 – 153.7)***	***(31.1 – 236.7)***	***(0.06 – 0.29)***

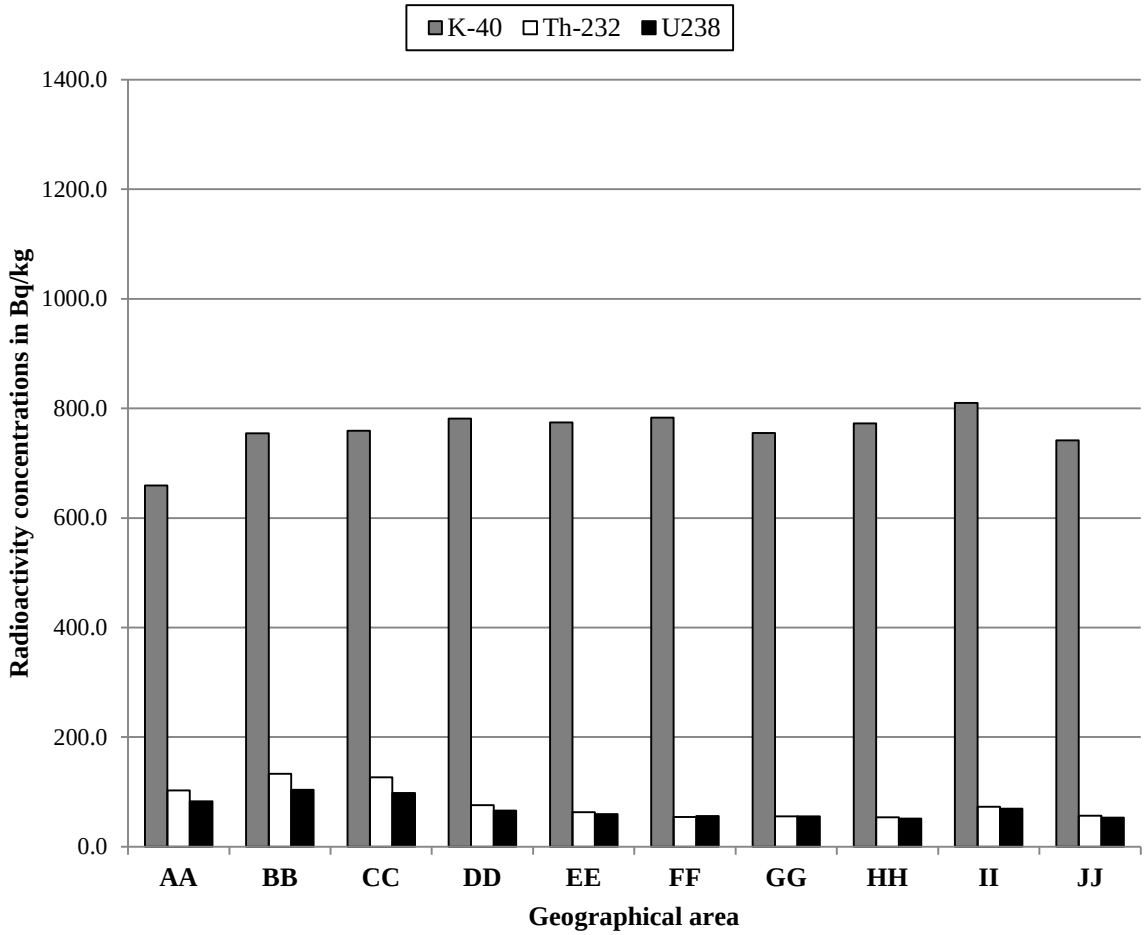

Figure 5.18: Comparison of mean activity concentrations of ^{40}K, ^{232}Th and ^{238}U for the ten geographical areas of Wlotzkasbaken.

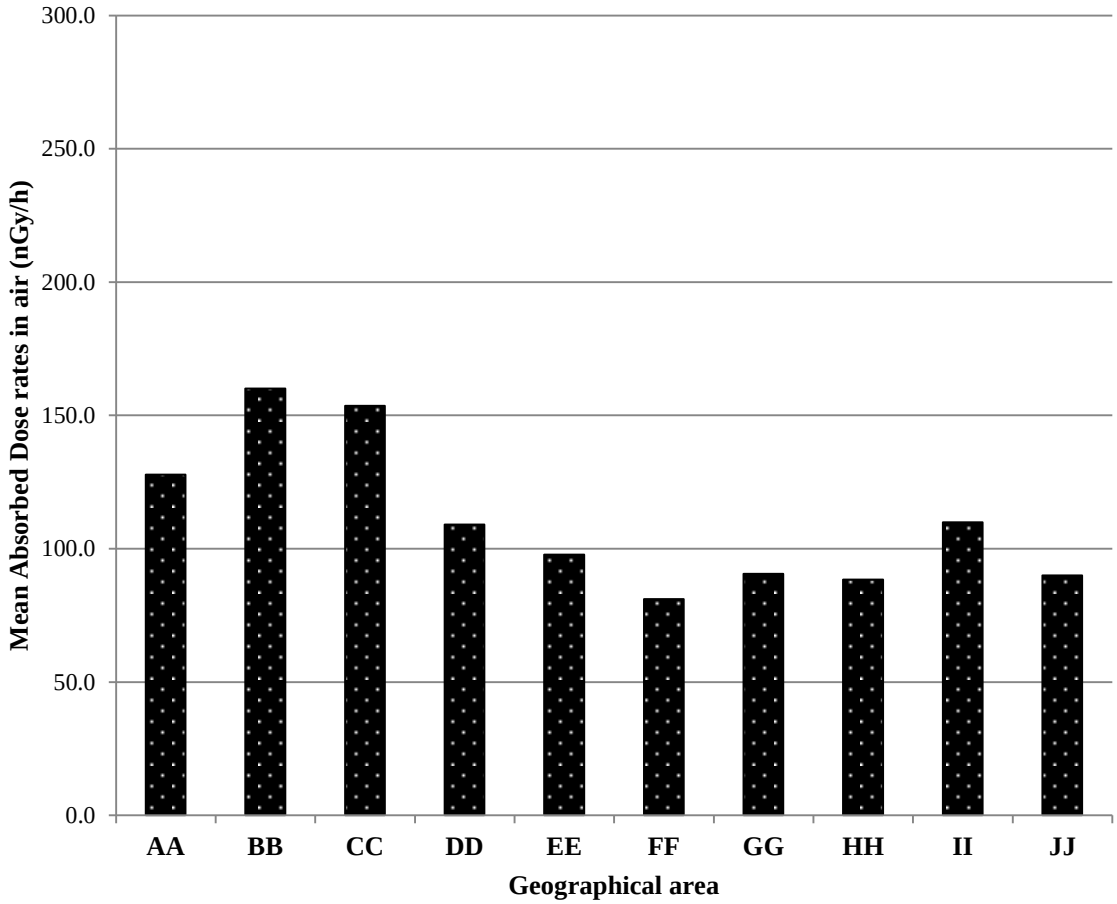

Figure 5.19: Comparison of mean absorbed dose rates for ten geographical areas for Wlotzkasbaken.

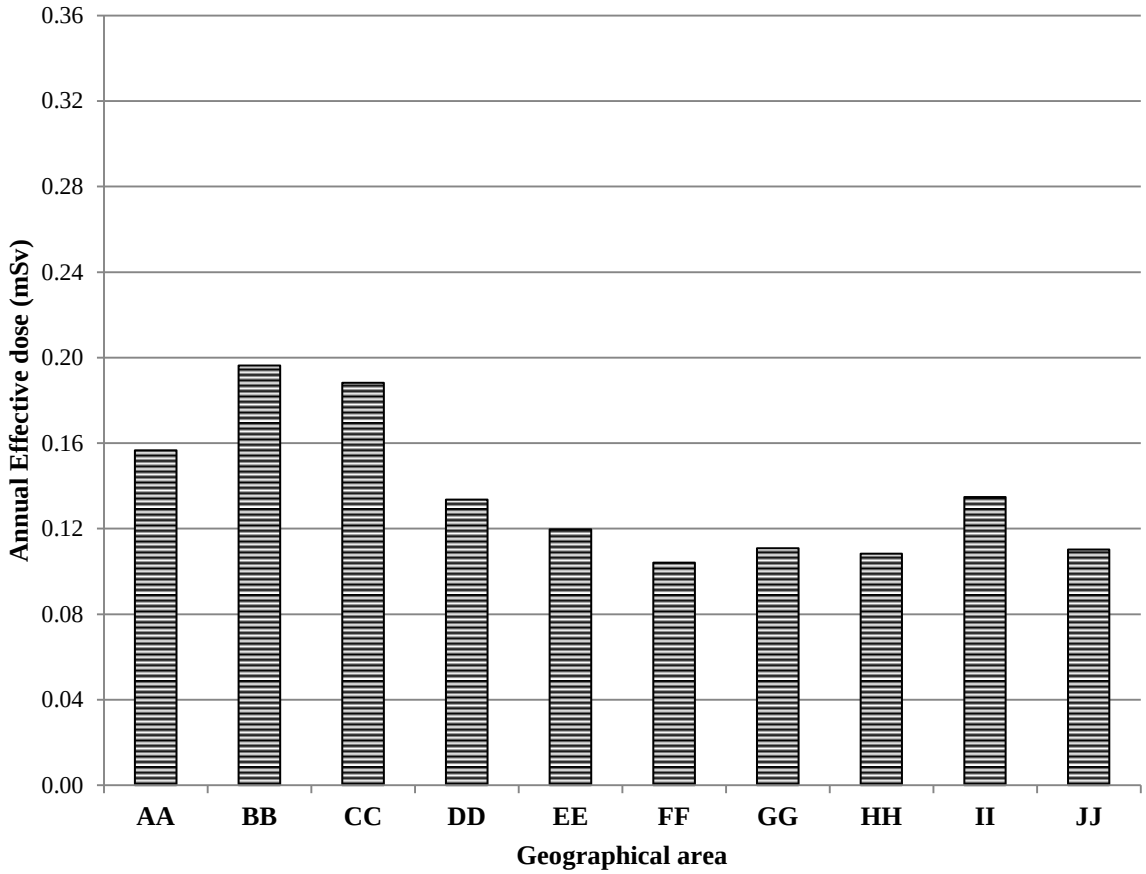

Figure 5.20: Comparison of mean annual effective dose for ten geographical areas of Wlotzkasbaken.

5.4.6 Natural radioactivity in Henties Bay

A total of fifty soil samples (five samples per area) were collected from the ten geographical areas of Henties Bay shown in Figure 5.21.The concentrations of ^{40}K, ^{238}U and ^{232}Th in the soil samples for the different sites were determined and the results are summarized in Table 5.6 (columns 2-4) and shown in Figure 5.22. As could be seen in the figure, the concentrations of ^{40}K was found to be the highest and varied from 790.2 ± 31.6 Bq kg^{-1} (at BU) to 1039.0 ± 38.7 Bq kg^{-1} (at MP) with a mean of 936.1 ± 68.5 Bq kg^{-1} (Table 5.6 column 2). The average concentration of ^{40}K (936.1 ± 68.5 Bq kg^{-1}) is much higher than the values obtained for ^{238}U (62.2 ± 20.0 Bq kg^{-1}) and ^{232}Th (97.1 ± 44.7 Bq kg^{-1}). This relatively high value of ^{40}K has also been observed in other parts of the world (Dabayneh, K.M., Mashal, L.A. and Hasan, F.I., 2008).

^{232}Th has the second highest concentration in the town and varies from 50.4 ± 4.5 Bq kg^{-1} (at BP) to 323.6 ± 12.7 Bq kg^{-1} (at ME) with an average of 97.1 ± 44.7 Bq kg^{-1} (Table 5.6 column 3). This average value is comparable to the corresponding value in Swakopmund (91.1 ± 39.6 Bq kg^{-1}). As could be seen in Figure 5.22 the average value of ^{232}Th varies slightly from one area to another area with the highest value observed at Marsbanker street/Elf street (ME).

Of the three radionuclides of interest, ^{238}U has the lowest concentration in all the samples (or sites) as could be observed in Figure 5.22. The concentration varies from 36.2 ± 2.7 Bq kg^{-1} (at KO) to 153.4 ± 4.8 Bq kg^{-1} (at ME) with a mean of 62.2 ± 20.0 Bq kg^{-1} as shown in Table 5.6 (column 4). The average concentration of ^{238}U (62.2 ± 20.0

Bq kg^{-1}) was found to be higher than the world-wide average value of 33 Bq kg^{-1} (UNSCEAR, 2008).

The absorbed dose rates obtained were calculated from the individual radioactivity concentration values of ^{40}K, ^{238}U and ^{232}Th and these values and their averages for all geographical areas are presented in table 5.6. These values varied from 91.2 ± 3.7 nGy h^{-1} (at area KO) to 304.0 ± 8.8 nGy h^{-1} (at ME) with an overall average of 126.4 ± 35.7 nGy h^{-1}. As could be expected, the average absorbed dose rates varied from one area to another as shown in Figure 5.24. The highest absorbed dose rate value is found at the Marsbanker street/Elf street area (ME). It should be noted that the area of Marsbanker street/Elf street is in a residential area that is close to the town's golf and recreational area.

All values obtained for the absorbed dose rate were used to calculate the annual effective dose in the different areas. These values were found to range from 0.11 ± 0.01 mSv (at KO) to 0.37 ± 0.01 mSv (at ME) with an average of 0.16 ± 0.04 mSv (Table 5.6 column 6). These values and the average value of 0.16 ± 0.04 mSv for the town are less than the average annual effective dose (0.48 mSv) due to exposure to natural terrestrial sources of radiation (UNSCEAR, 2000). Also, the average annual effective dose is much lower than the value of 1.0 mSv recommended for the public by the International Commission on Radiological Protection (ICRP). Therefore, the results indicate that the town of Henties Bay has a normal background radiation.

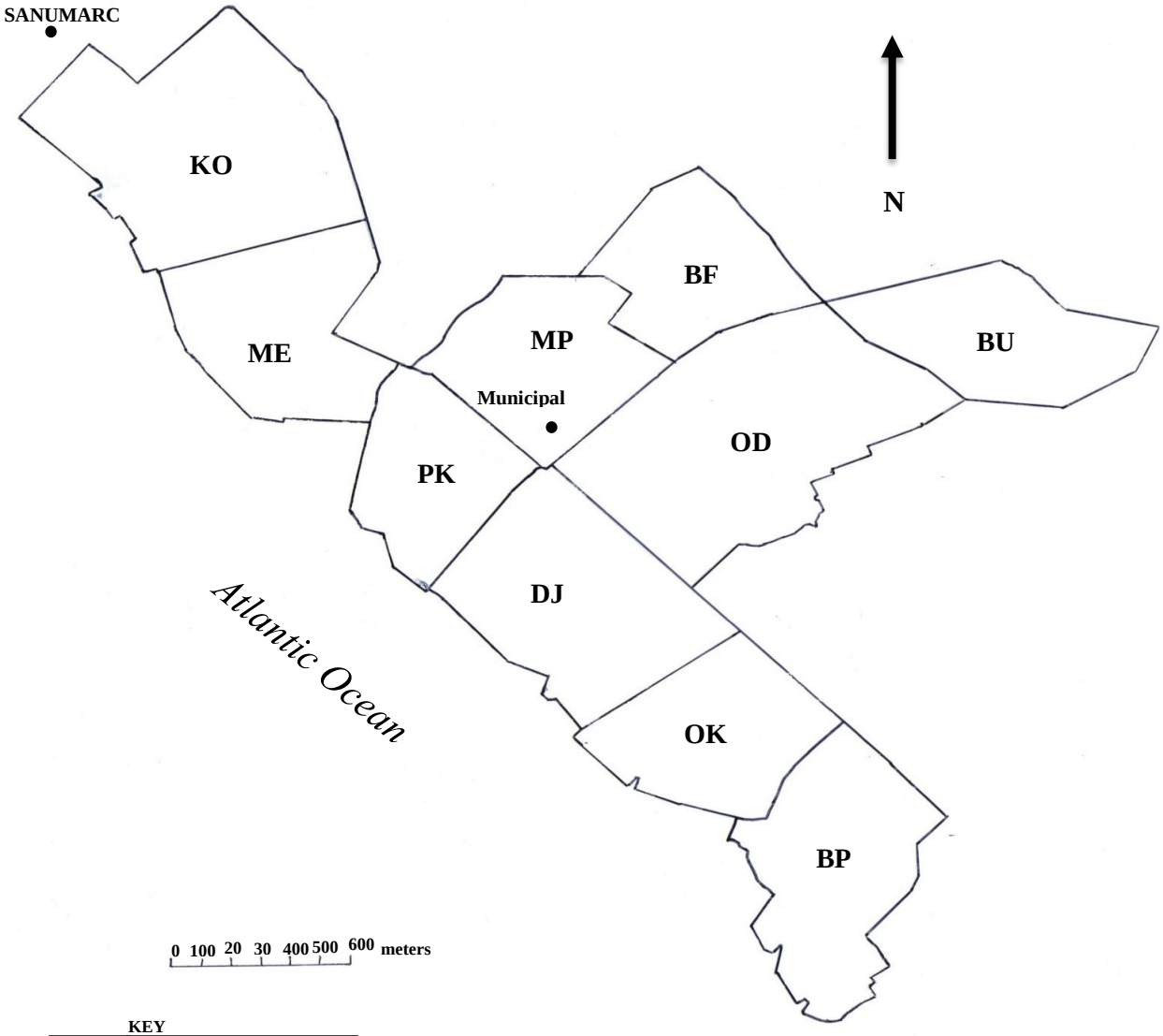

KEY

Area	Name
BP	Brandberg street/Paresis street area
OK	Orange street/Kavango street area
DJ	Duine road/Jakkalsputs road area
PK	Pelikaan street/Kabeljou street area
ME	Marsbanker street/Elf street area
KO	Kraai street/Omaruru street area
MP	Municipality area
OD	Omdel area
BF	Brick factory area
BU	Business area

Figure 5.21: Map showing the ten geographical areas where soil samples were collected in Henties Bay. 'Municipal office' and 'SANUMARC' show the locations of the Municipality and the Sam Nujoma Marine Research Centre (of the University of Namibia) respectively.

Table 5.6: Average (± standard deviation) radionuclide concentrations, absorbed dose rates and annual effective doses in ten geographical areas of Henties Bay. The corresponding range of values is given in parentheses.

Area	Radionuclide concentration (Bq kg^{-1})			Absorbed dose rate (nGy h^{-1})	Annual effect. dose (mSv)
	^{40}K	^{232}Th	^{238}U		
BP	959.0 ± 87.7	70.6 ± 14.0	56.0 ± 12.7	108.5 ± 10.4	0.13 ± 0.01
	(853.7 –1029.3)	*(50.4 – 84.6)*	*(45.7 – 72.1)*	*(95.0 – 119.1)*	*(0.12 –0. 15)*
OK	949.3 ± 59.3	82.2 ± 20.8	52.3 ± 6.8	113.4 ± 17.2	0.14 ± 0.02
	(868.3 –1014.6)	*(65.1 – 112.3)*	*(41.3–57.9)*	*(98.2 – 136.3)*	*(0.12 – 0.17)*
DJ	925.9 ± 34.0	81.1 ± 20.9	53.1 ± 6.7	112.1 ± 14.5	0.14± 0.02
	(892.7 – 970.7)	*(52.3 – 102.5)*	*(44.0 – 61.2)*	*(92.4 – 128.8)*	*(0.11 – 0.16)*
PK	893.7 ± 47.5	76.5 ± 9.9	53.2 ± 6.4	108.1 ± 8.2	0.13 ± 0.01
	(819.5 – 946.3)	*(66.2 – 88.2)*	*(46.4 – 60.4)*	*(99.3 – 116.3)*	*(0.12 – 0.14)*
ME	917.1 ± 63.8	143.1 ± 103.1	83.4 ± 40.4	163.2 ± 80.1	0.20 ± 0.10
	(819.5 – 990.2)	*(68.6 – 323.6)*	*(58.3 – 153.4)*	*(106.8 – 304.0)*	*(0.13 – 0.37)*
KO	933.7 ± 78.9	70.3 ± 12.1	54.3 ± 16.2	106.5 ± 11.7	0.13 ± 0.01
	(809.8 –1019.5)	*(53.0 – 82.6)*	*(36.2–79.4)*	*(91.2 – 117.6)*	*(0.11 – 0.14)*
MP	969.8 ± 83.7	98.3 ± 51.1	60.1 ± 26.7	127.6 ± 44.1	0.16 ± 0.05
	(824.4 –1039.0)	*(64.4 – 187.6)*	*(43.6 – 107.1)*	*(95.8 – 203.9)*	*(0.12 – 0.25)*
OD	963.9 ± 56.5	111.4 ± 23.9	66.2 ± 8.5	138.1 ± 19.1	0.17 ± 0.02
	(907.3 –1024.4)	*(71.3 – 133.6)*	*(52.0 – 73.4)*	*(104.9 – 152.4)*	*(0.13 – 0.19)*
BF	935.6 ± 61.3	124.3 ± 28.7	75.1 ± 15.9	148.8 ± 23.5	0.18 ± 0.03
	(868.3 –1009.8)	*(101.7 – 170.4)*	*(61.8 – 102.5)*	*(129.5 – 186.5)*	*(0.16 – 0.23)*
BU	913.2 ± 109.0	113.1 ± 38.5	68.0 ± 19.3	137.8 ± 32.8	0.17 ± 0.04
	(790.2 –1024.4)	*(68.0 – 171.9)*	*(46.2 – 97.9)*	*(96.4 – 187.4)*	*(0.12 –0. 23)*
All samples	**936.1 ± 68.5**	**97.1 ± 44.7**	**62.2 ± 20.0**	**126.4 ± 35.7**	**0.16 ± 0.04**
	(790.2 – 1039.0)	***(50.4 – 323.6)***	***(36.2 – 153.4)***	***(91.2 – 304.0)***	***(0.11 – 0.37)***

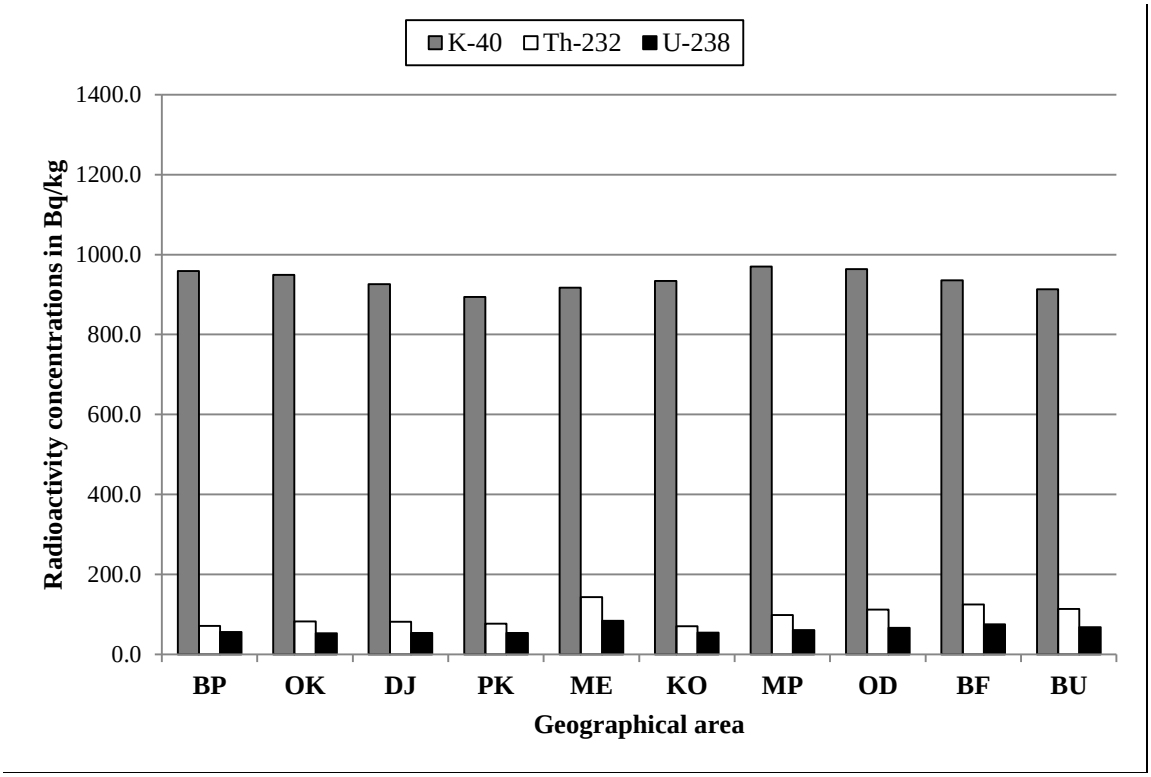

Figure 5.22: Comparison of mean activity concentrations of ^{40}K, ^{232}Th and ^{238}U for the ten geographical areas of Henties Bay.

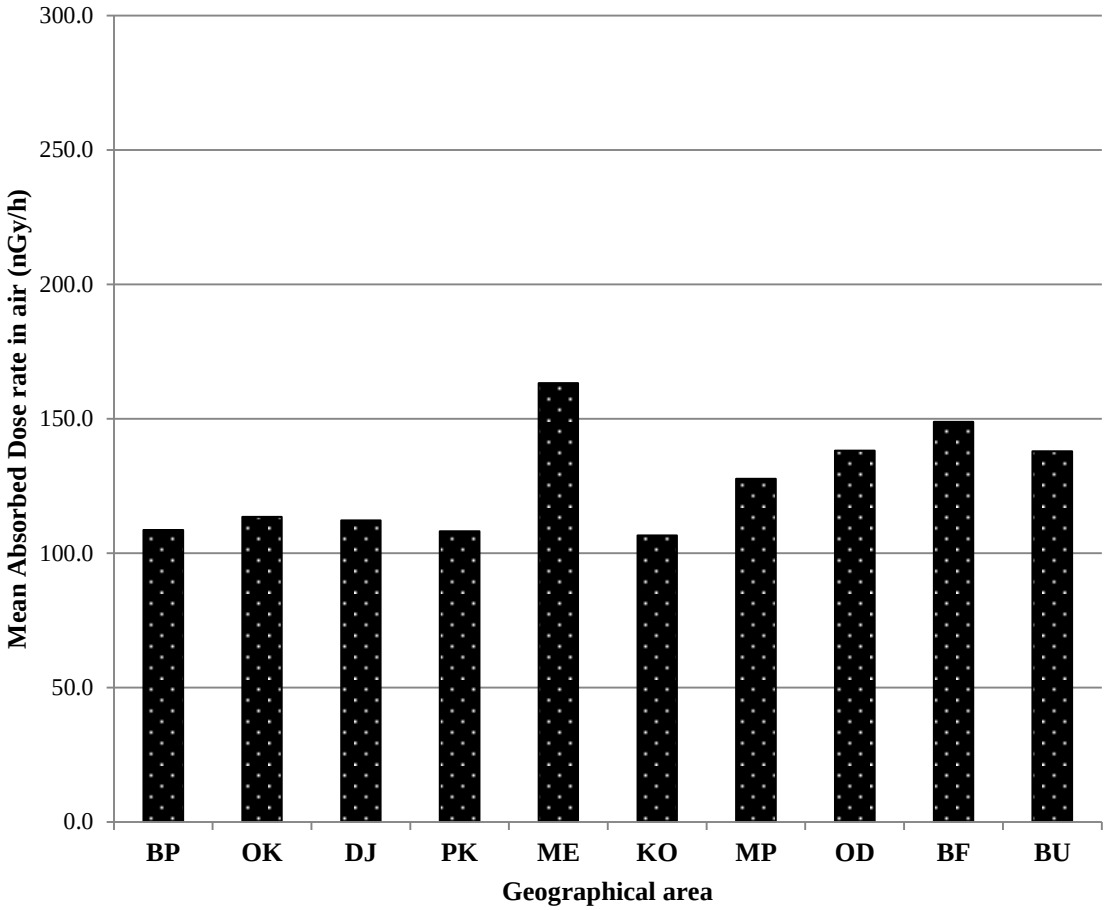

Figure 5.23: Comparison of mean absorbed dose rates for ten geographical areas of Henties Bay.

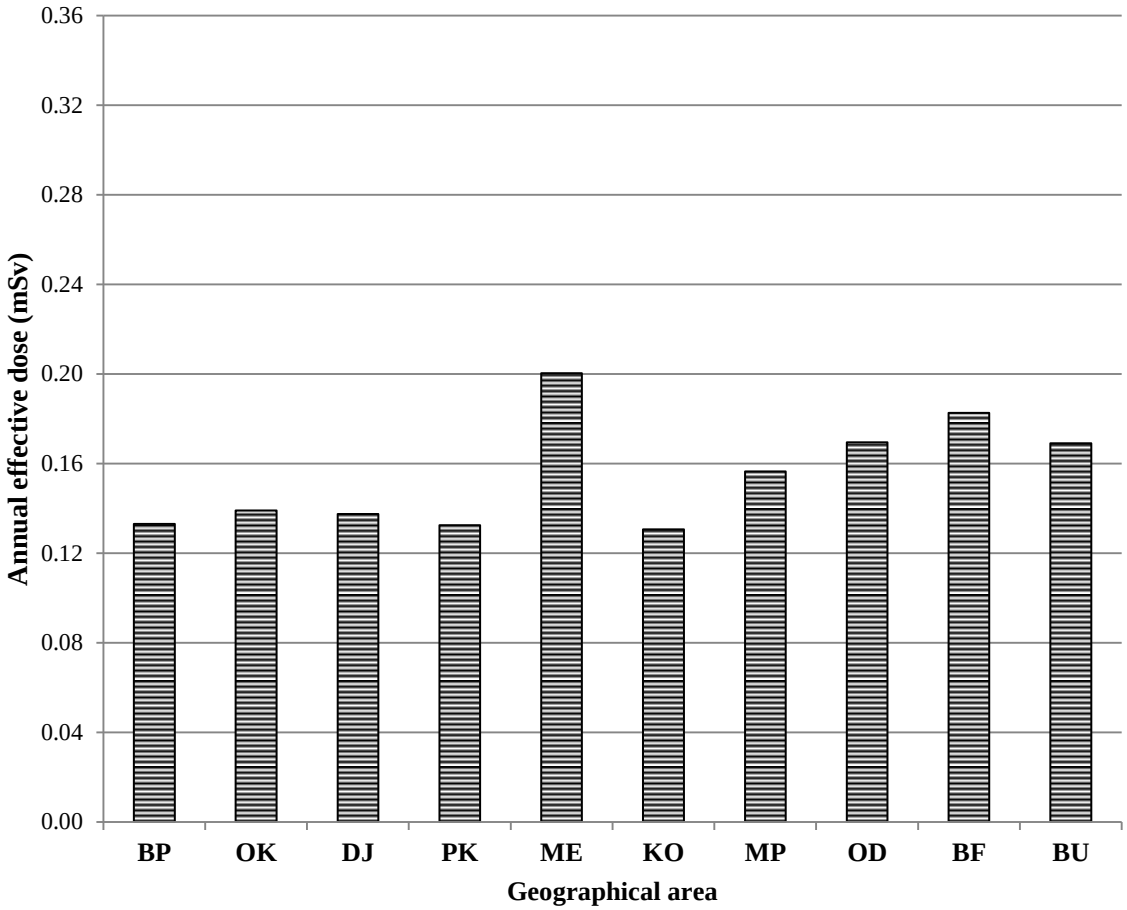

Figure 5.24: Comparison of mean annual effective dose for ten geographical areas of Henties Bay.

5.5 Comparison of activity concentrations and dose rates of different towns

The average activity concentrations of different radionuclides in the soils of the six towns in the Walvis Bay – Henties Bay coastal area are shown in Table 5.7 (columns 2-4) and figure 5.25. The range of average values in the different geographical areas of a town is shown in parentheses in the table. As could be observed in the figure, ^{40}K has the highest average concentration in each of the towns, while ^{232}Th has the next highest average concentration in each town and ^{238}U has the lowest average concentration in each of the towns. The lowest average concentration of ^{40}K is in Walvis Bay with a value of 460.3 ± 76.2 Bq kg^{-1} while the highest value is in Usakos with a value of 959.5 ± 194.7 Bq kg^{-1}. The mean value of ^{40}K in all the towns is 778.7 ± 204.6 Bq kg^{-1} as shown in Table 5.7 (column 2). Also, the lowest average concentration of ^{232}Th is in Walvis Bay with a value of 23.8 ± 8.4 Bq kg^{-1}, while the highest concentration is in Arandis with a value of 245.7 ± 87.4 Bq kg^{-1}. The mean value of ^{232}Th in the six towns is 104.3 ± 85.9 Bq kg^{-1} as shown in Table 5.7 (column 3). As observed for ^{232}Th the lowest average concentration of ^{238}U is in Walvis Bay with a value of 18.6 ± 4.6 Bq kg^{-1} while the maximum average concentration is in Arandis with a value of 72.4 ± 13.5 Bq kg^{-1}. ^{238}U has a mean value of 104.3 ± 85.9 Bq kg^{-1} in the six towns as shown in Table 5.7 (column 4). These results indicate that natural radioactivity will be highest in Arandis but lowest in Walvis Bay.

The corresponding absorbed dose rates and annual effective dose are shown in table 5.7 (columns 5 and 6) and Figures 5.26 and 5.27. As could be observed in Figure 5.26, the average absorbed dose rate is highest in Arandis with a value of 219.4 ± 58.5 nGy h^{-1}

while it is lowest in Walvis Bay with a value of 42.1 ± 9.2 nGy h^{-1} The average absorbed dose rate for the six towns is 119.6 ± 64.9 nGy h^{-1} as shown in Table 5.7 (column 5). Also, as could be observed in figure 5.27, the average annual effective dose is lowest in Walvis Bay with a value of 0.05 ± 0.01 mSv and highest in Arandis with a value of 0.27 ± 0.07 mSv. The average annual effective dose for the towns is 0.15 ± 0.08 mSv as shown in Table 5.7 (column 6). These results confirm that Arandis is having the highest natural radioactivity among the six towns while Walvis Bay is having the lowest radioactivity. Based on the average values of the annual effective dose in the towns, the level of radioactivity in a town decreases from Arandis to Henties Bay, Wlotzkasbaken, Swakopmund, Usakos and Walvis Bay.

A summary of the different geographical areas considered in this study and the average annual effective dose in each area is presented in Table 5.8. As could be seen in the table (values in parentheses), the area having the highest average annual effective dose of 0.35 ± 0.07 mSv is the Starling street area in the town of Arandis while the area having the lowest average annual effective dose of 0.04 ± 0.01 mSv is the Kuisebmond Civic Centre area in the town of Walvis Bay. However, this highest value (0.35 ± 0.07 mSv) is still below the recommended annual limit of 1.0 mSv so that the different areas have normal background radiation.

Table 5.7: Average (± standard deviation) radionuclide concentrations, absorbed dose rates and annual effective doses in six towns in the Walvis Bay-Henties Bay coastal area. The corresponding range of mean values are given in parentheses.

Town	Radionuclide concentration (Bq kg^{-1})			Absorbed dose rate (nGy h^{-1})	Annual effect. dose (mSv)
	^{40}K	^{232}Th	^{238}U		
Usakos	959.5 ± 194.7	74.8 ± 30.2	44.2 ± 9.7	105.7 ± 23.9	0.13 ± 0.03
	(774.6 – 1336.5)	*(45.7 – 118.9)*	*(33.1– 52.9)*	*(84.4 – 142.8)*	*(0.10 – 0.18)*
Arandis	899.7 ± 65.8	245.7 ± 87.4	72.4 ± 13.5	219.4 ± 58.5	0.27 ± 0.07
	(841.9 – 954.9)	*(128.9 – 334.4)*	*(57.5 – 88.2)*	*(139.5 – 281.0)*	*(0.17 – 0.35)*
Swakopmund	645.5 ± 69.5	91.1 ± 39.6	46.4 ± 14.2	103.4 ± 30.9	0.13 ± 0.04
	(572.0 – 747.3)	*(55.0 – 167.6)*	*(34.9 – 68.1)*	*(78.0 – 160.3)*	*(0.09 – 0.20)*
Walvis Bay	460.3 ± 76.2	23.8 ± 8.4	18.6 ± 4.6	42.1 ± 9.2	0.05 ± 0.01
	(363.2 – 586.9)	*(18.0 – 39.7)*	*(14.5 – 27.2)*	*(32.7 – 61.0)*	*(0.04 – 0.08)*
Wlotzkasbaken	759.2 ± 68.4	79.5 ± 44.1	69.6 ± 26.3	110.8 ± 40.3	0.14 ± 0.05
	(659.2 – 810.2)	*(53.6 – 133.2)*	*(51.5 – 104.1)*	*(84.8 – 160.0)*	*(0.10 – 0.20)*
Henties Bay	936.1 ± 68.5	97.1 ± 44.7	62.2 ± 20.0	126.4 ± 35.7	0.16 ± 0.04
	(893.7 – 969.8)	*(70.3 – 143.1)*	*(52.3 – 83.4)*	*(108.5 – 163.2)*	*(0.13 – 0.20)*
All samples	**778.7 ± 204.6**	**104.3 ± 85.9**	**52.6 ± 24.5**	**119.6 ± 64.9**	**0.15 ± 0.08**
	(363.2 – 1336.5)	***(18.0 – 334.4)***	***(14.5 – 104.1)***	***(32.7 – 281.0)***	***(0.04 – 0.35)***

Table 5.8: Geographical areas where soil samples were collected in six towns in the Walvis Bay – Henties Bay coastal area. The mean annual effective dose for a given area is written in parentheses.

Town	**Area**	Name (*dose in mSv*)
Usakos	HK	Hakaseb Community Centre/Hall area (*0.10 ± 0.01*)
	HA	Hakaseb (*Elifas Goseb Primary School*) area (*0.18 ± 0.03*)
	KS	Usakos (*Welcome sign*)/Erongo road area (*0.10 ± 0.01*)
	TS	Keets Scrap area (*0.12 ± 0.01*)
	HS	Wallis/ Conradie Street area (*0.13 ± 0.02*)
	CS	Bo-dorp area (*0.12 ± 0.03*)
	RS	Railway station (*Bahnhof*) area (*0.14 ± 0.05*)
	UE	Church area in Third Street (*0.12 ± 0.01*)
	UM	Usakos Municipality area (*0.16 ± 0.02*)
	PA	Usakos Children /Education Centre area (*0.12 ± 0.001*)
Arandis	PK	Police station/Koerboom Road area (*0.23 ± 0.04*)
	CS	Cormorant street area (*0.26 ± 0.08*)
	HA	Hospital/Albratross street area (*0.25 ± 0.05*)
	KL	Kudu lodge area (*0.29 ± 0.05*)
	HR	Hamerrop street area (*0.30 ± 0.07*)
	ST	Starling street area (*0.35 ± 0.07*)
	DL	Diamond lane area (*0.31 ± 0.07*)
	TH	Town hall/Zebra lodge (*0.28 ± 0.07*)
	CD	Cleaning depot/Sewing centre (*0.25 ± 0.08*)
	PP	Protea road/Parrot street area (*0.29 ± 0.07*)
	WL	Welwitschia lodge area (*0.17 ± 0.02*)
Swakopmund	DR	DRC residential area (*0.20 ± 0.03*)
	MD	Mondesa residential area (*0.14 ± 0.04*)
	TK	Tamariskia residential area (*0.12 ± 0.02*)
	TS	Transnamib Train Station area (*0.11 ± 0.01*)
	KR	Haus Petman/ Municipal Graveyard area (*0.10 ± 0.02*)
	JT	Swakopmund Jetty area (*0.12 ± 0.03*)
	WS	Welwitscha Sports grounds area (*0.10 ± 0.02*)
	VT	Vineta residential area (*0.09 ± 0.02*)
	HH	Hage Heights area (*0.13 ± 0.03*)
	OV	Ocean View suburb area (*0.15 ± 0.03*)
Walvis Bay	NR	Naraville residential area (*0.08 ± 0.00*)
	KS	Kuisebmond residential area (*0.05 ± 0.01*)
	MM	Kuisebmond civic centre area (*0.04 ± 0.01*)
	LI	Light Industrial Export Processing Zone (*E.P.Z*) area (*0.05 ± 0.00*)
	HI	Heavy Indst. - Nam. Ports Auth. area (*Namport*) area (*0.05 ± 0.01*)
	PO	Post Office CBD Area (*0.05 ± 0.01*)
	MP	Municipality of Walvis Bay civic centre area (*0.06 ± 0.01*)
	HP	Walvis Bay State Hospital area (*0.05 ± 0.00*)
	GC	Golf course area (*0.05 ± 0.01*)

	PK	Meersig residential area (*0.05 ± 0.01*)
Wlotzkasbaken	AA	House number 1- 8 area (*0.16 ± 0.06*)
	BB	House number 9 - 14 area (*0.20 ± 0.05*)
	CC	Houses close to Water point area (*0.19 ± 0.06*)
	DD	House number 50 and 78 area (*0.13 ± 0.04*)
	EE	MTC solar panel tower area (*0.12 ± 0.02*)
	FF	Area around house number 79 and 53 (*0.10 ± 0.03*)
	GG	Area close to house numbers 26,54,and 92 (*0.11 ± 0.02*)
	HH	Town's security building area (*0.11 ± 0.01*)
	II	House number 57,60,33 and 102 area (*0.13 ± 0.04*)
	JJ	Area around the sewerage/recycling house (*0.11 ± 0.04*)
Henties Bay	BP	Brandberg street/Paresis street area (*0.13 ± 0.01*)
	OK	Orange street/Kavango street area (*0.14 ± 0.02*)
	DJ	Duine road/Jakkalsputs road area (*0.14 ± 0.02*)
	PK	Pelikaan street/Kabeljou street area (*0.13 ± 0.01*)
	ME	Marsbanker street/Elf street area (*0.20 ± 0.10*)
	KO	Kraai street/Omaruru street area (*0.13 ± 0.01*)
	MP	Municipality area (*0.16 ± 0.05*)
	OD	Omdel area (*0.17 ± 0.02*)
	BF	Brick factory area (*0.18 ± 0.03*)
	BU	Business area (*0.17 ± 0.04*)

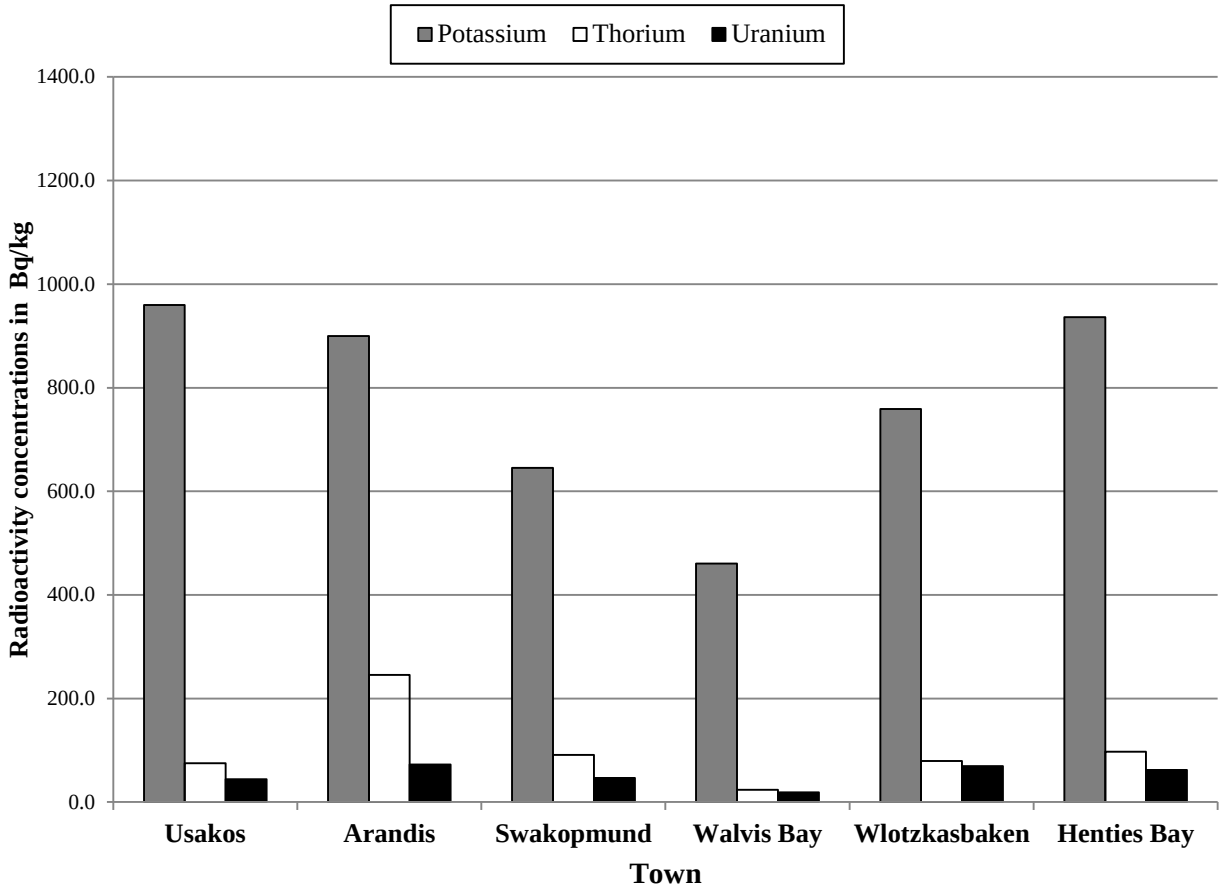

Figure 5.25: Comparison of the average concentrations of ^{40}K, ^{232}Th and ^{238}U in different towns.

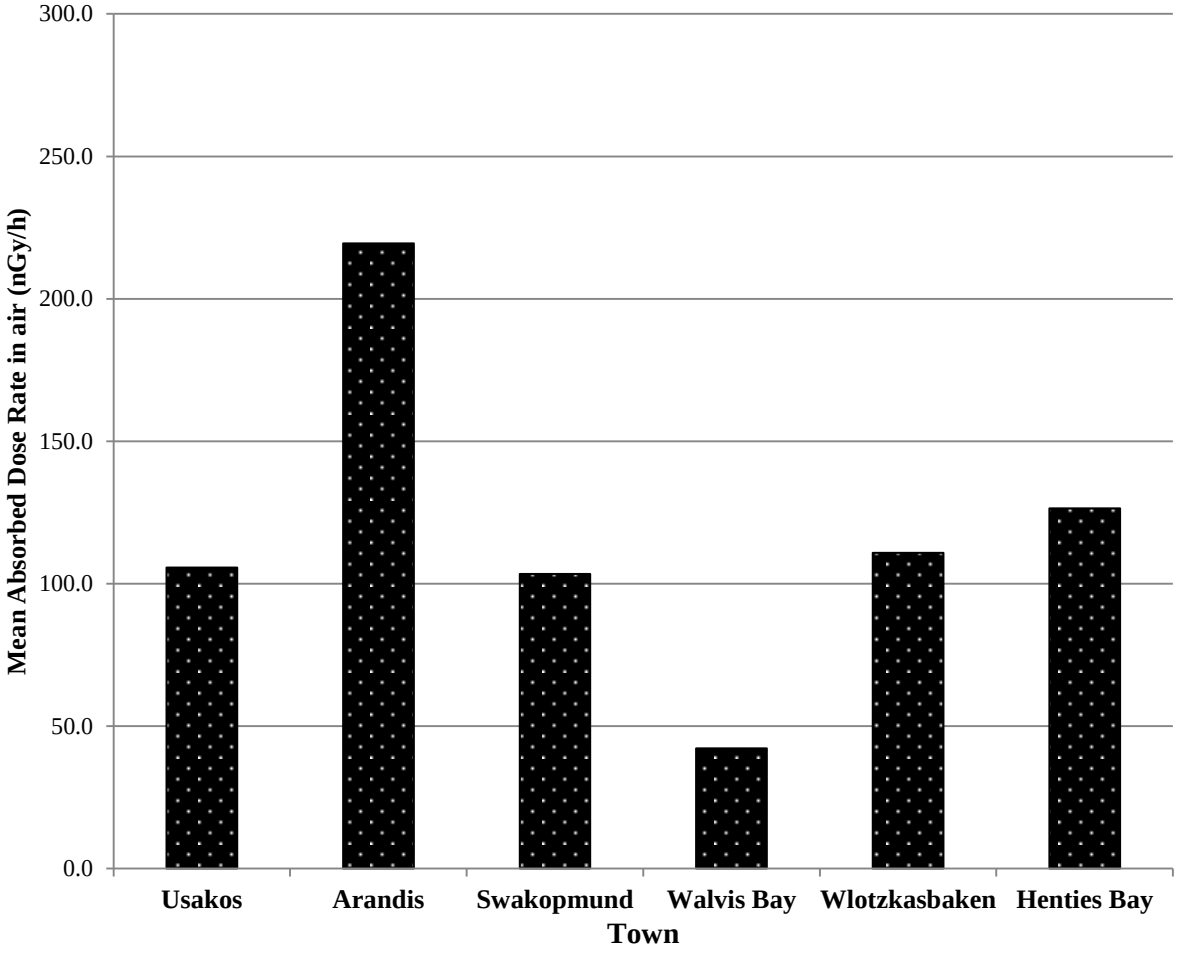

Figure 5.26: Comparison of the average absorbed dose rate in different towns.

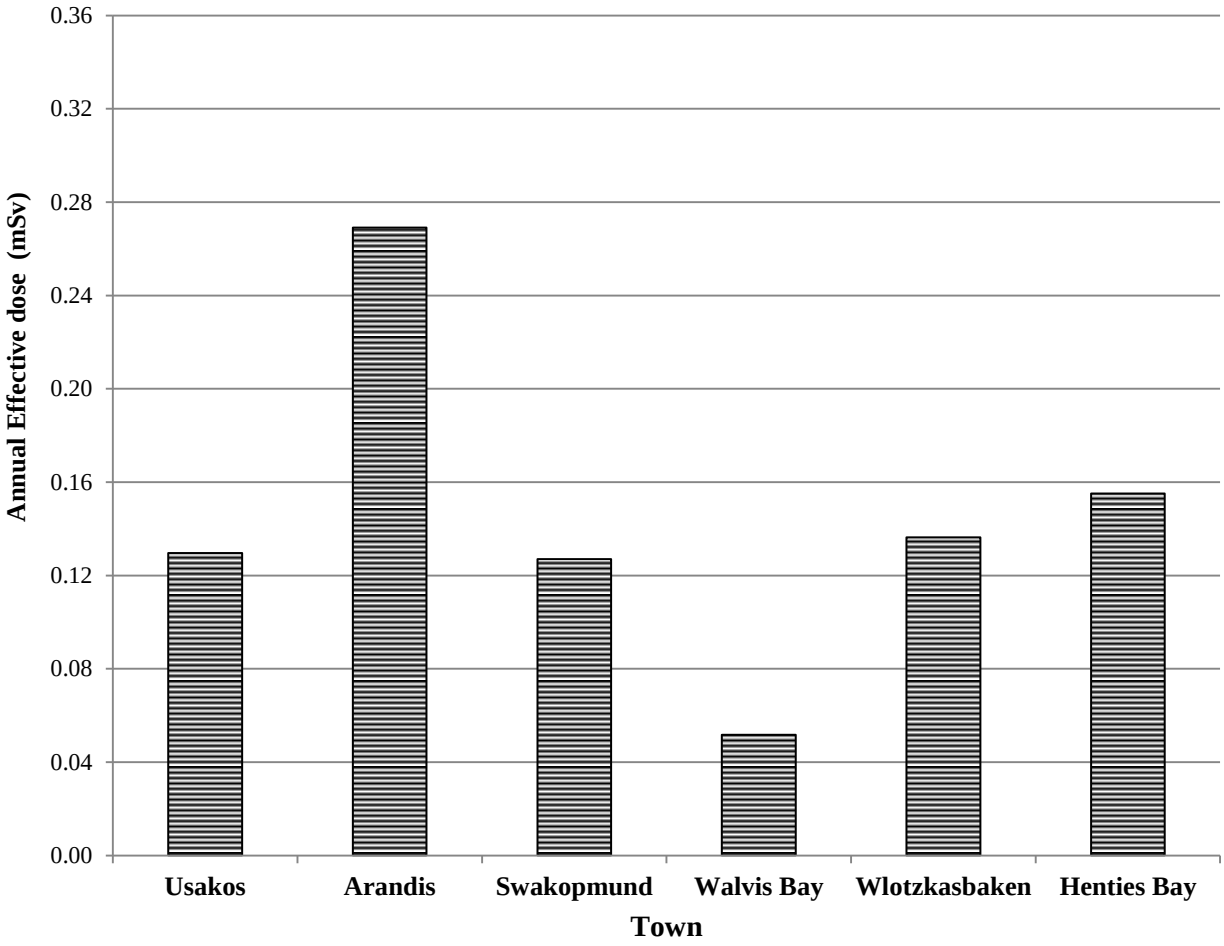

Figure 5.27: Comparison of the average annual effective dose rate in different towns.

CHAPTER 6

6. CONCLUSIONS AND RECOMMENDATIONS

6.1 Conclusion

The concentrations of ^{238}U, ^{232}Th and ^{40}K in 305 soil samples collected from Usakos, Arandis, Swakopmund, Walvis Bay, Wlotzkasbaken and Henties Bay have been determined by gamma spectroscopy. These towns are located in an area that is well known for its uranium mining activities in the country, and this necessitated the need to determine the radionuclide concentrations of these naturally occurring radionuclides in the soils of these towns. The corresponding absorbed dose rates and annual effective dose rates in these six towns have also been calculated.

From the results obtained for the concentrations and dose rates, the following observations were made;

- The activity concentration of ^{40}K is much higher than those of the other two naturally occurring radionuclides in the six towns. The concentration of ^{40}K is particularly high in Usakos, Arandis, Wlotzkasbaken and Henties Bay, thus making it the highest contributor to the radioactivity in the soils of these towns. Since no significant agricultural activities were observed in these towns, then the high concentration of ^{40}K is attributed to its natural abundance in the soils of the towns.
- The average activity concentration of ^{40}K (per area) varied from a minimum value of 363.2 Bq kg^{-1} in Walvis Bay to a maximum value of 1336.5 Bq kg^{-1} in

Usakos with an average of 778.7 ± 204.6 Bq kg^{-1} (Mean ± Standard deviation) for the six towns.

- The average activity concentration of ^{232}Th ranged from a minimum value of 18.0 Bq kg^{-1} in Walvis Bay to a maximum value of 334.4 Bq kg^{-1} at Arandis with a mean value of 104.3 ± 85.9 Bq kg^{-1} (Mean ± Standard deviation) for the six towns. Also, ^{232}Th was found to have the second highest mean concentration (out of the three radionuclides) in the towns.
- The average activity concentration of ^{238}U varied from a minimum value of 14.5 Bq kg^{-1} in Walvis Bay to a maximum value of 104.1 Bq kg^{-1} at Wlotzkasbaken with a mean value of 52.6 ± 24.5 Bq kg^{-1} (Mean ± Standard deviation) for the six towns. Also,^{238}U has the lowest activity concentration in the towns. These low values obtained for ^{238}U indicate that there exist no large deposits of uranium in these towns.
- Arandis has the highest concentrations of ^{238}U, ^{232}Th and ^{40}K in the soil while Walvis Bay has the lowest concentration in the soil.
- The average absorbed dose rate varies from a minimum value of 32.7 nGy h^{-1} at Walvis Bay to a maximum value of 281.0 nGy h^{-1} at Arandis. The mean value for the six towns was found to be 119.6 ± 64.9 nGy h^{-1} (Mean ± Standard deviation). This mean value is observed to be twice the world average of 58 nGy h^{-1} (UNSCEAR, 2000).
- The average annual effective dose rate varies from a minimum value of 0.04 mSv in Walvis Bay to a maximum value of 0.35 mSv in Arandis. The mean annual effective dose value of 0.15 ± 0.08 mSv obtained for the six towns is

much lower than the world average of 0.48 mSv (UNSCEAR, 2000). In addition, this value is far less than the annual maximum permissible dose of 1.0 mSv recommended by the ICRP for the public. Therefore, these baseline results indicate that the six towns in the Walvis Bay – Henties Bay coastal area have normal background radiation.

6.2 Recommendations and Suggestions for Further Work

This project aims to stimulate research work in nuclear science at the University of Namibia. The experimental procedure that was developed in the project should make it easier and more interesting for other postgraduate students and researchers in the subject area to use nuclear techniques or gamma spectrometry in their research work.

Based on the experience acquired in this research work, the following is suggested for further work:

- The establishment of a program for routine monitoring of towns located in the areas close to where uranium-mining activities are on going or envisaged.
- The extension of this study to include the determination of the level of radon in the air and the concentration of radionuclides in ground water, marine ecosystems and plant life. This information is important to determine the movement of naturally occurring radioactive material (NORM) in the terrestrial food chains that could lead to assessing the transfer ratios of soil-to-plant, plant-to-food and thus food-to-man.
- There is also a need to generate baseline data for areas outside the Walvis Bay - Henties Bay coastal area to assist in assessing the impact of high levels of

NORM on the physical environment in the country. This information is also important in assessing the extent of any nuclear emergency, since the Government of Namibia has pronounced itself on the possibility of obtaining a nuclear power plant for the generation of electricity for the country.

REFERENCES

Alatise, O. (2007). *Radioactivity concentrations and distrubution of some Naturally Occuring Radioactive materials in the soils of some coastal satates of Nigeria.* PhD Thesis, University of Agriculture, Abeokuta, Nigeria.

Antovic, N., Svrkota, N., & Antovic, I. (2011). Radiological impacts of natural radioactivity from soil in Montenegro. *Radiation Protection Dosimetry,* 1-8.

Arandis Town Council. (n.d). *Arandis Profile*. Retrieved July 22, 2011, from Arandis Town: http://www.arandistown.com/wp-content/uploads/2010/10/Arandis-Profile.pdf

Argonne National Laboratory, EVS. (2005, August). *Natural Decay Series: Uranium, Radium, and Thorium.* Retrieved June 23, 2011, from Argonne National Laboratory Environmental Science Division (EVS): http://www.ead.anl.gov/pub/doc/natural-decay-series.pdf

Atalise, O., Babalola, A., & Olowofela, J. (2008). Distribution of some natural gamma-emitting radionucuclides in the soils of coastal areas of Nigeria. *Journal of Environmental Radioactivity*(99), 1746-1749.

Atomic Energy Board of Namibia. (2011). *Atomic Energy Board of Namibia Annual Report 2009/2010.* Windhoek: Ministry of Health and Social Services.

Azarvand, B. (2011). Measurement of Radioactivity in soil samples of Sarein. *Middle-east Journal of Scientific Research, 7*(6), 859-863.

Beck, H., De Compo, J., & Gologak, J. (1972). *In-situ Ge (Li) and NaI(Tl) gamma-ray spectrometry.* Report 258, U.S Atomic Energy Commission , Health and Safety Laboratory.

Brazilian Academy of Sciences. (1977). International Symposium on Areas of High Natural Radioactivity, Pocos de Caldas, Brazil, 16-20 June 1975. Rio de Janeiro: Academia Brasileira de Ciencias.

Burcham, W. E., & Jobes, M. (1995). *Nuclear and particle physics.* United Kingdom: Longman Scientific & Technical.

Canberra. (1998). *Edition Ten Product Catalog.* Canberra Industries Inc., 800 Research Parkway, Meriden.

CERN. (1970). *The Bubble Chamber*. Retrieved April 23, 2012, from The European Organization for Nuclear Research.

Coastal Zone Management Project (CZM). (1999, August). *Coastal Profile of the Erongo Region.* (K. Bender, R. Barby, & J. Korrubel, Eds.) Retrieved July 25, 2011, from Environmental Information Service Namibia: http://www.the-eis.com/data/literature/Coastal%20profile%20of%20the%20Erongo%20Region.pdf

Coffey, J. (2010, March 3). *Cloud Chamber.* Retrieved July 23, 2012, from Universe Today: http://www.universetoday.com/58521/cloud-chamber/

Dabayneh, K., Mashal, L., & Hasan, F. (2008). Radioactivity concentration in soil samples in the southern part of the West Bank, Palestine. *Radiation Protection Dosimetry*(131), 265-271.

Damon, R. (2005). *Determination of the photopeak detection efficiency of a HPGe detector, for volume sources, via Monte Carlo simulations.* MSc Thesis, University of Western Cape, South Africa.

Firestone, R., Chu, S., Baglin, C., & Zipkin, J. (1996). *Table of Isotopes.* (V. Shirley, Ed.) New York: John Wiley & Sons.

Friend, J. F., Borshoff, J., Pretorius, L. E., Marsh, D., Siebert, T., Slabbert, J., et al. (2004). *Langer Heinrich Uranium Mine environmental assesment draft report.* Johannesburg, South Africa: Softchem.

Garimella, S., & Prasad, U. (2002). Distribution of ^{40}K, ^{232}Th and ^{238}U in soils of southern and western coasts of Viti Levu, Fiji. *South Pacific Journal of Natural Science*, 9-14.

Ghiassi-nejad, M., Mortazavi, S. M., Cameron, J. R., Niroomand-rad, A., & Karam, P. A. (2002). Very high background radiation areas of Ramsar, Iran: Prelimanary biological studies. *Health Physics*(82), 87-93.

Giancoli, C. G. (1998). *Physics.* New Jersey: Prentice Hall International Inc.

Goosen, L. (2009, April 17). *Wlotzkasbaken - to be or not to be?* Retrieved July 26, 2011, from Namibia Economist: http://www.economist.com.na/index.php?option=com_content&view=article&id=12593:wlotzkasbaken-to-be-or-not-to-be&catid=539:general-news&Itemid=60

Henckert, W. (2009). *History of Usakos*. Retrieved April 23, 2012, from Heckert Tourist Centre: http://www.henckert.com/karibib/index.php?option=com_content&view=article&id=31%3Ausakos&catid=1%3Ahistory&Itemid=7&lang=en

Henties Bay Tourism Association. (n.d). *Henties Bay Namibia History*. Retrieved July 25, 2011, from Henties Bay Namibia: http://www.hentiesbaytourism.com/history.htm

Heyde, K. (1999). *Basic ideas and concepts in nuclear physics.* Bristol, U.K: Institute of Physics Publishing.

Hodgson, P. E., Gadioli, E., & Gadioli Erba, E. (1997). *Introductory nuclear physics.* U.K: Oxford University Press.

IAEA. (2003). *IAEA-TECDOC-1363 Guidelines for radioelement mapping using gamma ray spectrometry data.* Vienna: IAEA Publication.

ICRP. (1991). *1990 Recommendations of the International Commission on Radiological Protection.ICRP Publication 60. Ann. ICRP 21 (1-3).* Oxford, UK: Pergamon Press.

ICRU. (1994). *International Commission on Radiation and Measurements. Gamma-Ray Spectrometry in the Environment. ICRU Report 53.* Bethesda,MD: International Commission on Radiation Units and Measurements.

ICRU. (1998). *International Commission on Radiation Units and Measurements. Fundamental Quantities and Units for Ionizing Radiation. ICRU Report 60.* Bethesda,MD: International Commission on Radiation Units and Measurement.

International Atomic Energy Agency. (1989). *Measurement of Radionuclides in food and the Environment - A Guidebook.* Vienna: IAEA Publication.

International Atomic Energy Agency. (2011). *Mission Report, IAEA International fact finding expert mission of the Fukushima Dai-ichi NPP accident following the great east Japan earthquake and tsunami, Tokyo, Fukushima Dai-ichi NPP, Fukushima Dai-ni NPP and Tokai Dai-ni NPP.* Vienna: IAEA Publications.

Jankovic-Mandic, L., & Dragovic, S. (2010). Assessment of terrestrial gamma exposure to the population of Belgrade (Serbia). *Radiation Protection Dosimetry, 4*(149), 369-377.

Kannan, V., Rajan, M., Iyengar, M., & Ramesh, R. (2002). Distribution of natural and anthropogenic radionuclides in soil and beach sand samples of Kalpakkam (India) using hyper pure germanium (HPGe) gamma ray spectrometry. *Applications Radiation and Isotopes*(57), 109-119.

Karunakara, N., Somashekarappa, H., Avadhani, D., Mahesh, H., Narayana, Y., & Siddappa, K. (2001). Radium-226, ^{232}Th and ^{40}K distribution in the environment of Kiaga of south west coast of India. *Health Physics*(80), 470-476.

Kebwaro, J., Rathorel, I., Hashim, N., & Mustapha, A. (2011). Radiometric assesment of natural radioactivity levels around Mirma Hill, Kenya. *International Journal of the Physical Sciences, 6*(13), 3105-3110.

Knoll, G. (2000). *Radiation Detection and Measurement.* New York: John Wiley & Sons.

Krane, K. (1988). *Introductory Nuclear Physics.* New York: John Wiley & Sons.

Latife, S., & Mustafa, C. (2008). Natural Radioactivity measurements in soil samples of Central Kutahya (Turkey). *Radiation Protection Dosimetry,* 1-5.

Municipality of Walvis Bay. (2011). *History of Walvis Bay*. Retrieved June 20, 2012, from Municipality of Walvis Bay: http://www.walvisbaycc.org.na/?page_id=56

Murty, V., & Karunakara, N. (2008). Natural radioactivity in the soil samples of Botswana. *Radiation Measurements*(43), 1541-1545.

Namibia Travel Adviser. (1998). *History of Swakopmund.* Retrieved June 20, 2012, from NamibWeb: http://www.namibweb.com/swakopmund.htm

NCRP. (1993). *Report No.116-Limitation of Exposure to Ionizing Radiation (Supersedes NCRP Report No.91).* NCRP.

Noureddine, A., Bouggoura, B., Larosa, J., & Vadja, N. (1979). Gamma and alpha emitting radionuclides in some Algerian soil samples. *Appl. Radiat. Isot.*(48), 1145-1148.

Oyedele, J. (2006). Assessment of the natural radioactivity in the soils of Windhoek city, Namibia, Southern Africa. *Radiation Protection Dosimetry, 3*(121), 337-340.

Oyedele, J. A. (2005). Natural Radioactivity in the soil samples of the University of Namibia, Windhoek, Namibia. *Proceedings of the East and Southern Afria Environmental Chemistry Workshop (ESAECW) and the 6th Theoretical Chemistry Workshop in Africa (TCWA).* Windhoek, Namibia.

Oyedele, J. A. (2006). Measurement of the natural radioactivity at the international high energy stereoscopic system (HESS) project in Southern Africa. *Applications Radiation and Isotopes*(64), 686-688.

Oyedele, J. A., Sitoka, S., & Davids, I. (2008). Radionuclide Concentration in soils of Nothern Namibia, Southern Africa. *Radiation Protection Dosimetry*(131), 482-486.

Patel, S. (1991). *Nuclear Physics: An introduction.* New York: John Wiley & Sons.

Pfeffer, J., & Nir, S. (2000). *Modern Physics: An Introductory Text.* Imperial College Press.

Ramli, A., Wahab, A., Hussein, M., & Wood, A. (2005). Environmental ^{238}U and ^{232}Th concentration measurements in an area of high level natural background radiation at palong, Johor, Malaysia. *Journal of Environmental Radioactivty*(80), 287-304.

Rossenfeld, C. (Ed.). (2011). *Human Effects of the Atomic Bomb.* Retrieved August 8, 2012, from Hiroshima & Nagasaki Remembered: http://www.hiroshima-remembered.com/photos/effects/index.html

Schreiber, U. (1996). *The Geology of the Walvis Bay Area. Explanation of Sheet 2214.* Windhoek: Geological Survey of Namibia.

Schreiber, U. (n.d). *Uranium Mineralisation in Namibia.* Retrieved August 3, 2007, from Ministry of Mines and Energy: Geological Survey of Namibia: http://www.mme.gov.na/gsn/pdf/URANium.pdf

Senthilkumar, B., Dhavamani, V., Ramkumar, S., & Philominathan, P. (2012). Measurement of gamma radiation levels in soil samples from Thanjavur using gamma-ray spectrometry and estimation of population exposure. *Journal of Medical Physics*(35), 48-53.

Tahir, S., Jamil, K., Zaidi, J., Arif, M., Ahmed, N., & Ahmad, S. (2005). Measurements of activity concentrations of naturally occuring radionuclides in soil samples from Punjab province of Pakistan and assessment of radiological hazards. *Radiation Protection Dosimetry*(113), 421-427.

Turner, J. (2004). *Atoms, Radiation, and Radiaiton Protection* (Second Edition ed.). Weinheim: Wiley-VCH Verlang GmbH & Co. KGaA .

Tykva, R., & Sabol, J. (1995). *Low Level Environmental Radioactivity Sources and Evaluation.* Pennsylvania: Technomic Publishing Company.

UNSCEAR. (1993). *Sources and effects of ionizing radiation.United Nations Scientific Committee on the Effects of Atomic Radiation, Report to the General Assembly with Annexes.* New York: United Nations Publication.

UNSCEAR. (2000). *Sources and effects of ionizing radiation. United Nations Scientific Committee on The Effects of Atomic Radiation, Report to the General Assembly, with Scienctific Annexes, Vol.I:Sources.* New York: United Nations.

UNSCEAR. (2008). *Sources and effects of ionizing radiation. United Nations Scientific Committee on The Effects of Atomic Radiation, Report to the General Assembly with Annexes. Vol. II.* New York: United Nations Publication.

V O Consulting. (2010, October). *Environmental radiation in Namibia.* Retrieved April 18, 2012, from V O Consulting -independent Namibian energy, environment and radiation consultants: http://www.voconsulting.net/htm/resources.html

Young, H., & Freedman, R. (2006). *University Physics with Modern Physics* (12th ed.). San Francisco, C.A: Pearson Addison-Wesley.

APPENDIX A

MatLab analyses code

function [Uc,Thc,Kc,Dt,Effective_Dose_Rate]=sample_concentration(Unpa, Thnpa, Knpa);

% [Uc, Thc, Kc, Dt, Effective_Dose_Rate]=sample_concentration(Unpa,Thnpa,
% Knpa) calculates the concentration (Bq/kg) of the nuclides 238-U, 232-Th, 40-K
% in a given sample with net peak area Unpa for 238-U, Thnpa for 232-Th and
%Knpa for 40-K.
% It also calculates the Dose rate in nGy/h and
% the Effective dose rate in mSv/y.
clear **% clear-:Ensures that the program runs in a cleared workspace in the Command Window.**
clc **% clc-: Removes all previously assigned variables in the command window.**
Data *=xlsread('C:\SA_Shimboyo\GamaAquisitionData_2008\Town_soil_samples_Net Peak Areas.xls');*
% Reads the data of the Net Peak Areas for the different nuclides of
% interest. We then assign the Net Peak areas and their errors to the
% coloums that we inputed our data in the Excel file '.xls'.
Unpa=Data(:,1); delta_Unpa=Data(:,2);
Thnpa=Data(:,3); delta_Thnpa=Data(:,4);
Knpa=Data(:,5); delta_Knpa=Data(:,6);
% Unpa=Data(:1) is the first coloumn in the data excel
% file,delta_Unpa=Data(:,2)is the second column in the data excel file.
% Each of the nuclides of interest net peak areas and their errors are
% inserted in the data excel file,e.g Unpa & delta_Unpa are in the first
% two columns respectively,Thnpa & delta_Thnpa are in the third and fourth
% respectively, Knpa & delta_Knpa are in the 5th and 6th column
% respectively.

StdC=[4940.00; 3250.00; 14000.00];Error_of_StdC=[30.00;90.00;400.00];
% StdC is the concentrations and Error_of_StdC is the error of the concentrations
% for the I.A.E.A(International Atomic Energy Agency)standards
% for 238-U,232-Th,40-K respectively.

StdData=xlsread('C:\SA_Shimboyo\GamaAquisitionData_2008\Town_samples_IAEA_ Standards_Net Peak Areas.xls');
% StdData reads the net peak areas of the I.A.E.A standards used to
% calibrate the Detector these data are inputed in the same order as those
% for the samples with RGU_nPa-: Net peak area for the Uranim
% standard,delta_RGU_nPa-: being the error in calculating the Net Peak
% Area of the Uranium standard.
RGU_nPa=StdData(:,1); delta_RGU_nPa=StdData(:,2);

```
RGTh_nPa=StdData(:,3); delta_RGTh_nPa=StdData(:,4);
RGK_nPa=StdData(:,5); delta_RGK_nPa=StdData(:,6);
nPA=[RGU_nPa;RGTh_nPa;RGK_nPa];Error_of_nPA=[delta_RGU_nPa;delta_RGTh
_nPa;delta_RGK_nPa];
% nPA is the net peak area and Error_of_nPA is the error in the net peak area
% calculated from the I.A.E.A standards using the HPGe detector software Genie
2000.
% These values changes if you calibrate the system again for samples from
% a different area or region of study.

x1=StdC(1);x2=StdC(2);x3=StdC(3); % We assign x1,x2,x3 to be the concentrations
of  the standards of 238-U, 232-Th and 40-K respectively.

y1=nPA(1);y2=nPA(2);y3=nPA(3); % We also assign y1,y2,y3 to be the net peak
areas of the standards of 238-U, 232-Th and 40-K respectively as calculated by
% the Gamma Aquisition and Analysis program in the Genie 2000 software.

kU=y1/x1;   % The constant K of the standard is calculated from it's
kTh=y2/x2;  % net peak area divided by it's concentration. This constant
kK=y3/x3;   % K(standard)==K(sample)for a given nuclide then we can use the
K(standard)
  % to calculate the concentrations of the nuclides of intrest namely, 238-U,
  % 232-Th and 40-K for a given sample.

Uc=Unpa/kU; Thc=Thnpa/kTh; Kc=Knpa/kK;
% the concentations of the nuclides of interest are calculated above.

delta_nPA_RGU=Error_of_nPA(1);delta_StdC_U=Error_of_StdC(1);
delta_nPA_RGTh=Error_of_nPA(2);delta_StdC_Th=Error_of_StdC(2);
delta_nPA_RGK=Error_of_nPA(3);delta_StdC_K=Error_of_StdC(3);

delta_kU= abs(kU)*sqrt((delta_nPA_RGU(1)/y1)^2+(delta_StdC_U/x1)^2);
delta_kTh= abs(kTh)*sqrt((delta_nPA_RGTh(1)/y2)^2+(delta_StdC_Th/x2)^2);
delta_kK= abs(kK)*sqrt((delta_nPA_RGK(1)/y3)^2+(delta_StdC_K/x3)^2);
% above error in constant Kstandard=Ksample of the nuclides are calculated.

delta_Uc= abs(Uc).*sqrt((delta_Unpa./Unpa).^2+(delta_kU./kU.^2));
delta_Thc= abs(Thc).*sqrt((delta_Thnpa./Thnpa).^2+(delta_kTh./kTh).^2);
delta_Kc= abs(Kc).*sqrt((delta_Knpa./Knpa).^2+(delta_kK./kK).^2);
% above error in the concentrations of the nuclides in a sample is calculated.

Dt= 0.0417.*Kc+0.462.*Uc+0.604.*Thc;
delta_Dt= sqrt((0.0417.*delta_Kc).^2+(0.462.*delta_Uc).^2+(0.604.*delta_Thc).^2);
% above we calculate the Dose rates in Grays per hour(Gy/h),Dt
% and also it's error we call delta_Dt.
```

```
Effective_Dose_Rate=Dt.*0.008760*0.7*0.2;
% above we calculate the Effective_Dose_Rates in milli Sievert per year(mSv/y)

fid=fopen('C:\SA_Shimboyo\GamaAquisitionData\Town_Soil_samples_Results.xls','wt')
% fid~: is a file identifier you use fopen to open a file to read and write
% results from a MatLab script.
fprintf(fid,'Town_Soil_Samples_Results\n')
fprintf(fid,'\n')
fprintf(fid,'Sample Uc(Bq/kg) Uc(Bq/kg) Thc(Bq/kg) Thc(Bq/kg) Kc(Bq/kg) Kc(Bq/kg)
Dose(Gy/h) Dose(Gy/h) EffectiveDoseRate(mSv/y) \n')
for i=1:55
fprintf(fid,'%1.0f %3.2f %2.2f %2.2f %2.2f %2.2f %2.2f %2.2f %2.3f\n',...
   [(i) Uc(i) delta_Uc(i) Thc(i) delta_Thc(i) Kc(i) delta_Kc(i) ...
   Dt(i) delta_Dt(i) Effective_Dose_Rate(i)]);
end
fprintf(fid,'\n')
fclose(fid);

% Written by Mr Simon Andrew Shimboyo. Copyright(c)August 2008
% Department of Physics, Faculty of Science
% University of Namibia
% Tel:(+264)61 2063374(w) , +26481 6771618(c)
% e-mail: sshimboyo@unam.na, andrewlorenzo2010@gmail.com
```

APPENDIX B

Activity Concentrations of ^{238}U, ^{232}Th and ^{40}K in Usakos

Sample	Uc (Bq/kg)	δUc (Bq/kg)	Thc (Bq/kg)	δThc (Bq/kg)	Kc (Bq/kg)	δKc (Bq/kg)
1	45.92	2.73	52.47	4.34	793.81	31.15
2	43.50	2.80	42.56	4.26	736.08	29.74
3	50.78	2.92	49.41	4.38	654.30	27.09
4	42.18	2.63	54.80	4.73	976.63	36.60
5	44.02	2.73	54.51	4.97	793.81	31.26
6	44.61	2.84	73.89	5.31	899.66	34.57
7	54.19	3.17	80.01	5.33	971.82	36.81
8	44.09	3.37	173.43	7.45	1308.59	46.64
9	39.10	2.60	64.56	4.87	822.68	32.07
10	28.73	2.46	58.59	4.93	1015.12	37.93
11	50.45	2.88	42.85	4.23	697.59	28.18
12	47.89	2.85	57.71	4.75	861.17	32.85
13	40.61	3.06	109.74	6.49	1178.69	42.50
14	48.74	2.97	58.44	4.80	779.38	30.97
15	50.52	3.06	72.72	4.95	827.49	32.25
16	51.76	3.12	41.83	4.21	659.11	27.14
17	43.63	2.86	51.74	4.63	894.85	34.16
18	43.95	2.73	42.99	4.38	846.74	33.04
19	39.89	2.86	46.64	4.64	856.36	33.14
20	85.29	3.22	45.47	4.12	615.81	26.38
21	46.71	2.92	66.02	5.02	880.41	33.66
22	52.81	2.98	52.61	4.78	808.25	31.57
23	42.91	2.88	67.19	5.01	923.71	34.95
24	41.79	2.83	49.84	4.70	942.96	35.81
25	41.86	2.91	96.77	5.89	899.66	34.55
26	63.37	3.37	82.63	5.79	986.25	37.03
27	39.23	2.89	86.57	5.61	1048.80	38.75
28	30.05	2.53	56.98	4.36	841.92	32.38
29	39.03	2.77	77.24	5.29	991.07	37.33
30	31.16	2.81	68.35	5.06	865.98	33.69
31	35.89	2.51	78.55	5.37	1145.02	41.46
32	33.79	2.90	113.09	6.55	1462.54	50.92
33	35.75	2.92	145.74	7.40	1246.05	44.62
34	33.59	3.04	167.60	8.14	1476.98	51.43

Sample	Uc (Bq/kg)	δUc (Bq/kg)	Thc (Bq/kg)	δThc (Bq/kg)	Kc (Bq/kg)	δKc (Bq/kg)
35	26.57	2.64	89.34	6.12	1351.89	47.67
36	50.58	2.98	75.78	5.29	726.46	29.32
37	43.82	2.79	62.96	4.87	1010.31	37.51
38	49.86	2.97	67.04	5.13	870.79	33.66
39	59.90	2.96	67.77	4.99	760.14	30.03
40	40.87	2.73	67.04	5.06	981.44	36.85
41	49.86	3.05	126.21	6.85	1053.61	39.11
42	34.77	3.00	97.06	5.90	1120.96	40.81
43	51.63	3.31	126.21	6.92	1130.58	41.46
44	47.10	3.15	78.55	5.52	909.28	35.06
45	50.52	2.92	81.61	5.59	1010.31	37.56
46	46.45	2.88	70.54	5.08	1092.10	40.33
47	37.46	2.75	65.00	4.74	1072.85	39.61
48	39.95	2.68	63.25	4.73	986.25	37.31
49	41.40	2.93	59.02	4.95	1106.53	40.67
50	33.20	2.75	60.63	4.64	1082.47	40.01

Activity Concentrations of ^{238}U, ^{232}Th and ^{40}K in Arandis

Sample	Uc (Bq/kg)	δUc (Bq/kg)	Thc (Bq/kg)	δThc (Bq/kg)	Kc (Bq/kg)	δKc (Bq/kg)
1	85.66	3.77	134.13	6.14	835.25	32.56
2	62.09	3.38	168.20	7.61	816.27	31.79
3	70.20	3.90	248.03	10.20	915.93	35.15
4	45.92	3.14	152.52	7.24	987.12	36.72
5	63.63	3.71	253.73	10.22	911.19	34.63
6	65.05	3.73	212.39	8.44	939.66	35.67
7	60.80	3.25	195.29	8.74	1020.34	37.78
8	58.22	3.58	175.33	7.98	972.88	36.41
9	94.68	4.71	410.53	14.91	849.49	33.54
10	64.41	3.48	196.71	8.52	991.86	37.02
11	78.58	4.05	313.60	11.98	930.17	35.78
12	72.78	3.65	165.35	7.76	740.34	29.61
13	70.85	3.52	209.54	9.14	901.69	34.75
14	80.51	3.99	235.20	9.08	939.66	35.83
15	65.69	3.14	142.54	7.56	911.19	34.87
16	79.22	3.99	253.73	10.37	953.90	36.21
17	67.63	3.63	222.37	9.53	987.12	36.99
18	97.25	4.79	379.17	13.31	963.39	36.73
19	74.71	2.69	186.73	8.21	868.47	33.53
20	79.22	4.32	366.34	12.92	920.68	35.37
21	85.66	4.22	300.77	11.49	882.71	34.3
22	79.86	4.29	329.28	12.65	873.22	33.78
23	49.85	3.16	183.88	8.22	920.68	35.02
24	84.37	4.20	277.96	11.02	844.75	33.29
25	98.54	4.73	392.00	14.45	882.71	34.61
26	78.58	3.88	263.71	10.39	830.51	32.16
27	94.03	4.48	329.28	12.41	906.44	35.2
28	88.24	4.60	421.93	14.53	987.12	37.64
29	101.76	4.70	421.93	14.54	963.39	36.83
30	78.58	4.00	235.20	9.91	901.69	34.59
31	69.56	3.44	203.84	8.80	977.63	36.79
32	63.70	3.68	230.92	9.66	778.31	30.88
33	73.42	3.88	334.98	12.01	911.19	35.1
34	69.56	4.16	347.81	12.34	759.32	31.11
35	74.71	4.05	239.47	9.95	887.46	34.36
36	52.43	3.12	138.41	6.90	901.69	34.37

Sample	Uc (Bq/kg)	δUc (Bq/kg)	Thc (Bq/kg)	δThc (Bq/kg)	Kc (Bq/kg)	δKc (Bq/kg)
37	83.08	4.49	356.36	12.57	963.39	36.93
38	68.92	3.80	236.62	9.81	901.69	34.24
39	74.07	4.20	295.07	10.86	873.22	33.71
40	70.20	4.19	280.81	10.43	930.17	35.65
41	72.14	3.91	249.45	9.51	840.00	32.74
42	90.81	4.65	359.21	13.21	873.22	34.22
43	67.63	3.91	226.64	9.48	868.47	33.54
44	46.24	3.20	145.39	7.13	854.24	32.86
45	56.48	3.31	134.13	6.87	887.46	34
46	65.69	3.38	173.90	7.95	911.19	34.85
47	71.49	3.79	193.86	7.94	925.42	34.32
48	84.37	4.48	349.23	12.48	1053.56	39.38
49	84.37	4.43	343.53	12.85	858.98	33.82
50	80.51	3.93	249.45	10.15	968.14	36.54
51	50.17	3.03	132.00	6.64	892.20	34.05
52	61.51	3.34	152.52	7.48	892.20	34.18
53	54.62	2.96	117.31	6.32	868.47	33.31
54	68.92	3.53	137.13	6.98	806.78	31.42
55	52.36	3.09	105.34	6.05	749.83	29.17

Activity Concentrations of ^{238}U, ^{232}Th and ^{40}K in Swakopmund

Sample	Uc (Bq/kg)	δUc (Bq/kg)	Thc (Bq/kg)	δThc (Bq/kg)	Kc (Bq/kg)	δKc (Bq/kg)
1	42.11	2.61	66.60	4.67	638.51	26.32
2	41.80	2.52	71.67	4.74	666.89	27.06
3	22.19	1.82	26.84	3.19	548.65	23.33
4	31.80	2.17	48.90	4.03	704.73	28.13
5	36.52	2.40	60.94	4.67	685.81	27.55
6	32.74	2.46	63.55	4.70	704.73	28.09
7	31.05	2.23	48.02	4.12	591.22	24.42
8	45.82	2.74	84.44	5.47	704.73	28.41
9	32.93	2.29	50.93	4.17	595.95	24.70
10	39.60	2.50	79.07	4.91	662.16	26.79
11	71.02	3.33	145.09	7.06	553.38	23.98
12	47.33	2.82	82.85	5.23	657.43	26.83
13	60.52	3.45	138.27	6.82	600.68	25.60
14	41.98	2.65	74.87	4.87	643.24	26.42
15	65.36	3.34	149.44	7.19	525.00	23.15
16	49.34	2.77	96.63	5.90	700.00	28.31
17	44.12	2.72	85.60	5.40	761.49	29.89
18	66.62	3.38	130.00	6.91	685.81	27.73
19	43.37	2.93	94.89	5.68	822.97	31.99
20	32.49	2.29	51.22	4.21	766.22	30.17
21	41.80	2.50	68.77	4.82	657.43	26.66
22	43.24	2.84	96.34	5.71	718.92	28.79
23	36.52	2.62	75.74	5.17	733.11	29.06
24	64.74	3.29	121.58	6.31	643.24	26.79
25	75.42	3.65	174.11	7.98	610.14	25.53
26	46.38	2.84	87.49	5.14	600.68	25.42
27	27.78	2.12	43.67	3.82	643.24	26.01
28	44.56	2.70	76.32	4.95	633.78	26.18
29	25.64	2.01	32.06	3.63	525.00	22.67
30	32.12	2.17	59.20	4.32	662.16	26.88
31	55.50	3.07	117.38	6.39	464.46	21.47
32	63.48	3.32	135.08	6.94	446.96	20.70
33	30.98	2.13	58.47	4.18	638.51	26.03
34	41.42	2.65	76.75	5.09	652.70	26.55
35	36.52	2.48	70.80	4.86	657.43	26.79
36	46.45	2.63	66.60	4.57	652.70	26.73
37	45.94	2.69	72.83	4.96	666.89	26.80

Sample	Uc (Bq/kg)	δUc (Bq/kg)	Thc (Bq/kg)	δThc (Bq/kg)	Kc (Bq/kg)	δKc (Bq/kg)
38	44.06	2.80	73.85	5.10	591.22	24.74
39	28.85	2.45	51.94	4.21	600.68	24.65
40	44.12	2.71	88.21	5.36	690.54	27.84
41	43.37	2.81	92.42	5.33	685.81	27.74
42	40.04	2.40	60.21	4.35	647.97	26.16
43	44.37	2.83	83.14	5.54	633.78	26.13
44	44.69	2.64	70.37	4.70	652.70	26.73
45	54.43	3.18	114.19	6.36	638.51	26.87
46	71.65	3.70	168.30	8.01	695.27	28.24
47	62.54	3.48	152.34	7.40	690.54	28.33
48	48.02	2.81	125.50	6.73	671.62	27.41
49	78.56	3.52	178.46	8.28	610.14	26.11
50	79.82	3.82	213.28	9.12	638.51	26.90

Activity Concentrations of ^{238}U, ^{232}Th and ^{40}K in Walvis Bay

Sample	Uc (Bq/kg)	δUc (Bq/kg)	Thc (Bq/kg)	δThc (Bq/kg)	Kc (Bq/kg)	δKc (Bq/kg)
1	17.73	1.83	19.36	2.64	408.93	19.00
2	12.10	1.69	18.93	2.93	329.07	16.39
3	15.45	1.76	19.64	2.73	427.22	19.75
4	11.78	1.63	19.36	2.83	333.40	16.34
5	15.39	1.47	12.73	2.66	317.53	15.86
6	16.40	1.79	18.79	2.79	397.39	18.56
7	16.91	1.64	12.80	2.68	356.49	16.97
8	11.91	1.55	18.23	2.65	364.19	17.76
9	13.36	1.62	15.54	2.60	348.80	17.02
10	26.60	2.01	37.16	3.28	449.35	20.34
11	14.95	1.67	18.09	2.62	514.78	22.05
12	15.64	1.57	14.12	2.38	495.53	21.72
13	11.40	1.69	14.55	2.42	436.36	19.75
14	23.18	1.89	27.70	3.10	495.53	21.60
15	15.52	1.76	16.82	2.75	509.97	21.87
16	17.92	1.92	23.74	3.34	509.97	22.04
17	19.63	1.89	19.50	2.92	472.44	21.15
18	20.20	2.04	25.58	2.96	567.70	24.05
19	21.28	1.85	18.09	3.06	654.30	26.52
20	17.35	1.63	19.22	2.82	447.42	20.10
21	23.31	1.97	32.50	3.38	421.92	19.67
22	16.21	1.56	16.96	2.45	330.03	16.31
23	12.41	1.62	15.68	2.72	391.13	18.71
24	16.34	1.65	19.22	2.48	451.27	20.42
25	21.72	1.84	19.36	2.86	485.91	21.20
26	14.50	1.84	23.03	2.84	468.11	20.95
27	18.11	1.75	19.50	2.50	458.01	20.64
28	16.02	1.85	23.60	2.82	464.74	20.75
29	16.02	1.79	18.65	2.73	420.96	19.46
30	20.33	1.86	27.55	3.12	443.57	20.06
31	13.55	1.66	17.66	2.64	439.24	20.03
32	24.70	1.92	29.67	2.92	495.53	21.56
33	16.72	1.69	30.24	3.16	500.34	21.87
34	24.57	2.02	45.08	3.75	495.53	21.76
35	18.94	1.56	24.59	3.08	404.60	18.82
36	16.78	1.94	22.18	3.22	500.34	21.82

Sample	Uc (Bq/kg)	δUc (Bq/kg)	Thc (Bq/kg)	δThc (Bq/kg)	Kc (Bq/kg)	δKc (Bq/kg)
37	15.71	1.79	22.47	3.05	467.15	20.64
38	16.72	1.86	20.21	2.60	442.61	20.11
39	17.16	1.77	19.78	2.62	434.91	19.84
40	23.24	2.00	31.79	3.47	444.05	20.25
41	27.17	2.22	52.14	3.99	663.92	27.02
42	26.92	2.21	36.88	3.61	567.70	23.96
43	29.51	2.25	36.74	3.88	548.45	23.58
44	24.51	1.99	33.91	3.03	582.13	24.30
45	27.68	2.08	38.58	3.53	572.51	24.07
46	17.99	1.81	26.42	3.13	462.34	20.79
47	17.86	1.92	25.43	3.01	471.00	21.20
48	17.04	1.88	22.18	3.09	442.61	20.08
49	20.71	1.90	28.12	3.34	505.15	22.24
50	20.39	1.78	19.92	2.88	404.60	19.00

Activity Concentrations of ^{238}U, ^{232}Th and ^{40}K in Wlotzkasbaken

Sample	Uc (Bq/kg)	δUc (Bq/kg)	Thc (Bq/kg)	δThc (Bq/kg)	Kc (Bq/kg)	δKc (Bq/kg)
1	74.61	3.47	89.85	5.59	649.48	27.29
2	92.63	3.93	121.62	6.67	769.76	30.59
3	117.07	4.58	154.41	7.77	798.63	31.68
4	34.73	2.31	26.76	3.34	385.36	18.81
5	95.2	3.85	119.85	6.86	692.78	28.4
6	96.48	4.06	111.03	6.43	745.7	30.12
7	84.26	3.77	100.88	6.04	764.95	30.33
8	91.98	3.83	106.62	6.43	764.95	30.41
9	93.91	3.99	124.12	6.86	760.14	30.38
10	153.73	5.41	223.53	9.61	736.08	30.18
11	153.73	5.41	223.53	9.61	736.08	30.18
12	77.19	3.54	80.74	5.46	793.81	31.02
13	75.9	3.54	91.47	5.7	779.38	30.9
14	80.4	3.75	106.91	6.3	736.08	29.41
15	102.27	4.17	131.91	6.86	750.52	29.94
16	91.98	3.94	128.53	6.71	774.57	30.88
17	43.48	2.5	37.94	4.16	779.38	30.35
18	79.76	3.62	94.56	6.09	803.44	31.55
19	67.54	3.13	72.21	4.93	755.33	29.67
20	48.11	2.78	46.03	4.35	793.81	31.21
21	67.54	3.14	91.03	5.47	764.95	30.38
22	54.03	2.97	53.38	4.61	745.7	29.51
23	62.39	3.01	63.09	4.76	779.38	30.5
24	46.89	2.79	40.44	4.07	779.38	30.41
25	66.25	3.21	65.88	4.84	803.44	31.35
26	54.22	3.01	57.5	4.87	827.49	32.12
27	48.44	2.85	45.15	4.35	793.81	4.05
28	46.7	2.56	40.15	3.79	832.3	32.15
29	72.04	3.38	86.18	5.36	755.33	29.81
30	58.47	2.98	42.94	4.05	707.22	28.36
31	42.77	2.6	32.94	3.56	798.63	31.16
32	70.11	3.42	76.18	5.25	726.46	29.16
33	69.47	3.45	83.97	5.48	673.54	27.63
34	52.68	2.77	47.21	4.05	793.81	30.91
35	41.55	2.63	36.76	3.69	784.19	30.67

Sample	Uc (Bq/kg)	δUc (Bq/kg)	Thc (Bq/kg)	δThc (Bq/kg)	Kc (Bq/kg)	δKc (Bq/kg)
36	47.47	2.81	55.88	4.57	817.87	31.79
37	45.54	2.73	38.53	3.93	803.44	31.16
38	53.39	2.99	59.56	4.76	784.19	30.74
39	49.79	2.57	49.12	4.15	731.27	29.02
40	61.36	3.13	64.85	4.88	726.46	29.16
41	65.61	3.26	69.26	4.67	769.76	30.53
42	97.13	4.14	135.74	7.2	822.68	32.24
43	58.28	2.92	42.94	4.28	822.68	31.74
44	69.47	3.34	61.18	4.88	827.49	32.16
45	55.83	3.07	55.88	4.61	808.25	31.84
46	30.88	2.23	27.65	3.4	659.11	26.78
47	45.6	2.62	35.44	3.71	779.38	30.38
48	84.91	3.75	103.68	6.1	789	31.28
49	40.01	2.52	38.97	4.17	755.33	29.68
50	64.97	3.17	78.38	5.1	726.46	29.16

Activity Concentrations of ^{238}U, ^{232}Th and ^{40}K in Henties Bay

Sample	Uc (Bq/kg)	δUc (Bq/kg)	Thc (Bq/kg)	δThc (Bq/kg)	Kc (Bq/kg)	δKc (Bq/kg)
1	63.55	3.48	108.38	6.09	1014.63	37.98
2	97.87	4.25	171.81	8.21	921.95	35.01
3	72.74	3.67	122.84	6.76	790.24	31.64
4	59.39	3.31	94.64	6.05	1024.39	38.30
5	46.23	3.13	68.01	4.99	814.63	31.71
6	67.45	3.44	84.61	4.17	873.17	33.57
7	48.14	2.73	67.86	5.01	1024.39	38.30
8	45.70	2.85	66.72	4.95	1014.63	37.91
9	72.08	3.50	83.18	5.27	853.66	33.04
10	46.82	2.88	50.40	4.49	1029.27	37.98
11	43.58	2.75	68.29	4.83	824.39	32.36
12	46.56	3.13	78.31	5.32	995.12	37.33
13	107.13	4.57	187.56	8.77	985.37	37.90
14	47.02	3.01	64.43	4.81	1004.88	37.87
15	56.41	3.19	93.06	5.42	1039.02	38.73
16	61.44	3.49	95.64	6.04	990.24	37.28
17	153.42	5.76	323.57	12.69	902.44	35.36
18	58.33	3.24	68.58	4.98	921.95	35.23
19	83.33	3.93	127.85	6.81	819.51	32.19
20	60.64	3.41	99.79	6.16	951.22	36.09
21	57.20	3.16	82.61	5.19	946.34	35.86
22	36.17	2.70	52.97	4.66	1019.51	37.91
23	79.36	3.64	78.03	5.46	809.76	31.92
24	45.37	2.76	62.85	5.05	917.07	35.08
25	53.37	3.20	75.02	5.22	975.61	36.78
26	57.93	3.34	95.50	5.81	1014.63	37.91
27	51.25	3.05	65.14	5.04	868.29	33.39
28	41.33	2.88	66.29	5.11	936.59	35.48
29	53.24	3.17	71.73	5.25	926.83	35.32
30	57.93	3.49	112.25	6.35	1000.00	37.79
31	67.45	3.59	110.24	6.71	1009.76	37.72
32	70.76	3.40	101.65	5.92	912.20	34.97
33	61.83	3.43	105.09	6.08	897.56	34.47
34	102.50	4.62	170.37	8.16	868.29	33.81
35	72.74	3.71	134.01	6.80	990.24	37.44
36	51.98	3.04	71.30	5.15	907.32	34.76

Sample	Uc (Bq/kg)	δUc (Bq/kg)	Thc (Bq/kg)	δThc (Bq/kg)	Kc (Bq/kg)	δKc (Bq/kg)
37	72.08	3.83	133.58	6.96	921.95	35.23
38	73.41	3.66	121.70	6.76	941.46	35.73
39	66.07	3.38	109.81	6.13	1024.39	38.04
40	67.45	3.61	120.55	6.42	1024.39	38.24
41	46.75	2.89	66.15	4.89	917.07	34.77
42	46.42	2.89	66.57	4.94	902.44	34.48
43	54.36	3.01	78.74	5.26	882.93	33.80
44	57.93	3.22	82.90	5.49	946.34	35.73
45	60.44	3.31	88.19	5.43	819.51	32.08
46	49.27	3.06	73.88	5.26	892.68	33.97
47	56.87	3.20	76.31	5.21	946.34	35.87
48	43.98	2.86	52.26	4.59	970.73	36.42
49	54.16	3.10	100.51	5.72	892.68	34.37
50	61.17	3.34	102.51	6.09	926.83	35.37